

Road map for the tuning of hadronic interaction models with accelerator-based and astroparticle data

J. Albrecht^{1,2,3}, J. Becker Tjus^{1,4,5}, N. Behling², J. Blazek⁶, M. Bleicher⁷,
J. Boelhaue², L. Cazon⁸, R. Conceição^{9a,9b}, H. Dembinski^{1,2}, L. Dietrich², J. Ebr⁶,
J. Ellbracht², R. Engel¹⁰, A. Fedynitch¹¹, M. Fieg¹², M.V. Garzelli¹³, C. Gaudu¹⁴,
G. Graziani¹⁵, P. Gutjahr², A. Haungs¹⁰, T. Huege^{10,11}, K. Hymon², M. Hünnefeld²,
K.-H. Kampert^{15,1}, L. Kardum², L. Kolk², N. Korneeva¹⁷, K. Kröninger^{1,2},
A. Maire¹⁸, H. Menjo¹⁹, L. Morejon¹⁵, S. Ostapchenko¹⁴, P. Paakkinen^{20, 20b},
T. Pierog¹⁰, P. Plotko²¹, A. Prosekin¹², L. Pyras^{21,22,23}, T. Pöschl²⁴,
J. Rautenberg¹⁵, M. Reininghaus¹⁰, W. Rhode^{1,2,3}, F. Riehn^{1,2}, M. Roth¹⁰,
A. Sandrock¹⁵, I. Sarcevic²⁶, M. Schmelling²⁷, G. Sigl¹⁴, T. Sjöstrand²⁸, D. Soldin²³,
M. Unger¹⁰, M. Utheim²⁰, J. Vicha⁶, K. Werner²⁹, M.E. Windau², and V. Zhukov³⁰

¹*Ruhr Astroparticle and Plasma Physics Center (RAPP Center), Bochum, Germany*

²*Department of Physics, TU Dortmund University, D-44221 Dortmund, Germany*

³*Lamarr Institute for Machine Learning and Artificial Intelligence, Dortmund, Germany*

⁴*Theoretical Physics IV: Plasma Astroparticle Physics, Ruhr University Bochum, 44780 Bochum, Germany*

⁵*Department of Space, Earth and Environment, Chalmers University of Technology, Gothenburg, Sweden*

⁶*FZU – Institute of Physics of the Czech Academy of Sciences, Prague, Czech Republic*

⁷*Institute for Theoretical Physics, Goethe University Frankfurt, Frankfurt am Main, Germany*

⁸*Instituto Galego de Física de Altas Enerxías (IGFAE), Universidade de Santiago de Compostela, Santiago de Compostela, Spain*

^{9a}*Physics Department, Instituto Superior Técnico (IST), University of Lisbon, Lisbon, Portugal*

^{9b}*Laboratório de Instrumentação e Física Experimental de Partículas (LIP), Lisbon, Portugal*

¹⁰*Institute for Astroparticle Physics, Karlsruhe Institute of Technology (KIT), Karlsruhe, Germany*

¹¹*Astrophysical Institute, Vrije Universiteit Brussel, Brussels, Belgium*

¹²*Institute of Physics, Academia Sinica, Taipei, Taiwan*

¹³*Department of Physics and Astronomy, University of California, Irvine, CA, USA*

¹⁴*II Institute for Theoretical Physics, Hamburg University, Hamburg, Germany*

¹⁵*Faculty of Mathematics and Natural Sciences, University of Wuppertal, D-42119 Wuppertal, Germany*

¹⁶*INFN, Sezione di Firenze, Florence, Italy*

¹⁷*School of Physics and Astronomy, Monash University, Clayton, VIC 3800, Australia*

¹⁸*IPHC – Institut Pluridisciplinaire Hubert Curien, CNRS-IN2P3 / Université de Strasbourg, UMR 7178, Strasbourg, France*

¹⁹*Institute for Space-Earth Environmental Research (ISEE), Nagoya University, Nagoya, Japan*

²⁰*Department of Physics, University of Jyväskylä, Jyväskylä, Finland*

^{20b}*Helsinki Institute of Physics, University of Helsinki, Helsinki, Finland*

²¹*Deutsches Elektronen-Synchrotron (DESY), Platanenallee 6, 15738 Zeuthen, Germany*

²²*Erlangen Center for Astroparticle Physics (ECAP), Friedrich-Alexander-Universität Erlangen-Nürnberg, Nikolaus-Fiebiger-Straße 2, 91058 Erlangen, Germany*

²³*Department of Physics and Astronomy, University of Utah, Salt Lake City, UT 84112, USA*

²⁴*European Organization for Nuclear Research (CERN), Geneva, Switzerland*

²⁵*Instituto Galego de Física de Altas Enerxías (IGFAE), Universidade de Santiago de Compostela, Santiago de Compostela, Spain*

²⁶*Department of Physics, University of Arizona, Tucson, AZ, USA*

²⁷*Max-Planck-Institut für Kernphysik, Heidelberg, Germany*

²⁸*Department of Physics, Lund University, Lund, Sweden*

²⁹*SUBATECH – Laboratory of Subatomic Physics and Associated Technologies, University of Nantes, IMT Atlantique, CNRS/IN2P3, Nantes, France*

³⁰*Institute for Experimental Physics 1b, RWTH Aachen University, Aachen, Germany*

Monday 1st September, 2025

Abstract

In high-energy and astroparticle physics, event generators play an essential role, even in the simplest data analyses. As analysis techniques become more sophisticated, e.g. based on deep neural networks, their correct description of the observed event characteristics becomes even more important. Physical processes occurring in hadronic collisions are simulated within a Monte Carlo framework. A major challenge is the modeling of hadron dynamics at low momentum transfer, which includes the initial and final phases of every hadronic collision. Phenomenological models inspired by Quantum Chromodynamics used for these phases cannot guarantee completeness or correctness over the full phase space. These models usually include parameters which must be tuned to suitable experimental data. Until now, event generators have primarily been developed and tuned based on data from high-energy physics experiments at accelerators. However, in many cases they have been found to not satisfactorily describe data from astroparticle experiments, which provide sensitivity especially to hadrons produced nearly parallel to the collision axis and cover center-of-mass energies up to several hundred TeV, well beyond those reached at colliders so far. In this report, we address the complementarity of these two sets of data and present a road map for exploiting, for the first time, their complementarity by enabling a unified tuning of event generators with accelerator-based and astroparticle data.

1 Introduction

The simulation of high-energy particle collisions is an essential task in many fields of science, such as high-energy nuclear and particle physics or high-energy astroparticle physics. The simulation involves several steps, namely the event generation, hadronization and particle decay, particle propagation, and detector response simulation. The predictions of the event generators are usually based on the Standard Model (SM) of particle physics [1] with new phenomena being tested against the SM predictions. So far, event generators are essentially developed and tuned solely based on data from accelerator-based experiments. We define *tuning* as the process of adjusting free parameters of phenomenological models in event generators based on comparisons with data. Specific tunes of event generators based on accelerator experiments have been found to be inconsistent with data from astroparticle experiments. To address this issue, we explore the opportunities and challenges of incorporating data from particle and astroparticle experiments simultaneously into the development and tuning of event generators. We also outline how to achieve such a *global tuning*.

There is a clear need for such an effort, as improved event generators have the potential to benefit a wide range of applications. Event generators are used to simulate signal events, from which measurements of signal-related experimental parameters are inferred. They also predict event signatures that can be used to develop data analysis methods and even design entirely new experiments. Additionally, they also predict particle interactions within the detector material. When searching for rare events or processes, such as Higgs production at the Large Hadron Collider (LHC), background contamination of the data typically occurs, and event generators help to find experimental designs and analysis methods that allow one to reduce this contamination [2]. For this purpose, they need to predict the frequency and distribution of signal and background events with a high degree of accuracy, since the efficiency and purity of an event selection can often only be calculated on the basis of a full end-to-end simulation of the entire experiment. The need for accurate event generators becomes more important as better experimental data become available. This is particularly true when applying machine learning methods, which tend to outperform classical analysis methods, e.g. in terms of classification performance, at the cost of being more sensitive to mismatches between simulated and experimental data.

In astroparticle physics experiments, event generators are used to simulate interactions between cosmic particles and the Earth and its atmosphere. In specific applications, they also to simulate interactions between particles within cosmic ray sources and during their journey to Earth. Because high-energy charged cosmic rays, cosmic neutrinos, and gamma-rays are characterized by low fluxes ($\phi \lesssim 1 \text{ m}^{-2} \text{ yr}^{-1}$ at cosmic ray energies above a few 10^{15} eV), large aperture ground-based experiments are required to detect them. These experiments indirectly observe cosmic particles through showers of secondary particles [3]. The showers themselves originate from the collisions of high-energy primary particles with matter, most importantly air, water, or ice. They are typically detected by their light emission (fluorescence or Cherenkov radiation), radio emission, or classically by sparse arrays of charged particle detectors distributed over an extended area or volume [3, 4]. Recently, experiments have begun combining two or more of the above methods to observe the same shower in different ways. This is known as *hybrid detection* and was pioneered as an integral concept at the Pierre Auger Observatory [5]. Event generators simulate the development of the particle cascade in order to determine the relationship between the detector response and the initial cosmic particle. If the simulation is inaccurate, the interpretation of the data will be biased. While the energy scale of TeV gamma-ray experiments can in principle be calibrated against the GeV gamma rays detected by satellite experiments using standard candles such as the Crab Nebula [6, 7], there is no equivalent calibration source for high-energy cosmic rays and neutrinos, making the theoretical uncertainties in the event generators a major source of uncertainty in these experiments. A prime

Table 1: Key characteristics of HEP accelerator-based experiments and astroparticle experiments. We use A as a placeholder for nuclei. When nuclei are involved, \sqrt{s} refers to the nucleon-nucleon CM energy.

	Accelerator		Astroparticle	
	Fixed-target	Collider	Cosmic rays	Neutrinos
Collision energy (\sqrt{s})	up to 100 GeV	100 GeV to 14 TeV	up to 500 TeV	up to 10 TeV
Collision systems	e+e, e+p, p+p, p+A, A+A		$(\pi, K, p, A, e, \gamma, \mu, \nu) + A$	
Initial state	fixed		variable (energy and system)	
Acceptance range	backward to central	central to forward	very forward	
Final state: flavour	light	light and heavy	light	light and heavy
Resolution	single interaction		cascade	single interaction, cascade

example of this is the *muon puzzle* [8] in extensive air showers (EAS), which causes an ambiguity in the inferred mass composition of ultra-high energy cosmic rays [4].

A major source of uncertainty in event generators is the treatment of hadronic interactions with low momentum transfer ($Q = \mathcal{O}(\text{GeV})$), where the strong coupling in quantum chromodynamics (QCD) is large and perturbative methods are not applicable [9]. The most important example here is the copious production of light-flavor particles which dominate the development of secondary particle cascades in various media. In high-momentum transfer interactions, such as heavy-flavor production, the initial and final stages (parton momentum distribution and hadronization, respectively) are also non-perturbative.

QCD-inspired phenomenological models are used to describe non-perturbative processes, which may not be entirely correct nor complete across the entire phase-space. Recent examples of surprises in QCD include the discovery of collective flow and enhanced strangeness production, which was previously only known to occur in high-energy in nucleus-nucleus collisions, but has also been observed in proton-proton and proton-lead collisions at the TeV scale, see e.g. [10, 11].

To arrive at a highly complete and accurate description of QCD phenomena, and to reduce uncertainties and ambiguities in the interpretation of data from astroparticle experiments, it is important to develop event generators using data from all sources. So far, data from astroparticle experiments have not been widely used in this context, apart from a few pioneering studies, see for example [12]. While previous generations of astroparticle experiments were not precise enough for this purpose, the latest generation provides a great wealth of data.

A comparison of specific aspects of accelerator and astroparticle physics data is provided in Table 1. There are several challenges to using astroparticle data. The initial state of a collision is variable and not well known, and air shower detector arrays observe the final state of a cascade of interactions in a medium, such as air, rather than a single interaction. Optical and radio observations track the evolution of the entire shower particle ensemble along the shower axis. However, astroparticle data complement accelerator data: they are sensitive to light and heavy flavor production at forward rapidities¹ and probe collisions at center-of-mass (CM) energies of up to 500 TeV. They also probe collisions that are not easily accessible at colliders, such as those initiated by pions

¹The rapidity of a particle is defined as $y = \frac{1}{2} \ln \frac{E+p_{\parallel}}{E-p_{\parallel}}$, where E is the total energy and p_{\parallel} the longitudinal momentum. The rapidity behaves additively under a Lorentz transformation along the beam axis, meaning the shape of a rapidity distribution remains unchanged. This makes it an attractive observable in particle physics experiments.

and kaons [13, 14]. Exploiting complementary data from both fields can further reduce theoretical uncertainties in event generators. This also provides a powerful test of the effective phenomenological models employed. Ultimately, event generators that include sufficiently general models should be able to describe all the data from particle and astroparticle experiments without inconsistencies.

Currently, new event generators are manually tuned and verified by comparing them to a set of accelerator data. Then, the effect of changes is studied by comparing EAS predictions to observational data. The first step toward global tuning is automating the comparison and tuning to accelerator data. This will allow for the rapid testing of new models and quick retuning as new models or data become available. Including EAS data in the second step is challenging due to fundamental differences between the measurements in the two fields. Most of the complexity arises from the unknown initial state of the first and subsequent collisions and the computational resources needed for full EAS simulations. Developing standardized tools is a crucial prerequisite for this effort.

Recent Cross-Section for Cosmic Rays (XSCRC) workshops at CERN have addressed the lack of cross-section data necessary for improving hadronic interaction models for modeling the propagation of cosmic rays in our galaxy. These workshops provide a roadmap for closing key cross-section data gaps [15].

This review is based on discussions among representatives of particle and astroparticle physics during a workshop in Wuppertal that focused more generally on the deficits and tuning of hadronic interaction models. As a result, we present for the first time a road map showing how to tune event generators simultaneously using data from both accelerators and astroparticle physics experiments. In Section 2, we summarize the theoretical approaches implemented in current event generators and recent developments towards event generators that are applicable to both high-energy and astroparticle physics. In Section 3, we summarize recent developments in the simulation of particle transport in matter, which are essential for the interpretation of high-energy astroparticle experiments and for global tuning. In Section 4, we give an overview of the most important measurements from accelerator and astroparticle experiments that provide input for global tuning. In Section 5, we summarize the current state of tuning of event generators and discuss how the tools involved need to be extended or replaced to enable global tuning, followed by a discussion of current challenges and possible solutions to achieve global tuning in Section 6. We conclude with a summary in Section 7.

2 Theoretical foundations and event generators

Despite significant progress both in the predictions of perturbative QCD (pQCD) and in measurements at the LHC, it is still not possible to calculate from first principles the bulk of particle production processes at high energies. Only processes with large momentum transfer, also known as hard interactions, are accessible to the perturbative methods. To obtain a complete description of hadron collisions in accelerator experiments, it is necessary to combine results from pQCD and general theoretical constraints with phenomenological modeling. To make predictions for particle production in hadron collisions in the astroparticle context, one must also extrapolate the distributions measured at accelerators into unmeasured regions of phase-space, projectile and target combinations and to much higher energies.

Processes in which heavy quarks are produced in the final state are necessarily hard, and pQCD calculations can be quite accurate, but even in these calculations non-perturbative parts enter to model long-distance physics effects governing the parton-to-hadron transition and vice versa (fragmentation functions/hadronization, parton distribution functions).

Event generators use Monte Carlo simulations to describe QCD interactions. Table 2 present

Table 2: Comparison of five event generators. Acronyms are defined in the text. Further details on the individual event generators and their interfaces are provided in Appendix A, while the particle transport codes mentioned in the last row are discussed in Section 3 and Appendix B.

	EPOS4 [16]	EPOS LHC-R [17, 18]	QGSJET-III [19]	SIBYLL 2.3d [20]	PYTHIA 8 [21, 22]
Primary domains	HIC, HEP	EAS, HIC	EAS	EAS	HEP, (HIC via Angantyr)
Theoretical basis	parton-based GRT, pQCD, energy sharing, saturation	parton-based GRT, pQCD, energy sharing	GRT, pQCD (DGLAP+HT)	GRT, pQCD (minijet)	MPI, pQCD, ISR, FSR
Nuclear collisions	idem	idem	idem	extended superposition	Glauber via Angantyr
Collective effects	✓	✓	None	None	✓
Tuning collision systems	e^+e^- , pp, pA	e^+e^- , pp, pA	pp, pA	pp, pA	e^+e^- , pp
Tuning parameters accessibility	model authors	model authors	model authors	model authors	any users
Tuning-related interface	HepMC, RIVET	HepMC	HepMC	HepMC	HepMC, RIVET
Transport code interface	None	CORSIKA 7/8, CONEX	CORSIKA 7/8, CONEX	CORSIKA 7/8, CONEX, MCEq	CORSIKA 8

the latest generation of event generators that are used in both high-energy accelerator physics and astroparticle physics. Apart from basic physics concepts employed in each model, the table also summarizes how the models are tuned and interfaced. A more detailed description of each generator can be found in Appendix A. There are many other generators in the high energy physics (HEP), heavy ion (HIC) (e.g. UrQMD [23]), and nuclear physics communities. However, we focus exclusively on generators that are commonly used in air shower simulations or those offering all the necessary capabilities for air shower simulations and support tuning, as in the case of PYTHIA 8. In this discussion, we also neglect low-energy hadronic interaction models ($\sqrt{s} \leq 10 \text{ GeV}$) and nuclear physics ($\sqrt{s} = \mathcal{O}(\text{MeV})$) codes. Interactions at these energies were found to be much less important for ultra-high energy showers, see e.g. [24]. They may, however, be included in the tuning at a later stage once the process is established.

PYTHIA 8 [21] is an event generator often used in high-energy physics (HEP) and more recently also applied for cosmic ray physics [22]. Its core is built on the pQCD model. A (semi-)hard scattering is the starting point of each inelastic interaction, accompanied by emissions of partons before, or after the hard scattering (so-called initial/final state radiation implemented in parton shower algorithms). Multiple (semi-)hard scatterings are also allowed. The soft physics effects are described by phenomenological models. The cross sections for (semi-)hard scattering are determined from pQCD using a threshold in the transverse momentum (suppressed by a smooth damping factor). The modeling of the total elastic, diffractive, and inelastic cross sections in PYTHIA 8 is decoupled from the particle production mechanism.

In other event generators, like FRITIOF [25] used in GEANT4 [26] or the models used in astroparticle physics, a different, more inclusive approach is used, where the interaction of hadrons is modeled as the exchange of specifically structured "networks" of interacting quarks and gluons (so-called Pomeron and Reggeon exchanges). The mathematical framework for these exchanges, an effective quantum field theory, is the so-called Gribov Regge theory (GRT) [27], see Refs. [28] for a

pedagogical introduction. It allows one to connect the wide range of processes that occur in hadron collisions, such as elastic scattering, diffractive scattering and soft multi-particle production up to multiple hard parton scattering. The energy evolution of the hadron multiplicity and the total cross section are thus linked in GRT-based models.

SIBYLL [20] is a GRT model that describes inelastic collisions with a soft and a hard part, where the hard part is based on the pQCD cross section calculated with an energy-dependent cutoff in transverse momentum (similar to PYTHIA), while the soft part is purely phenomenological. The EPOS [16, 17] and QGSJET [19] families of models use a semi-hard pomeron that consistently mixes aspects of the GRT and pQCD descriptions. The semi-hard pomeron provides the analog of initial and final state radiation (ISR and FSR), which in particular leads to broader hadron spectra in rapidity. The EPOS family of generators is based on so-called parton-based GRT, where the pomerons are exchanged between partons instead of hadrons and energy conservation is ensured at the amplitude level. The QGSJET family of generators implements pomeron-pomeron interactions. Both are mechanisms that slow down the growth of the total cross section at high energies, which is necessary to describe the measurements.

Single diffraction dissociation, which occurs in events where only one of the incoming hadrons is dissociated, is an important contribution to hadron production in the forward region. In GRT models, this is described by the exchange of a specific colorless (quantum number-less) configuration of quarks and gluons (the so-called diffractive pomeron). This is either explicitly included in the amplitude or added using the Good-Walker model [29].

In the context of air showers, the models need to be reliably extrapolated from hadron-hadron to hadron-nucleus and nucleus-nucleus interactions. In the EPOS and QGSJET models the nuclear amplitudes are constructed from the basic pomeron amplitude using the Glauber formalism [30]. In SIBYLL, a mixture of Glauber (for hadron-nucleus) and an extended superposition model (for nucleus-nucleus) [31] is used. PYTHIA can model nuclear interactions in air showers using either the Angantyr [32] model or PythiaCascade [33] class, both of which now support an essential feature for realistic air shower simulations as discussed in [22]: (1) generate single events at arbitrary energies without costly reinitialization, (2) event-by-event modifications of the projectile, target, and center-of-mass energy. PYTHIA can optionally use nuclear parton distribution functions (PDFs) for collisions with nuclei, which differ from the PDFs of free protons [34, 35].

The description of heavy ion collisions (HIC) requires the inclusion of effects such as collective flow, jet quenching, and possible modifications of the final-state hadron composition (which may affect e.g. the strangeness enhancement). In EPOS, this is described by distinguishing between hadronization of the high-(energy) density part of the collision (core), modeled by the formation of a quark-gluon plasma that evolves hydrodynamically and then decays statistically, and hadronization of the low-(energy) density part (corona), based on string fragmentation [36] (similar to the standard PYTHIA hadronization mechanism). This is followed by a phase of hadronic rescattering. Similarly, in PYTHIA 8, color reconnection [37], rope fragmentation [38], string shoving [39], and hadron rescattering [40] are means to modify standard hadronization in vacuum to describe the effects observed in HIC. SIBYLL and QGSJET do not include these types of HIC effects. HIJING [41, 42] and other generators that are exclusively developed for heavy ion collisions typically do not include the interaction of pions and kaons nor do they provide reliable predictions for particle production in the forward direction. Both of these are essential for simulating extensive air showers, which is why pure HIC generators are not usually used in air shower simulations.

Heavy quark production has traditionally not been implemented in event generators used for EAS simulation, since the effect on most air shower observables is negligible [43], but the need to model the prompt atmospheric lepton flux in the latest generation of neutrino observatories has led to the inclusion of charm production in SIBYLL 2.3d, EPOS4, and EPOS LHC-R. PYTHIA natively

produces quarks of all flavors. Next generation neutrino observatories may even be sensitive to the contribution from b-quarks [44].

Important to note that EPOS LHC-R is a simplified version of EPOS4 designed to reduce computation times, enabling its practical use within air shower simulation codes. In the future, EPOS4 and EPOS LHC-R are intended to be merged into a single unified EPOS framework.

Event generators are stand-alone codes often with non-standard interfaces. However, software packages such as CRMC [45] and Chromo [46] simplify the use and comparison of the previously listed event generators by providing a common interface and unified output. Further detail can be found in Appendix A.8.

3 Particle transport in matter

Transport codes in astroparticle physics simulate the propagation, decay, and interaction of high-energy particles with a medium such as air, water, ice, or interstellar gas. They employ event generators, including current and/or previous versions of the models summarized in Table 2, to handle interactions and decays. This section provides an overview of the most relevant particle transport codes and some of their applications. A recent review of transport codes used in astroparticle physics is also given in Ref. [8]. In Table 3, transport codes are compared from the perspective of their use in tuning event generators. They link the physics of hadronic interactions in a cascade to “macroscopic” experimental astrophysical observables, such as the depth of the electromagnetic shower maximum, X_{max} , the number of muons produced, or the atmospheric high-energy lepton flux. Theoretical uncertainties in particle transport mainly arise from the theory and the phenomenological assumptions implemented in the hadronic event generators. For neutrino observatories such as IceCube [47] and underground laboratories, uncertainties related to the propagation of secondary leptons through the atmosphere or overburden are also significant [48].

Table 3: Comparison of transport codes in the context of tuning. References are given the text.

	Monte Carlo simulation	Cascade equation solver	3D Hybrid simulation
Examples	CORSIKA, AIRES, CR-PROPA	CONEX, MCEQ, SENECA	CORSIKA+CONEX, SENECA
Observables	all	limited (see text)	limited (no radio or Cherenkov emission)
Shower-to-shower fluctuations?	yes	no	yes
Energy dependence of computational cost	$\propto E_{\text{cosmic ray}}$	$\approx \text{constant}$	$\propto E_{\text{cosmic ray}}$

In the case of transport codes used in HEP, such as GEANT4 [26] or FLUKA [49], the focus is slightly different. Here, transport codes are mostly used to simulate particle transport through the “detector material” and generate observable signals starting from a list of primary particles provided by an event generator like PYTHIA. In accelerator-based experiments, theoretical uncertainties are reduced by minimizing the amount of material the particles must pass through and by sophisticated calibration schemes. In astroparticle experiments, the amount of material is usually large, often complex and its detailed structure unknown. For example, the Earth’s atmosphere and magnetic field can be considered as part of the detector of an air shower experiment, and must be carefully

monitored, as these properties change daily and seasonally. It is important to track the vertical density profile of the atmosphere and its optical properties, which are monitored using laser and electron beams [50, 51], local weather balloon flights [52], and satellite-based models [53]. For all of these reasons, great care is taken to make not only the interaction but all models entering the transport codes as accurate as possible.

Computational speed and efficiency of transport codes is a key aspect to be considered in tuning procedures, since calculating a change in an air shower observable as response to a change in an event generator may require simulating hundreds of air showers in order to average out shower-to-shower fluctuations. Full Monte Carlo simulation, as employed by CORSIKA [54], AIRES [55] and CRPROPA [56], is the gold standard, but very demanding in terms of computational resources. The computational effort is proportional to the number of particles that need to be tracked. For air showers, this number is proportional to the cosmic-ray energy, which in turn spans over 11 orders of magnitude. Full simulation becomes impractical above 10^{17} eV. At higher energies, the thinning technique [57] in which only a representative subset of particles is simulated can be used. The shower-to-shower variation in computation time depends on the interaction model, through both the runtime of individual hadronic interactions and the nature of the final-state particles, which influence how much energy is fed into the electromagnetic or hadronic cascades. Electromagnetic cascades dominate the overall runtime, so models producing more electromagnetic secondaries results in longer simulations. The computational load further increases if detailed Cherenkov or radio emission has to be simulated, which is needed for some observables.

The numerical solution of cascade equations is an alternative technique for simulating air showers and calculating particle fluxes. This approach is used by CONEX [58] and MCEQ [59]. It describes hadronic cascades by a large system of differential (cascade) equations, one for each particle species, containing source and sink terms describing energy loss, particle interaction and decay [60]. The input particles are binned in energy and atmospheric depth, and the differential equations are then solved numerically. This enables e.g. the computation of atmospheric lepton fluxes using as input the cosmic ray flux at the top of the atmosphere or an “average” air shower from monoenergetic cosmic rays as input. Examples of outputs include longitudinal shower density profiles and energy distributions of secondary particle fluxes. However, this approach only works for calculating some of the air shower observables. Those that require the simulation of shower-to-shower fluctuations or lateral particle distributions at the detector sites, typically required by ground-based air shower arrays, require full Monte Carlo or 3D hybrid simulations. In these simulations, implemented in CORSIKA or SENECA [61], the initial and final stages of an air shower are simulated using Monte Carlo, and the cascade equations are solved numerically for the middle part. 3D hybrid simulations that omit full particle trajectories cannot produce radio or Cherenkov emissions, which require complete space-time shower evolution. Observables that are already defined as an average over many similar showers (e.g. the depth of the shower maximum or the number of muons produced) can be obtained directly from these solvers.

Numerical solvers of cascade equations use precomputed tables of the energy spectra of secondary particles for colliding particles at different energies. These tables allow air showers to be computed in seconds, but generating them from event generator calls is computationally expensive, requiring on the order of (10–1000)k events, depending on the desired smoothness of the tables and whether charmed hadrons, which have a lower production cross section, are to be simulated. However, cascade equation solvers have a computational advantage when computing air shower observables of different primary cosmic ray energies and masses multiple times during the tuning process.

Further details of the transport codes are discussed in Appendix B.

As mentioned above, factorization and reweighting techniques can reduce the computational cost of CPU-intensive transport codes. In the factorization approach [62, 63], intermediate “high-

level” key variables that have a strong influence on the air shower observables are identified. These variables include the inelastic cross section and the hadron multiplicity. Assuming that these high-level quantities scale logarithmically with the cosmic-ray energy, one can precalculate their impact on the air shower observables. This drastically reduces the effort required for an event generator to calculate a high-level variable at a fixed cosmic-ray energy. An example of such an analysis is discussed below (*cf.* Fig. 2). In the reweighting approach [64], on the other hand, weights are applied to the precomputed tables used by a cascade equation solver, or to a set of air showers previously simulated by Monte Carlo. These air showers must be stored as complete graphs, including all particle interactions and decay histories. The weights are chosen to reflect the change in the event generator. Reweighting can be effective when the change in the event generator only has an isolated effect, such as on selected particle types. Both strategies have the potential to considerably speed up tuning, but they require making strong assumptions that must be carefully validated. They also run the risk of missing unexpected side effects of changes to event generators.

4 Input from experiments

Traditionally, event generators are tuned using input from accelerator-based experiments (classic tuning). Classic tuning uses measurements such as production cross sections, hadron multiplicity spectra, energy flow, and rapidity gap distributions. Global tuning adds a variety of air shower observables, such as the mean and fluctuations of the depth of the shower maximum, the mean and fluctuations of the produced number of muons, and other observables related to these. The mean number of muons is sensitive to small changes in secondary hadron yields, which are amplified by the hadronic cascade [8, 62], while the other air shower observables are dominated by the first interaction. Further input can be obtained from the atmospheric muon flux at PeV energies. The conventional component of this flux (*i.e.*, the component arising from light-flavor production, hadronization, and decay) is sensitive to hadron production over a wide range of energies. In contrast, the prompt component (*i.e.*, the component arising from heavy-flavor production) is sensitive to charm production.

Inputs from air shower and accelerator experiments complement each other, and both have their respective limitations. The highest CM energy achieved at an accelerator on Earth so far amounts to 13.6 TeV. In air showers, the CM energy of the first collision can be significantly higher, reaching several hundred TeV. In many cases, air shower measurements are precise enough to place constraints on quantities that accelerator measurements only loosely constrain. For example, fluctuations in the number of muons in air showers constrain the inelasticity, *i.e.* the fraction of energy taken by the secondary particles, which is challenging to measure at the LHC.

Another complementarity lies in the accessible rapidity range. Measurements from accelerator-based experiments are often expressed as a function of the transverse momentum p_{\perp} , and rapidity (y) or pseudorapidity (η)² of the products. At the TeV scale, the production cross sections of hadrons near projectile rapidities are most important for air showers [8], but detailed measurements of identified hadrons are mostly limited to mid-rapidity, *i.e.* to polar angles near $\theta_{\text{CM}} = 90^\circ$.

Finally, a third complementarity in the collision systems. At the LHC, so far only p+p, p+Pb, and Pb+Pb collision systems were investigated (see *e.g.* [11]), while the most common system in air showers is $\pi + (N, O)$. The properties of $\pi + A$ collisions beyond the CM energies of fixed target experiments have to be inferred from data on p+A collisions, since pion beams are not available at colliders. Until results of the recent oxygen beams at the LHC become available, the extrapolation

²In contrast to the rapidity, y , the pseudorapidity $\eta = -\ln(\tan(\theta/2))$ does not require particle identification capabilities and $\eta \approx y$ for highly relativistic particles.

from p+p and p+Pb to p+O and p+N remains uncertain at the TeV scale.

Global tuning will likely reveal discrepancies between models and data. In terms of experimentation, hidden systematic effects in the measurements may exist that are not covered by the quoted uncertainties. Theory-wise, models may lack the necessary physical content, robustness, and flexibility to reproduce all available measurements. In either case, it will not be possible to achieve a good statistical fit between the models and the available data. However, global tuning is necessary to reveal these discrepancies, so that the community can address them.

4.1 Accelerator-based experiments

We will focus our discussion primarily on experiments using hadron beams, such as those provided at the LHC and its pre-accelerator the Super Proton Synchrotron (SPS). Nevertheless measurements at the Brookhaven Relativistic Heavy Ion Collider (RHIC) and older data from the Tevatron and other accelerators also provide important input by constraining event generators across a wide range of collision energies. Note that experiments conducted at lepton-lepton and lepton-hadron colliders, such as LEP and HERA, are also included in the tuning process because they allow us to fix string fragmentation parameters, as discussed e.g. in Ref. [65] and the parton distribution functions of hadrons [66]. For further details on tuning see Subsection 5.2. Future machines, such as the Electron Ion Collider [67] and the planned FCC-ee [68] at CERN, will probe hadrons at new scales.

Accelerator data are available from either fixed-target and colliding-beam experiments. The main differences between these two types of experiments lie in the CM energy scale being probed, the kinematic coverage, and the flexibility in studying different collision systems. Current fixed-target experiments probe nucleon-nucleon CM energies up to about 100 GeV, while LHC experiments in colliding-beam configurations currently reach up to 13.6 TeV.

An advantage of fixed-target experiments is the ability to study a wide range of beam and target combinations. The target is typically a thin foil or small block of material that can easily be replaced. Liquid and gaseous targets are used. Experiments can use primary beams, such as proton and lead beams from the LHC or SPS, or secondary beams produced by colliding the primary beam with a production target. Currently, this is the only way to study $\pi + A$ or $K + A$ interactions.

Another advantage of fixed-target experiments at the SPS, such as NA61/SHINE [69], is the ability to cover a large part of the rapidity range with good particle identification, making them relevant for tests and improvements of hadronic interaction models (*cf.* Fig. 1).

Collider experiments are typically best instrumented in the mid-rapidity region in the CM frame of the collision system because most particles are produced there. In contrast, the forward region ($|y| \gg 2$), into which most of the beam energy flows, is usually sparsely instrumented. The four large LHC experiments –ATLAS [72], CMS [73], ALICE [74], and LHCb [75] – are all designed as general-purpose detectors, but each with a different focus. ATLAS and CMS were primarily designed to discover new heavy particles, such as the Higgs boson and heavy supersymmetric candidates. Thus, their main instrumentation provides good lepton-hadron separation capabilities in the mid-rapidity region ($|y| < 2.5$) and it compromises on hadron identification capabilities. The main focus of ALICE is studying the QCD phase transition to a quark-gluon plasma, particularly in nucleus-nucleus and proton-nucleus collisions. For this reason, ALICE is equipped with excellent hadron identification capabilities over a large momentum range and tracking in the presence of high charged particle multiplicities. The main focus of LHCb is studying the production of hadrons containing heavy flavor, i.e. charm and bottom quarks. Therefore, LHCb does not need a symmetric acceptance w.r.t. $y = 0$ and is mainly instrumented in the forward region with very good particle identification capabilities for hadrons with momenta up to 100 GeV/c. LHCb is equipped with a system that enables the injection of gases into the beam pipe. This allows the LHCb detector to

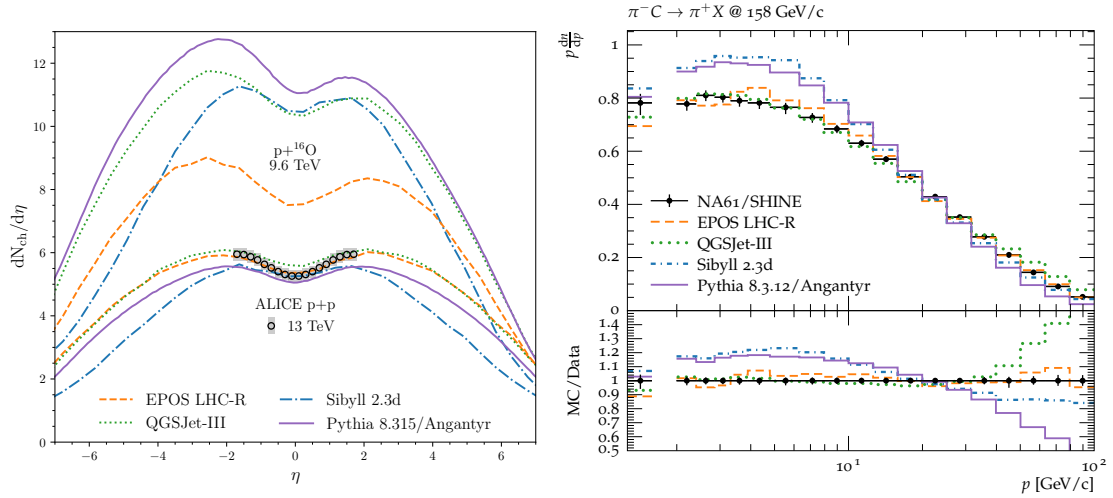


Figure 1: Left: $dN_{ch}/d\eta$ distributions for proton-proton collisions at $\sqrt{s} = 13\text{ TeV}$ and proton-oxygen collisions at 9.6 TeV. Experimental data are from ALICE [70]. Model predictions include EPOS LHC-R (dashed), QGSJET-III (dotted), Sibyll 2.3d (dash-dotted), and PYTHIA 8/Angantyr (solid). Right: π^+ production in π^-C collisions at 158 GeV as a function of the outgoing π^+ momentum. Experimental data are from NA61/SHINE [71], using a RIVET plugin listed in Table 6.

operate as a fixed-target experiment [76] and provides a unique opportunity to study proton-nucleus and nucleus-nucleus collisions with different gaseous targets using the LHC beams. Recently, the system was upgraded to allow gases other than noble gases to be injected into the beam pipe, most notably nitrogen and oxygen [77]. Important observables in these experiments include total and differential cross sections, multiplicity distributions, and energy flow. Results from proton-proton, proton-nucleus and nucleus-nucleus collisions help us to understand nuclear and collective effects. The relevance of the different quark flavors can be probed by studying the production of particles containing strange, charm or bottom quarks.

In addition to general-purpose experiments, there are experiments dedicated to covering the very forward rapidities, which are most relevant for EAS: TOTEM [78] measured the charged particle multiplicity [79], CMS-CASTOR has measured the energy flow [80], LHCf [81] the π^0 and neutron production cross sections at $y > 8$ and FASER [82] the sum of the production spectra of charged pions, kaons and D-mesons at $y > 8.5$. These data are not well described by the interaction models [83–86] and provide important additional input for tuning of the models (*cf.* Sec. 5.2).

A comprehensive overview of data from accelerator experiments that is useful for tuning hadronic interaction models is given in Ref. [8]. The most important experiments for the tuning of QCD-inspired models, along with their most relevant results, are summarized in Appendix C.

For air shower simulations, it is important to understand nuclear effects, which alter the production cross sections relative to collisions involving free nucleons. So far, LHC beams have probed proton-proton, proton-lead, and lead-lead collisions, representing the extremes of collision systems. Additionally, a short pilot run with xenon beams was conducted in 2017 [87]. However, these reference systems are not ideal for air showers, in which collisions with nitrogen and oxygen dominate. It is unclear how features of hadron production can be interpolated to this point. As Figure 1 illustrates, current event generators used to simulate air showers show a considerable spread in

their predictions for the hadron multiplicity in proton-oxygen collisions at mid-rapidity, reaching up to 25%. In contrast, they agree within 5% in proton-proton collisions in the mid-rapidity region, because they are tuned to these data [88].

Fortunately, after an extensive preparation period, the first oxygen run was successfully delivered to experiments at the LHC during a pilot run in July 2025. This enabled the first study of p+O and O+O collisions [89]. Analyzing this and future data will be particularly interesting for cosmic ray physics and tuning hadronic interaction models.

Figure 1 also shows that the different hadronic interaction models agree with one another and with the experimental data for p+p at mid-rapidity but deviate in the forward region, highlighting the importance of measurements in this region. In addition to the forward experiments listed above, such measurements could be provided by experiments at the proposed Forward Physics Facility [90].

4.2 Astroparticle experiments

High-energy astroparticle experiments measure gamma rays, neutrinos, and cosmic rays from about 10^{12} eV to beyond 10^{20} eV. The flux of these particles decreases sharply as a function of energy, according to a power law. Therefore, large apertures are needed for measurements at very high energies. This is achieved with ground-based experiments that measure the characteristics of particle showers initiated by the primary particle in the Earth’s atmosphere, water bodies, or ice shields.

The properties of the primary particle can be inferred from the observed features of the particle shower. The direction of the projectile is inferred from the arrival times of shower particles at ground-level detectors. The energy can be derived either by integrating the longitudinal energy deposition profile in the atmosphere – a nearly model-independent technique – or by counting the number of particles at observer level. The latter method requires a detailed simulation of the particle cascade in order to calibrate the number of particles at ground against the primary energy.

The mass A of a cosmic-ray projectile can be inferred from the depth of the electromagnetic shower maximum, X_{max} , the depth of the maximum muon production, $X_{\mu,\text{max}}$, or the number of muons, N_{μ} , at ground [4]. Other mass-sensitive observables can be reduced to these three fundamental observables. They probe different aspects of the hadronic interactions in the cascade, whose evolution is dominated by soft QCD interactions. Complementary information is obtained from stochastic shower-to-shower fluctuations in a narrow energy interval, such as $\sigma(X_{\text{max}})$ and $\sigma(N_{\mu})$ [4]. These fluctuations are very sensitive to the first interaction of the primary particle, which is also true for $\langle X_{\text{max}} \rangle$, while $\langle N_{\mu} \rangle$ and $\langle X_{\mu,\text{max}} \rangle$ are sensitive to the entire evolution of the hadronic cascade. Therefore, one can probe QCD features of the first interaction at hundreds of TeV in the CM frame, and features of the entire chain down to the GeV scale. Figure 2, adapted from [8, 62], illustrates how air shower observables observed at a slant depth of 1000 g/cm^2 react to changes in hadronic interactions. For example, increasing the interaction cross section shifts X_{max} to higher altitudes and reduces its fluctuations. However, such a change has only a slight effect on the number of muons and their fluctuations. Note that the changes to the hadronic observables in Figure 2 are applied at the level of the final state particles produced by the generator, e.g. the multiplicity is increased by artificially multiplying the number of final state particles, etc. The internal parameters of the event generator remain unchanged. Table 4 summarizes how the air shower observables relate to QCD features and cosmic ray properties. Regarding the muon number, N_{μ} , additional information can be obtained from the lateral distribution function of muons at observer level. The characteristic width of this function is inversely proportional to the muon detection threshold [91, 92].

While the direction and energy of a cosmic ray can be determined in a model-independent manner, other observables are sensitive to the *a priori* unknown mean and variance of the logarithmic mass number $\ln A$. This additional uncertainty poses a challenge to the tuning of event generators,

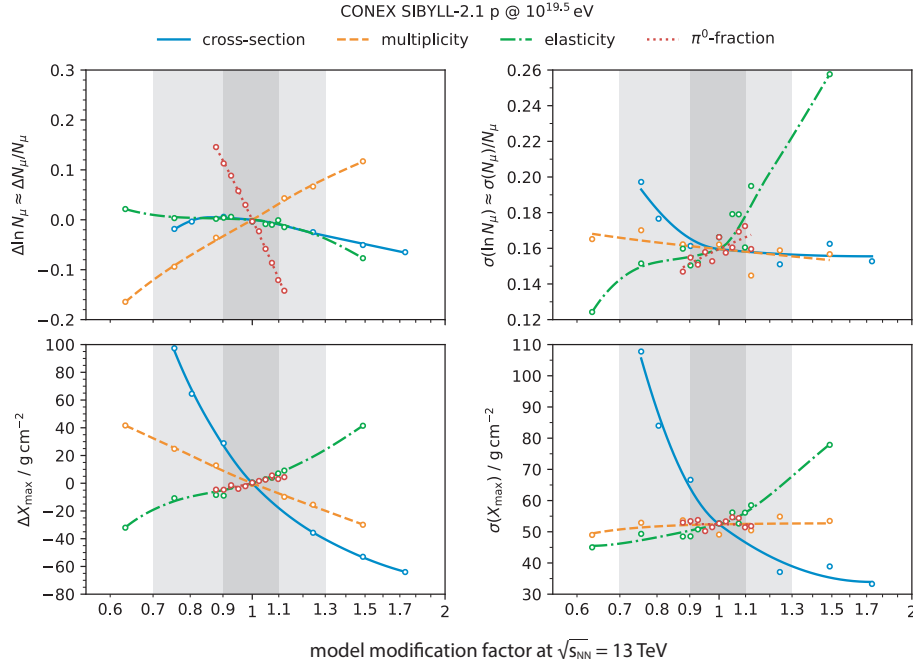


Figure 2: Effects of changing basic observables of hadronic interactions to different EAS observables for $10^{19.5}$ eV proton showers simulated with CONEX using SIBYLL 2.1 as the baseline model. The abscissa shows the modification factors applied to the cross section (green), multiplicity (orange), elasticity (green), and π^0 -fraction (red) at $\sqrt{s} = 13$ TeV. Effects to the means and standard deviations of the logarithm of the muon number N_μ and the depth of the shower maximum X_{\max} are shown in the top and bottom row, respectively. The shaded bands highlight a $\pm 10\%$ and $\pm 30\%$ modification, respectively. The data are based on [62] and the figure is adapted from [8].

but can be addressed in two ways. First, a clean sample of proton-induced air showers can be prepared within the energy window (1–3) EeV, where the primary mass is dominated by protons [93]. Selecting showers with a deep shower maximum from that sample further eliminates contamination from heavier primaries. This method has effectively been used to derive the p-Air cross section at $\sqrt{s} = 57$ TeV [93]. Second, one can take advantage of hybrid measurements to compare different observables that are sensitive to the same properties of the primary particle. For example, measuring the primary energy in a model-independent way from the integrated longitudinal shower profile and comparing the simulated muon number from such showers to observations revealed the muon deficit in air shower simulations [94, 95].

Finally, Neutrino telescopes, measuring the flux of atmospheric leptons and astrophysical neutrinos, provide additional observables for tuning. As discussed in Section 2, the atmospheric lepton fluxes result from the cascade generated by cosmic-ray interactions with the atmosphere. At energies up to approximately 1 PeV, the conventional flux resulting from the decay of pions and kaons in the atmosphere is dominant. At higher energies, the prompt flux takes over. It originates from the decay of short-lived hadrons containing charm and bottom quarks. These hadrons are generally produced in the first few interactions of the primary cosmic ray. In the case of the muon fluxes, other short-lived resonances also contribute. Although most charm mesons are produced at

Table 4: Observables in air shower experiments (described in the text) and their sensitivity to QCD features and properties of the cosmic rays [62]. Legend: σ_{inel} : inelastic (p, π)-air cross section, N_{mult} : average number of secondary hadrons, E_{max}/E : elasticity (energy fraction carried by most energetic product), E_{π^0}/E : energy fraction carried by neutral pions, $\sigma_{D,B}$: production cross section for D and B mesons, C_1 : mean free path to first collision, E : primary energy, $\langle \ln A \rangle$: mean logarithmic mass, $\sigma(\ln A)$: standard deviation of logarithmic mass.

Observable	Sensitivity to QCD feature					Sensitivity to cosmic ray feature			
	σ_{inel}	N_{mult}	$\frac{E_{\text{max}}}{E}$	$\frac{E_{\pi^0}}{E}$	$\sigma_{D,B}$	C_1	E	$\langle \ln A \rangle$	$\sigma(\ln A)$
$\int (dE/dx) dx$							✓		
$\langle X_{\text{max}} \rangle$	✓	✓	✓			✓	✓	✓	
$\sigma(X_{\text{max}})$	✓		✓			✓	✓	✓	✓
$\langle X_{\mu, \text{max}} \rangle$	✓	✓	✓			✓	✓	✓	
$\sigma(X_{\mu, \text{max}})$	✓		✓			✓	✓	✓	✓
$\langle N_{\mu} \rangle$		✓		✓			✓	✓	
$\sigma(N_{\mu})/N_{\mu}$			✓	✓		✓	✓	✓	✓
$\Phi_{(\nu, \mu), \text{conv}}$	✓	✓	✓	✓		✓	✓	✓	
$\Phi_{(\nu, \mu), \text{prompt}}$			✓		✓	✓	✓	✓	

mid-rapidity, the steeply falling cosmic-ray flux means that charm mesons produced at rapidities $\gtrsim 4.5$ contribute most to the prompt neutrino flux. Thus, the atmospheric lepton flux is sensitive to QCD features over a wide range of energies. At the level of a single neutrino interaction event, one cannot distinguish between the atmospheric and the extraterrestrial neutrino fluxes. However, the combined neutrino flux can still be used for tuning, as both sources contribute differently at different energies. Conversely, the atmospheric and extraterrestrial neutrino fluxes are expected to exhibit distinct features and shapes [96], and correlations with sources could be a powerful tool for distinguishing them. Thus, it is possible that each of these two fluxes could be used separately for tuning purposes.

In summary, a wealth of data from astroparticle experiments is available for tuning. The precision of modern air shower experiments rivals that of accelerator-based experiments and calls in question the accuracy of event generators tuned to accelerator measurements. To disentangle the complex dependencies between the microscopic properties of hadronic interactions (e.g. multiplicity or momentum distributions) and the macroscopic observables of extensive air showers (e.g. the X_{max} distribution or number of muons at the ground level), several observables should be used together in the tuning process. This process must also carefully consider the systematic uncertainties and correlations in the measurements. Hybrid experiments, such as the Pierre Auger Observatory [5] and IceCube, offer the greatest value for tuning, because they can measure several observables simultaneously. A detailed discussion of the most relevant astroparticle experiments and their recent measurements in the context of event generator tuning is presented in Appendix C.

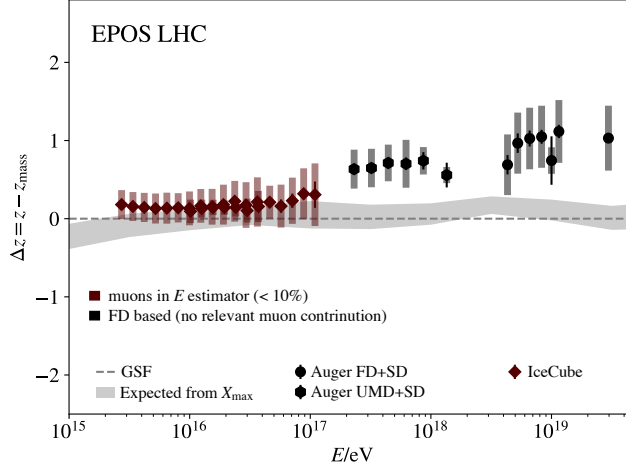


Figure 3: Muon content of air showers encoded in the values of Δz (see text) as a function of the shower energy E from different experiments. Only data with minimal (red-brown) or no (black) muon contribution to the energy estimator and with muon detection thresholds of $E_\mu \leq 1 \text{ GeV}/c$ are shown. The Δz values show the deviation of the measured muon content from the expectation based on the data-driven GSF model [97] and the event generator EPOS LHC. The gray band shows the expected value when the mass is inferred from Auger X_{max} measurements instead of the GSF model. The error bars show the statistical and systematic uncertainties, added in quadrature. Figure adapted from Ref. [98].

4.3 Clash of high-energy accelerator and astroparticle physics: the muon puzzle

A prominent example that illustrates the need for a coordinated effort by both the particle physics and the astroparticle physics communities is the so-called *muon puzzle* in air shower data [8]. Over the past decade, an increasing number of datasets have revealed a consistent systematic discrepancy between the number of muons observed in EAS and those predicted by standard interaction models. This discrepancy persists even when including data from the LHC in the tuning of the hadronic interaction models, which were previously tuned only from other HEP experimental data.

Apart from the cosmic ray energy E , the observed muon density at ground level depends on the atmospheric depth of the ground array, the lateral distance at which the muon density is measured, the zenith angle of the considered showers, and the effective energy cutoff introduced by the shielding of the detectors. Due to the diversity of the measurements the Working Group for Hadronic Interactions and Shower Physics (WHISP), consisting of representatives from most of the experiments, was formed. To facilitate the comparison of the observed vs. expected number of muons under very diverse experimental conditions, the group defined an abstract Δz -scale. These values are proportional to the relative difference between the observed number of muons in an experiment and the calculated expectation using an event generator and a model for the primary flux. The scale is defined such that the dependence on the details of the experimental conditions and the air shower simulation is minimal [98–101]. An overview of all the muon measurements is presented in Appendix C.10.

At first glance, a coherent, global picture does not emerge from 1 PeV to 10 EeV. However, two groups of experiments can be identified. Experiments that determine the shower energy largely

or almost independently of the muon number, such as IceCube and Auger, show a muon deficit in simulations that grows at a constant rate with increasing energy (see Figure 3). Conversely, no clear picture emerges from experiments without independent energy measurements (see Appendix C.10). This is presumably because the shower energy is reconstructed (at least in part) from the number of muons, thereby masking the deficit.

In addition to the scientific interest in the nature of hadronic multiparticle production at high energies, unfortunately, the muon puzzle introduces large systematic uncertainties in the analysis and interpretation of EAS data. This is especially problematic when training machine learning algorithms with simulations that do not fully align with the data.

4.4 Challenges in describing EAS data and approaches to address the muon puzzle

As noted above, it is difficult for current event generators to provide a consistent description of EAS data. This is not only because of the muon deficit; the muon production depth, $X_{\mu,\max}$, is also not reproduced by all event generators. EPOS LHC predicts an excessive depth in simulations, while QGSJET-II.04 is consistent [102]. Some possible causes of these model deficits will be discussed below.

Strangeness enhancement The influence of enhanced strangeness production on muon production in air showers has been studied using a core-corona model in high multiplicity events, where the core is responsible for the strangeness enhancement [63]. These studies were based on a modified version of EPOS LHC. Using the Ω/π ratio measured by ALICE as a function of hadron multiplicity as a reference and assuming that strangeness production for all collision systems depends only on the hadron multiplicity, the LHC results were extrapolated with the core-corona model to ultra-high energy air showers. It was found that this leads to an increase in the muon number of about 10% , which is not sufficient to resolve the observed muon deficit in air shower simulations.

Standard Model uncertainties The impact of Standard Model uncertainties on the predictions of the muon number N_μ and the muon production depth $X_{\mu,\max}$ has been studied in [103]. The EAS observables were computed with CONEX and the event generators QGSJET-II-04, EPOS LHC, SIBYLL 2.3, and a modified variant of QGSJET-III. Modifications to the latter were made within the experimental constraints of collider data. The influence of the following modifications was studied: a change in the pion energy distribution; an enhanced gluon content of the pion; a modified energy dependence of pion exchange; and a possible enhancement of (anti)nucleon and kaon production. It was found that none of these variations could increase N_μ by more than 10%, which is insufficient to align with the data from the Pierre Auger Observatory. Furthermore, these variations increase $X_{\mu,\max}$ which exacerbates the tension with the Pierre Auger Observatory observations.

Sibyll★ A similar study was performed with a modified version of SIBYLL 2.3d, called SIBYLL★ [104], with *ad hoc* modifications to the final state that ignore internal model consistency. Simulations were performed to study scenarios that increase the muon production in air showers. This includes increased baryon (and hyperon) production, increased ρ^0 production, increased K^\pm production, and a mixture of baryon and ρ^0 production. All scenarios were found to match the Auger data; however, the scenarios with increased ρ^0 do so without introducing sudden jumps in the production cross section as a function of the collision energy. However, the forward/high x_F production cross section of the ρ^0 is expected to decrease with increasing energy; in contrast, it remains constant or even increases in the modified scenarios that match Auger data.

Strangeball model The muon production in air showers can also be increased using a so-called strangeball model [105], an evolution of the fireball model described in [106]. The latter assumes that a quark-gluon plasma droplet (the fireball) forms in a fraction of the collisions. The fireball and the aforementioned core-corona models are similar, in that they increase strangeness production by switching to statistical fragmentation (the fireball). However, in the latter model, the core (fireball) and the corona (string fragmentation) contribute simultaneously. In contrast, the fireball in the strangeball model is the sole product of the collision once formed. The authors found that the strangeball model could not consistently describe the mean and variance of X_{max} in air showers due to the inelasticity enhancement associated with forming a plasma state. This problem does not arise in core-corona models, because the core component does not extend to very forward rapidities, which reduces its effect on inelasticity. The strangeball model solves this problem by increasing only the strangeness produced in Standard Model hadronic interactions relative to other flavors, without forming a quark-gluon plasma state. Strangeball parameters consistent with the muon production seen in Auger data have been found. However, constraints from measured shower-to-shower fluctuations of the muon number require strangeness enhancements already at the TeV scale. A comparison with relevant measurements from the LHCf and LHCb detectors does not directly exclude this scenario. Further measurements with the LHCb detector in Runs 3 and 4 at the LHC could constrain this model further.

This discussion shows that that our current modeling of non-perturbative QCD is incomplete and that – besides tuning model parameters – new physics may need to be implemented in event generators to resolve the current discrepancies between EAS data and simulations. In such attempts, it will be of key importance to verify the consistency of new or revised event generators in standardized processes also with HEP data. Global tuning would undoubtedly help to guide us toward appropriate extensions of the standard theory.

5 Tuning of event generators

Event generators use effective models with tens to hundreds of parameters that must be adjusted to experimental data, in a process called *tuning*. A *tune* refers to one given set of these parameters. Many event generators have switches that enable or disable physics processes or select alternative physics models, which are also stored in the tune. Depending on the enabled processes, a tune can be more conservative or more speculative.

Parameter tuning often targets multiple physics blocks, such as total and diffractive cross sections, multiple-parton interactions (MPIs), parton showers, fragmentation and hadronization, baryon and strangeness yields, nuclear collision settings, collective effects, and decay handling options. A focused tune addresses a restricted set of observables and uses a small number of parameters, $\mathcal{O}(10-20)$. An intermediate tune covers a broader set of observables and uses a larger number of parameters, $\mathcal{O}(30-50)$, typical of comprehensive collider fits. Some examples are discussed in Appendix D.

A prerequisite for tuning is providing experimental measurements in a machine-readable format. In the particle physics community, the High-Energy Physics Database (HEPData) [107] provides this. It is an open-access repository for sharing experimental particle physics data. A project with a similar goal in the astroparticle physics community is the Cosmic Ray Database (CRDB) [108]. Specific datasets from IceCube are available at [109]. The open data of KASCADE-Grande [110] and the Pierre Auger Observatory [111] go beyond this and provide not only high-level tabulated data, but also full raw data. Next, one must compare the output of an event generator to the measurement to compute a residual. This step is not trivial due to the different internal implementations chosen

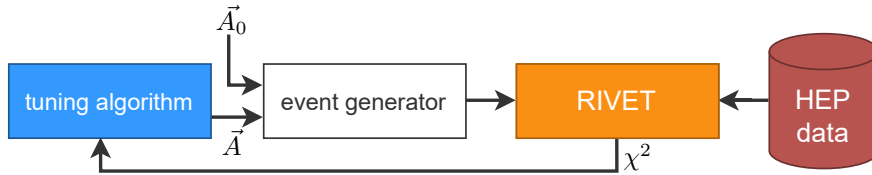


Figure 4: A schematic of classic tuning. The classic tuning loop proceeds as follows: 1) A new vector of parameter values \vec{A}_0 is used to configure the event generator. 2) The event generator is used to simulate all collision systems fitting the required initial conditions of the RIVET plugins. 3) The RIVET plugins process the simulated raw event samples to produce binned distributions comparable to experimental HEP data. 4) A chi-square value is computed from the differences between simulated and experimental distributions for all RIVET plugins and fed back into the tuning algorithm. 5) The tuning algorithm computes a new vector of parameter values based on this input. Generalization derived from [115].

by each event generator and the diversity of measurements.

Event generators suitable for tuning provide a documented interface that allows one to change parameters without recompiling the code. PYTHIA 8 is exemplary in this regard. Most event generators used in the astroparticle physics, as shown in Table 2, are not designed to allow for tuning by a generic user. Instead, the authors manually tune these generators by changing parameters until the generator predictions match the experimental results in a set of control plots. While the reference data that these models are tuned to are documented in the respective publications (see e.g. Ref. [20] or Ref. [112]), the internal tuning interface is not documented. Moreover, the authors determine the relative weights of different data sets as needed.

Obviously, performing automatic tuning by a multi-dimensional fit makes the results more reproducible and eases the incorporation of new data.

5.1 Automatic tuning

In automatic tuning, a suitable distance measure, such as a least-squares-type cost function, is used to quantify the agreement of the event generator output with a set of measurements, taking into account experimental uncertainties. The best set of parameters is found either by minimizing the least-squares-type cost function via gradient descent, or in a Bayesian framework by computing the posterior probability density of the parameters from the likelihood function and priors. Further details on these methods are presented in Appendix D.

Before tuning, the raw output of an event generator must be converted into a prediction that can be compared to the measurement. In particle physics this step is performed by the RIVET [113] software which has been specifically designed to support the development, validation and tuning of event generators. The experimental data are entered via so-called RIVET plugins which are programs that emulate the published experimental analysis but starting from the generator output, instead of the original experimental data. RIVET stores measurements in a human readable format, usually imported from HEPData. Some event generators, such as PYTHIA 8, can feed the raw events directly into RIVET, while others use interface programs [45, 46, 114].

The classic tuning loop used in particle physics is illustrated in Figure 4, where a *tuning algorithm* iteratively optimizes the event generator, such as those listed in Table 2, to describe the HEP data. Specifically, RIVET handles the processing of both experimental data and simulated

events to produce comparable distributions, while the tuning algorithm performs the chi-square minimization to determine optimal parameters. Additional details regarding tuning algorithms can be found in Appendix D. Note that the figure is conceptual only; in practice, tuning introduces a few complications to this basic model. First, weights must be assigned to each observable when calculating the least-squares-type cost function, because event generators are incomplete models of nature and usually do not perfectly match measurements of their implemented physics processes. Some observables are known much more precisely than others, and possibly more precisely than the corresponding theory. Without weights, a fit can be dragged into an implausible parameter space. Introducing weights or imposing additional common model uncertainties is an *ad hoc* way of balancing experimental versus theoretical error to avoid this problem. Second, producing predictions with the event generator is computationally expensive. To reduce this cost, a *surrogate model*, typically a multidimensional polynomial in the simplest case, is constructed from the output of the actual event generator and used instead of the generator to evaluate the chi-square. Depending on the tuning algorithm, an analytical surrogate model may be needed to compute gradients. Appendix D.1 discusses tuning procedures that avoid surrogate models altogether, highlighting how such approaches could streamline the process by bypassing the need for efficient parameter-space sampling.

Examples of automatically tuned models are SIBYLL and PYTHIA. While PYTHIA has many tunes, often several per LHC experiment, for example the Monash tune [116], for SIBYLL automatic tuning was used to determine the best parameters [20].

Using an interface like RIVET simplifies tuning, but expert knowledge is still needed to select the right measurements that are sensitive to a given range of tuning parameters, to avoid measurements that the event generator was not designed to describe, and to choose between measurements that contradict each other. To facilitate this process, the MCPlots [117, 118] website has been created. It is based on RIVET and provides comparisons between the established particle physics event generators in many code bases and tunes whose results can be compared to a large set of measurements (RIVET plugins). The website assembles plots of pre-generated results produced on the computers of citizen scientists who contribute to the project via the LHC@home initiative [119]. In addition to the visual comparison of generator predictions with measurements, the website also computes a chi-square test statistic for the goodness-of-fit between the experimental data and an event generator version or tune, allowing non-generator experts to easily select the appropriate tune for their task.

5.2 Early tuning efforts for astroparticle physics

An early version of the global tuning using HEP and astroparticle data we envision here was carried out for the EPOS generator [12]. In that work, relying on the expert knowledge from the EPOS and CONEX authors, parameters relating to diffraction dissociation were tuned to selected measurements from CMS/CASTOR and the X_{max} data from the Pierre Auger Observatory. One of the major shortcomings of all current HEP tunes of PYTHIA 8 is the difficult description of particle production at very forward rapidities, most notably the failure to describe the spectra of neutrons and neutral pions measured at the LHCf experiment. Specifically, the π^0 spectra predicted by PYTHIA 8 are too hard while the neutron spectra are too soft [83–85]. It is worth noting that the event generators used to simulate air showers, such as EPOS LHC, QGSJET, and SIBYLL also do not perform well. This is very important for simulating air showers, as well as for physics in the forward direction such as the FASER [82] or SND@LHC [120] experiments.

In the context of FASER/SND, a dedicated “forward physics” tune of PYTHIA 8 was developed [121]. Starting with various configurations and tunes of PYTHIA 8 [37, 116], a satisfactory description of the LHCf data was achieved by adjusting the hadronization model and the parameters of the so-called beam remnants using RIVET and the APPRENTICE [122] toolkit. It is expected

that the “forward physics” tune will improve air shower simulations, though this remains to be confirmed through further study.

Building on the successful “forward physics” tune of PYTHIA 8, efforts are underway to produce a first “air shower” tune from HEP data. Notable ongoing examples include the PYTHIA 8 “Wuppertal” tune discussed in [115], and a combined analysis of LHC, LEP, and fixed-target data, presented in [123]. The goal is to more accurately describe the processes important for air shower simulations, such as forward hadron production measured e.g. by LHCb and NA61, as well as the total and inelastic cross sections in different collision systems, spanning several orders of magnitude in energy. For the full set of measurements suggested for the tuning, see Table 6 in Appendix D. The tune parameters will be fixed step-by-step for each collision system, beginning with e^+e^- to fix fragmentation and hadronization parameters, progressing to $p+p$, $\pi^\pm+p$ and $K^\pm+p$ for parameters associated with hadronic structure, moving to $p+A$ and $\pi^\pm+A$, and finally with $A+A$ for nucleon structure and collective effects. This is partially done for manually tuned models, see Table 2. Ideally, the nucleus A should be in the CNO group, since nitrogen is the most abundant nucleus in the atmosphere, and intermediate-mass nuclei are abundant in the flux of ultra-high-energy cosmic rays near the spectral cutoff. To achieve a more accurate model of an air shower development, we tune to $p+A$, $\pi^\pm+A$, and $A+A$ to constrain the first interaction, and in turn, to $\pi^\pm+p$, $K^\pm+p$, and $p+p$ for secondary interactions. Therefore, the recent proton-oxygen runs at the LHC will provide important validation data set and a future reference point at the TeV scale for this and subsequent tunings. Parameters related to beam remnants and hadronization are highly relevant for the tuning, as is the dependence of the parameters on the CM energy of the collision system. This is because the CM energy must be extrapolated to higher projectile energies. It will also be important to arrive at a tune that describes the mid- and forward-rapidity data without major inconsistencies.

An essential first step toward global tuning to particle and astroparticle data is demonstrating the feasibility of tuning to air shower data. To this end, we performed a study based on the event generator PYTHIA 8 and the air shower simulation code CORSIKA 8 [124] by generating mock air shower data using the default settings in PYTHIA 8. Using Bayesian tuning [125, 126] these default values were successfully recovered by tuning PYTHIA to X_{\max} and N_μ in the mock data. This study shows that tuning to air shower observables is possible in principle and that the Bayesian tuning approach is a promising method for global tuning to particle and astroparticle data. Further details are provided in Appendix D. The experiment also highlights the need for fast air shower simulations. The next step is to perform an initial tuning to the data.

6 Towards global tuning

In this section, we outline a vision for simultaneous, automatic tuning of MC generators with data from particle and astroparticle physics. While HEP experiments probe specific regions of phase space, air shower measurements capture the integrated outcome of all interactions in the shower development. This yields a need to tune to a broad set of measurements across collision systems and energies for consistency, and requires a framework to be built in collaboration with the developers of the event generators and both experimental communities. At the same time the air shower measurements promise to provide new constraints for models across a wide range of energies, projectile-target combinations and phase space regions. Many of the necessary ingredients are already available or under development. Encouraging first steps towards a global tune were listed in Section 5.

The basic training loop as envisioned for a global tuning is illustrated in Figure 5. The particle physics tuning loop as discussed in Figure 4 is complemented by a second iterative loop where the

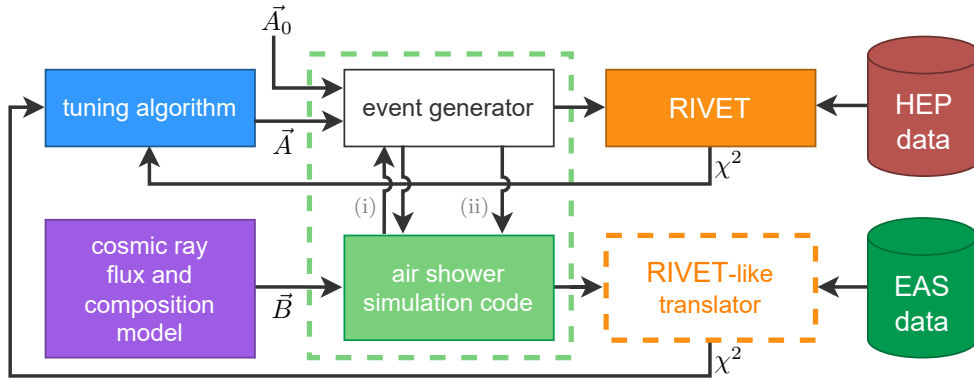


Figure 5: A schematic of global tuning. The global tuning loop proceeds as follows: 1) An initial vector of parameter values \vec{A}_0 is used to configure the event generator. 2a) The event generator is used to simulate all collision systems fitting the required initial conditions of the RIVET plugins. 2b) The event generator either (i) runs inside the air shower simulation code CORSIKA to simulate air showers, or (ii) simulates all collision systems required to build interaction tables for CONEX or MCEQ, which are then used to simulate air showers. 3) The energy spectrum and mass composition of the primary cosmic rays follow a cosmic ray flux and composition model (parameters \vec{B}) (This may be a monocular beam following a simple power-law distribution used as reference). 4a) The RIVET plugins compute predictions comparable to their respective HEP data from the raw HEP event sample. 4b) RIVET-like translators compute predictions comparable to their respective EAS data based on the raw air shower sample. 5) A chi-square value is computed from all RIVET plugins and the translator plugins and fed back into the tuning algorithm. 6) The tuning algorithm computes a new vector of parameter values based on these inputs. Note that the RIVET-like translator still needs to be developed.

input from the particle physics event generator and the cosmic ray flux model are combined in the air shower simulation code to derive the prediction for the observables that is to be compared with the air shower data. The cosmic ray flux model parameters (\vec{B}) are fixed for this vision of global tuning; see Subsection 6.2 for details. The task of the RIVET-like translator is to choose the appropriate configuration for the air shower simulation for each observable. This includes selecting the method of calculation, which can be a full MC simulation (CORSIKA) or solving cascade equations (CONEX, MCEQ).

6.1 A RIVET-like translator for astroparticle data

Global tuning is an automatic process that adjusts multiple parameters in the event generator to multiple data sets simultaneously. When tuning only to HEP data, it is possible to select data sets that correspond to only a small subset of parameters in the event generator and perform a manual tuning. This approach is not feasible when including EAS data, which are sensitive to many correlated parameters. In order to enable global tuning that incorporates EAS measurements, a translator software analogous to RIVET discussed in Subsection 5.1, or an extension of the RIVET software is required. Clearly, this effort should build on the existing infrastructure developed within the HEP community.

A translator for EAS data can function like a RIVET plugin, but with simulated air showers as the input. For each analysis, the relevant energy range of air showers, the atmospheric profile, the zenith angle range, and the observation level are to be defined. In addition, the most suitable type of calculation (cascade equation, hybrid, full MC) for each observable needs to be selected. Air showers are then simulated according to these specifications. The translator applies any selections that bias the air shower sample. For example, it applies cuts on the depth of shower maximum X_{max} that correspond to the field of view of the fluorescence telescopes.

The existing RIVET software can be extended to serve as the new translator, but this is not a simple task. Several arguments support this approach: The internal RIVET file format is flexible enough to describe EAS data. Tuning software can already interface with RIVET plugins and integrating EAS plugins would be relatively easy. Additionally, the MCPlots website could be used to show comparisons with EAS data. However, the main problem is that RIVET is designed for input in the form of a particle graph, which cannot represent air showers. An air shower consists of longitudinal density profiles for electrons, photons, and muons, and a list of millions of particles that reach the observation level. The HepMC format is not designed to represent density profiles or to store millions of particles. Handling this input would likely require significant changes to RIVET, which would need to be discussed with the RIVET developers to evaluate their feasibility.

The alternative is to construct a new RIVET-like translator from scratch. With this approach, the tuning and plotting software would need to be adapted to interface with the new translator. One advantage would be the decoupling from the RIVET release cycle and the ability to write the translator in Python instead of C++, which would allow us to benefit from a development cycle and easy prototyping. In conclusion, whether by extending the existing RIVET software or developing a new translator from scratch, enabling global tuning that incorporates EAS data requires significant technical advancements and close collaboration within the scientific communities to ensure compatibility, maintainability, and effective utilization of this new capability.

6.2 Cosmic ray flux and composition model

An optional yet natural extension of global tuning is including cosmic ray flux model parameters, which provides additional benefits. The distribution of air shower observables depend on the cosmic ray flux and its composition, which are *a priori* unknown and must be inferred from these observables. The latest generation of hybrid observatories measures the all-particle cosmic ray flux in a nearly model-independent way, which is now fairly well understood [97]. The remaining uncertainty in the all-particle flux is primarily due to uncertainties in the energy scale, which has little effect on most air shower observables of interest. Exceptions are the atmospheric muon and neutrino fluxes.

It appears that this introduces a circular dependency: we want to use air shower observables to tune event generators, but the predicted observables depend on the composition inferred by comparing event generator predictions with air shower observables. However, this is not actually a circular dependency because there are many observables sensitive to different aspects of the event generators. The composition is typically inferred from the depth of the shower maximum, X_{max} , and predictions based on this value are then compared with other observables. This approach is successful because the theoretical uncertainty in predicting X_{max} is smaller than that for other variables.

Another option is to incorporate a cosmic ray composition model into the tuning process. In this case, the tuning algorithm would also adjust the parameters of the flux model. This *universal tuning* would infer the composition from *all* air shower observables, not just from X_{max} . However, this approach can only work if the tuned event generator can consistently describe all air shower observables. Currently, this is not the case, so naive universal tuning would lead to incorrect results.

However, this approach could be used if X_{max} measurements were given more weight in the least-squares-type cost function used for the tuning.

In addition to conceptual consistency, universal tuning provides an additional benefit: the cosmic ray composition model obtained in this way would have a propagated uncertainty band from all air shower and HEP observables used in the tuning. Currently, the uncertainty is estimated from the scatter of results obtained using different event generators. However, this uncertainty estimate may over- or underestimate the true uncertainty.

7 Summary and next steps

In this article, we demonstrated that a global tuning of event generators with data from both high-energy accelerators (HEP) and extensive air showers (EAS) could help solve some of the puzzles we currently face when interpreting astrophysical measurements. As an example, we discussed ways to increase the muon production in air showers in order to better describe observations. Global tuning will either resolve these tensions or lead us to extend the standard theory. Similarly, global tuning may also reveal additional tensions between experimental results that have not been previously brought into comparison, or challenge the systematic uncertainties quoted by some experiments. Either way, it promises valuable new insight into air shower data.

Global tuning requires the use of automatic tuning software, which extends the classic tuning loop by incorporating a model of the cosmic ray fluxes and air shower simulations. To facilitate the use of EAS data, a translator similar to RIVET in HEP data needs to be developed. This report can serve as a starting point for that development.

Another requirement for global tuning is an event generator with a documented tuning interface that includes all the necessary physical processes to simulate hadron-nucleus and nucleus-nucleus collisions up to hundreds of TeV. PYTHIA 8/Angantyr currently best meets these requirements and is therefore the first target for tuning, but other event generators should follow. However, PYTHIA remains poorly integrated with several air shower simulation codes, including CONEX and MCEq. In contrast, EPOS, SIBYLL, and QGSJET are well integrated but they often suffer from insufficient documentation, which limits their usability for user-friendly tuning. Closing these gaps will be a key focus of future development to improve usability and compatibility across simulation frameworks.

Established tuning methods are ready to be used for global tuning, as demonstrated in toy studies. One concern is the significant additional computational cost of running air shower simulations. This cost can be significantly reduced by using cascade equation solvers, such as CONEX and MCEQ, instead of full CORSIKA simulations. An interface is being developed between MCEq and PYTHIA 8/Angantyr to enable fast atmospheric lepton flux calculations and to broaden compatibility with air shower simulation codes. Future methods based on stochastic gradient descent may perform better for tuning of many parameters at once, but such methods have yet to be developed. In the near future, air shower simulations will also benefit from ongoing efforts to improve the description of forward hadron production in event generators, as well as from data collected using oxygen beams in the LHC.

In summary, global tuning is within reach. Prototypes and smaller-scale studies have demonstrated the effectiveness of the tuning process in addressing the primary challenges associated with simulating EAS and HEP data. With the combined efforts of the community, we can turn global tuning into a standard tool that anyone can use. Global tuning can improve tuning methods themselves, benefiting the astroparticle physics and HEP community as a whole. Many interesting results can be expected in the near and mid-term future.

Acknowledgments

This paper is a comprehensive overview of work that has been advanced with a collaboration of experts during the workshop *Tuning of hadronic interaction models*³ at the Bergische Universität Wuppertal in January 2024. The international workshop was organized as part of the Collaborative Research Center SFB1491, *Cosmic Interacting Matters — From Source to Signal*. We acknowledge the support of the workshop and the related research by many of the workshop participants and authors of this paper by SFB1491, funded by the Deutsche Forschungsgemeinschaft (DFG, German Research Foundation) under project number 445052434.

J. Albrecht acknowledges additional support from the Heisenberg Programme of the Deutsche Forschungsgemeinschaft (DFG, German Research Foundation) under project number AL 1639/5-1, and from the Bundesministerium für Bildung und Forschung (BMBF, Federal Ministry of Education and Research) under grant number 05H21PECL1 within ErUM-FSP T04. H. Dembinski acknowledges funding from the DFG under project number 449728698. C. Gaudu acknowledges funding from the DFG via the Collaborative Research Center SFB1491: Cosmic Interacting Matters – from Source to Signal (F4) – project no. 445052434. Karl-Heinz Kampert acknowledges additional support from the BMBF under grant numbers 05A20PX1 and 05A23PX1 and from DFG under project no. 445990517. G. Sigl acknowledges support from the DFG under Germany’s Excellence Strategy — EXC 2121 *Quantum Universe* — 390833306, and from the BMBF under grants 05A20GU2 and 05A23GU3. N. Korneeva acknowledges support from the Monash Warwick Alliance as part of the Monash Warwick Alliance in Particle Physics, and from the LHC Physics Centre at CERN (LPCC). S. Ostapchenko acknowledges support from the DFG under project numbers 465275045 and 550225003. F. Riehn has received funding from the European Union’s Horizon 2020 research and innovation programme under the Marie Skłodowska-Curie grant agreement number 101065027. T. Sjöstrand has been supported by the Swedish Research Council under contract number 2016-05996. L. Cazon thanks Ministerio de Ciencia e Innovacion / Agencia Estatal de Investigación (PID2022-140510NB-I00 and RYC2019-027017-I), Xunta de Galicia (CIGUS Network of Research Centers, Consolidación 2021GRCGI-2033, ED431C-2021/22 and ED431F-2022/15), and the European Union (ERDF). J. Blazek, J. Ebr and J. Vícha have received funding from the following grants: CAS LQ100102401, GACR 21-02226M and MEYS CZ.02.01.01/00/22_008/0004632. P. Paakkinen acknowledges the support from the the Research Council of Finland (projects 330448 and 331545) and as a part of the Center of Excellence in Quark Matter of the Research Council of Finland (project 364194).

A Details on event generators

Further details on the event generators are presented in Table 5 and discussed below. We emphasize the distinct theoretical frameworks and concepts underlying each model. Notably, EPOS, with a strong focus on heavy-ion collisions, and PYTHIA were primarily developed for high-energy particle physics. The EPOS LHC models are an adaptation of the EPOS model family specifically for extensive air shower simulations. In contrast, the SIBYLL and QGSJET models were designed from the outset for extensive air shower modeling.

³<https://indico.uni-wuppertal.de/event/284/>

Table 5: Detailed comparison of five event generators, as an extension of Table 2. Acronyms are defined in the Section 2.

	EPOS4 [16]	EPOS LHC-R [17, 18]	QGSJET-III [19]	SIBYLL 2.3d [20]	PYTHIA 8 [21, 22]
Primary domains	HIC, HEP	EAS, HIC	EAS	EAS	HEP, (HIC via Angantyr)
Theoretical basis	parton-based GRT, pQCD, energy sharing, saturation	parton-based GRT, pQCD, energy sharing	GRT, pQCD (DGLAP+HT)	GRT, pQCD (minijet)	MPI, pQCD, ISR, FSR
Nuclear collisions	idem	idem	idem	extended superposition	Glauber via Angantyr
Pomeron	semi-hard, dynamical saturation	semi-hard	semi-hard	soft+hard	soft+hard
Parton distributions	generated	custom (GRV for valence)	Pomeron PDFs + DGLAP + HT	GRV	various
Diffraction dissociation (low mass)	diffractive Pomeron	diffractive Pomeron	Good-Walker (3-channel eikonal)	Good-Walker (2-channel eikonal)	longitudinal strings
Diffraction dissociation (high mass)	Pomeron exchange	Pomeron exchange	cut-enhanced graphs	Pomeron exchange	MPI
String fragmentation	area law	area law	early Lund type	Lund	Lund
Forward-central correlation	strong	strong	strong	weak	strong
Charm production	pQCD	parameterised + intrinsic	None	parameterised + intrinsic	pQCD
Collective effects	core-corona, hydrodynamical flow, hadronic rescattering	core-corona, parameterised flow, hadronic rescattering	None	None	colour reconnection, rope fragm., string shoving, hadronic rescattering
Programming language	C/C++, Fortran90, Fortran	Fortran	Fortran	Fortran	C++
Tuning collision systems	e^+e^- , pp, pA	e^+e^- , pp, pA	pp, pA	pp, pA	e^+e^- , pp
Tuning parameters accessibility	model authors	model authors	model authors	model authors	any users
Tuning-related interface	HepMC, RIVET	HepMC	HepMC	HepMC	HepMC, RIVET
Event generator frontend	None	CRMC, Chromo	CRMC, Chromo	CRMC, Chromo	Chromo
Transport code interface	None	CORSIKA 7/8, CONEX	CORSIKA 7/8, CONEX	CORSIKA 7/8, CONEX, MCEq	CORSIKA 8

A.1 EPOS4

The theoretical basis of EPOS4⁴ [16, 127–129] is the so-called parton-based Gribov-Regge field theory (GRFT) [130] with energy conservation at the amplitude level and a bare amplitude based on the parton model. The main new development in EPOS4 is the ability to accommodate simultaneously rigorous parallel scattering, energy-momentum sharing, perturbative QCD, and the validity of the Abramovsky-Gribov-Kancheli (AGK) theorem [131].

The AGK theorem is central for describing multiparticle production in providing a framework for the calculation of the relative contributions of various parallel parton interaction processes. The theorem shows that interference terms between different diagrams cancel under certain conditions, leading to specific proportionalities between elastic scattering, single diffractive dissociation, and multiparticle production. This simplifies the computation of inelastic cross-sections and connects unitarity constraints with experimentally measurable quantities.

The combination of energy-momentum sharing in parallel scattering, perturbative QCD, and ensuring the validity of the AGK theorem in EPOS4 leads to binary scaling in $A + A$ scattering and factorization in p+p for hard processes, by introducing saturation in a way that is compatible with recent “low- x -physics” considerations. Energy-momentum sharing is mandatory for a consistent picture and offers a connection between factorization and saturation.

The validity of AGK allows one to perform the same analyses as those based on the QCD factorization theorem to study inclusive cross sections and much more. As mentioned in the introduction, many important observables go beyond inclusive cross sections and require access to complete events. The unique feature of EPOS4 is that it starts from a parallel multiple scattering scenario while ensuring that it breaks down to a description using PDFs for inclusive cross sections. Other models begin with inclusive cross sections and then introduce multiple scattering via the eikonal formula. This strategy is also relevant for nuclear collisions, where one starts with unordered parallel scatterings (a unique feature). Performing nuclear scattering in EPOS4 is a natural extension of the p+p approach.

A number of pre-hadrons are obtained from the initial stage of parallel instantaneous partonic scatterings. In the core-corona approach, the pre-hadrons are separated into “core” and “corona” pre-hadrons, depending on their energy loss when traversing the “matter” composed of all the others. Corona pre-hadrons (per definition) can escape and become final hadrons, whereas core pre-hadrons lose all their energy and constitute what we call “core”, which acts as an initial condition for the hydrodynamical evolution of a quark gluon plasma.

The evolution of the core ends when the energy density falls below a critical value, resulting in the formation of hadrons. EPOS4 uses a new procedure for energy-momentum flow through the “freeze-out hypersurface”, which is defined by the critical energy density value. This procedure allows one to define an effective invariant mass. This mass then decays into hadrons according to microcanonical phase space, and the hadrons are Lorentz boosted according to the flow velocities computed at the hypersurface. New efficient methods were developed for the microcanonical procedure to make this feasible. Energy-momentum and flavors are conserved in the full scheme for all hadrons from the core and corona.

EPOS4 is written partly in Fortran and partly in C++. It supports HepMC output and additionally provides a direct RIVET interface [132]. EPOS4 must be rebuilt after any change to its tuning parameters for the updates to take effect.

⁴Available at <https://klaus.pages.in2p3.fr/epos4/>

A.2 EPOS LHC-R

EPOS LHC-R⁵ [17, 18] is an updated and re-tuned version of EPOS LHC[65]. As EPOS4, it is based on the parton-based GRFT with energy conservation at amplitude level, but without the new saturation treatment. It uses a custom model for the parton distributions, and the valence quarks are based on the Glück-Reya-Vogt (GRV) parameterization [133]. It also uses the core-corona approach. The calculation of the hadronization in high-energy/density environments, such as high-multiplicity events or heavy-ion collisions, is implemented in a simplified manner compared to EPOS4. Rather than running a full hydrodynamic evolution of the core, collective flow is calculated from a parameterization matched to the full simulation. These simplifications speed up event simulation, which is an important feature for the computationally expensive EAS simulations, which are dominated by the computation time consumed by the hadronic event generator.

EPOS LHC-R is tuned to newer and more detailed data sets than EPOS LHC, which was released in 2012, when only early LHC data was available. This results in a lower extrapolated cross section and better pseudorapidity distributions. Some missing physics phenomena have been introduced, such as color transparency for a better description of multiplicity fluctuations in nuclear interactions, and a real pion exchange process for very forward neutron production, as measured by the LHCf experiment. Particular attention is given to the details of the hadronization chain, especially to the production of ρ mesons in string fragmentation and to how the energy is shared between the core and corona contributions. EPOS LHC-R is intended as a transition between EPOS LHC and EPOS4, which includes newer features such as saturation effects and is much more advanced.

Both versions of EPOS LHC are written in Fortran. EPOS LHC-R provides a HepMC output and can be used with RIVET through its CRMC interface. Changes to tuning parameters in EPOS LHC-R require rebuilding the entire model before they take effect.

A.3 QGSJET-III

QGSJET-III⁶ [19, 112] is a recent update of QGSJET-II-04 [134, 135], from which it inherits its principal feature: a microscopic treatment of nonlinear interaction effects, based on all-order resummation of the underlying Pomeron-Pomeron interaction diagrams. The evolution of parton densities is calculated according to the DGLAP equations [136–138]. The new theoretical mechanism implemented in QGSJET-III is the treatment of higher twist (HT) corrections to hard parton scattering processes, based on a phenomenological extrapolation of the corresponding approach of Qiu and Vitev [139, 140], regarding deep inelastic and proton scattering on heavy nuclei, towards collisions of hadrons with protons and light nuclei. Although HERA data on deep inelastic electron–proton scattering strongly constrain the magnitude of such HT corrections, their impact on the predicted cross sections and particle production yields in p+p and hadron-air collisions is rather moderate. Nevertheless, the mechanism effectively controls the increase of inclusive cross sections for (mini)jet production in the limit of small jet transverse momenta [112].

Besides that, an important technical improvement implemented in QGSJET-III involves the treatment of the pion exchange process in hadron–proton and hadron–nucleus (nucleus–nucleus) collisions [19]. This mechanism significantly affects predictions of the muon content of extensive air showers (EAS) initiated by primary cosmic rays [135]. The process is described in a theoretically more consistent way here than in QGSJET-II-04, which is restricted to pion–proton and pion–nucleus collisions. Furthermore, data on forward neutron production from the NA49 [141] and LHCf [142]

⁵Available in Chromo [46] and CRMC [45].

⁶Available in Chromo [46] and CRMC [45]. Code is available upon request.

experiments have been used to verify the validity of the approach, regarding the energy dependence of the process, over six decades in energy.

When applying the QGSJET-III model to EAS simulations, rather small differences are obtained with respect to QGSJET-II-04 for basic EAS characteristics, such as the shower maximum depth, X_{\max} , and the muon number, N_{μ} , at ground level [19]. This suggests that relevant aspects of hadronic interaction physics are sufficiently constrained by existing accelerator data. A recent study further corroborates this conclusion by demonstrating that the predicted EAS muon content cannot increase by more than 10% while remaining within the standard physics picture (here excluding core-corona and similar approaches), without contradicting relevant accelerator data [103].

The QGSJET models are also written in Fortran. QGSJET-III includes a HepMC capability and can be run through RIVET via the CRMC interface. To apply changes to the tuning parameters in QGSJET-III, the code must be recompiled.

A.4 SIBYLL

SIBYLL⁷[20, 144, 145] is designed to describe the general features of hadronic multi-particle production, like the leading-particle effect, the formation of high- p_{\perp} jets predicted in QCD, the production of diffractively excited states of the projectile and target, and approximate scaling of leading-particle distributions with interaction energy. The focus is on the most relevant physics aspects for the development of extensive air showers, such as energy flow and particle production in the forward phase space region. The model is kept as simple as possible, while implementing important microscopic physics concepts and the general principles of scattering theory and unitarity to allow for extrapolation to energies and phase space regions beyond the reach of colliders.

The interaction model in SIBYLL is based on the two-component dual parton model with soft and hard minijets [146]. Nuclear collisions are treated with an extended superposition model [31]. The model also includes low- and high-mass diffraction, as well as a model for the excitation of beam remnants [147]. Hard scattering is distinguished from soft scattering by an energy-dependent cut-off, $p_{\perp 0}$, in transverse momentum. The cross section for hard scattering is calculated to leading order (LO) in QCD at the scale $p_{\perp 0}$. For soft scattering, a parameterization based on the Regge field theory [148] is used. The energy evolution of parton densities and saturation is effectively included by increasing the value of $p_{\perp 0}$ with energy. The QCD cross section includes contributions from quarks of all flavors and gluons. In the subsequent fragmentation, based on the Lund model [149, 150], only hadrons containing (u, d, s) and c quarks are produced.

The above description applies to all versions 2.Xy of the SIBYLL model. Differences between the sub-versions are listed in the appendix of Ref. [20]. SIBYLL is written in Fortran. SIBYLL 2.3d supports HepMC output and can be analyzed with RIVET via the CRMC interface. Updates to tuning parameters in SIBYLL 2.3d also require rebuilding the model before running simulations.

A.5 PYTHIA 8

PYTHIA 8⁸ [21] is a general-purpose event generator. At the LHC, it is primarily used to simulate soft and hard processes in the central rapidity range of p+p collisions. An MPI (multiparton interaction) is the basic building block of an event. It involves a perturbative $2 \rightarrow 2$ QCD process, where the $p_{\perp 0}$ parameter is introduced to dampen the low- p_{\perp} divergence. A varying impact parameter, with a non-zero Poissonian number of MPIs at each, builds up the MPI multiplicity spectrum. This is

⁷Available in Chromo [46] and CRMC [45], CORSIKA [54, 124, 143], and all air shower codes. Code and source documentation are available upon request.

⁸Available at <https://pythia.org/>, a detailed (HTML) manual is distributed with the code.

similar to, but not equivalent to traditional Gribov–Regge. The p_{\perp} -ordered initial- and final-state showers are added to each MPI.

The Lund string fragmentation model is used to hadronize events. Naively, each MPI would have strings stretching out to the beam remnants. However, color reconnection is applied to reduce the total string length, both to the beam remnant and in the central region itself. Diffractive events are handled as if a Pomeron acts like a glueball [151].

In recent years, PYTHIA 8 has been extended to enable its use in EAS simulation [22]. PDFs were introduced for over 20 different hadron species. Total and partial cross sections were introduced for corresponding hadron–nucleon collisions. These were smoothly matched to the low-energy hadronic rescattering framework [152]. Thus, PYTHIA can be used from nearly threshold energies up to and beyond center-of-mass energies of 100 TeV, aside from increasing problems with numerical precision. A simple kludge was introduced to handle nuclear targets, and was tuned to approximately reproduce the ANGANTYR (see below) results at collider energies. As a nonstandard feature not fully available in the public version, rope hadronization [38] and shoving [39] can be used to enhance the fraction of strange baryons and to generate asymmetric flow, respectively.

ANGANTYR [32] is a PYTHIA 8 module that extends its functionality from $p+p$ to $p+A$ and $A+A$. It is inspired by the Fritiof model and pays special attention to fluctuations in the nucleon wave function. The Good–Walker formalism [29] is used to obtain the relevant cross sections. Glauber modeling is used to determine which nucleons collide. Then, all non-diffractive sub-collisions are considered in order of increasing impact parameter. Overall, a reasonable description of multiplicity and pseudorapidity distributions is obtained. ANGANTYR should be able to offer a better alternative to the current kludge for cosmic ray evolution and has been investigated in [153, 154].

PYTHIA 8 is written in C++. It natively supports HepMC output and integrates seamlessly with Rivet. Angantyr inherits the same interface and full Rivet compatibility. In PYTHIA 8/Angantyr, tuning parameters can be modified at runtime through the configuration without recompiling the code.

A.6 UrQMD

The UrQMD⁹ [23, 155] (Ultra-relativistic Quantum Molecular Dynamics) model is based on the propagation of hadrons according to Hamilton’s equation of motion, as derived from the Ritz variational principle. The model allows to obtain the full time evolution of the collision, from the initial state to the final particles. The decoupling of the particles from the system is governed by their individual scatterings. The propagation uses relativistic kinematics and includes all n -particle correlations, as is typical for QMD-type models. This differs from test-particle-based approaches, which solve certain Boltzmann-type equations and therefore only allow 1-particle distribution functions to be obtained (meaning that they do not propagate particle correlations). UrQMD includes potential interactions of Skyrme type, but it can also include other potentials. It allows for the use of soft and hard potential interactions. Current data suggest that hard potentials, meaning a stiff equation-of-state, is appropriate at low energies ($\sqrt{s_{NN}} < 7$ GeV), while a soft equation-of-state with momentum dependent nucleon–nucleon interactions is favored at higher collision energies [156]. Hadrons interact according to a 2-particle collision term involving elastic interactions and inelastic reactions. The inelastic reactions include resonance creation and decay as well as string formation and fragmentation. At very high energies ($\sqrt{s_{NN}} > 50$ GeV), the model uses PYTHIA to account for hard scatterings. The table of included hadrons typically extends up to 3 GeV in mass, depending on the particle type. The latest version includes charm degrees of freedom, although charm production has only been benchmarked in the low-energy range ($\sqrt{s_{NN}} < 7$ GeV). Generally, applying

⁹Available at www.urqmd.org.

such a model set-up leads to a natural transition from the central collision area to the periphery of the interaction zone. This is often referred to as the core–corona transition, because it leads to substantial thermalization in the central region due to high interaction rates. Then, it naturally transforms into single nucleon-nucleon interactions towards the edges of the collision zone. For a recent review of transport models the reader is referred to Ref. [157]. UrQMD is also available in CORSIKA as an optional low-energy interaction model.

A.7 FLUKA

FLUKA [49, 158]¹⁰ is a general-purpose Monte Carlo code for particle transport and interactions in matter. It incorporates detailed physics models for electromagnetic and hadronic processes down to thermal energies, including nuclear effects and particle decays. FLUKA serves as the default low-energy hadronic interaction model in CORSIKA 7 and CORSIKA 8, typically handling interactions below a given energy threshold in the range of 70–100 GeV. It simulates the production and transport of secondary particles, nuclear fragmentation, and decay processes in the later stages of air-shower development, complementing high-energy models such as EPOS LHC-R, QGSJET-III, SIBYLL 2.3d or PYTHIA 8/Angantyr.

A.8 Unified interfaces for hadronic interaction models

Event generators are standalone codes without a uniform interface. Two software packages simplify using and comparing the previously listed event generators by providing a unified interface and unified output in HepMC format, which tuning tools can read. CRMC¹¹ [45] is written in C++ and Fortran and supports many high-energy event generators, including PYTHIA 6, as well as most event generators used in astroparticle experiments. CRMC offers a command-line interface to generate events. Chromo¹² [46], written in Python and Fortran, is a newer package with the same goal. It can be used as a command-line tool, and as a library in Python scripts and Jupyter notebooks. It greatly simplifies access to event generators by offering precompiled packages for Linux, macOS, and Windows, that can be installed from the PyPI repository and are immediately ready to use (no compilation by users is required). A continuous integration service automatically compiles and tests the software after every change, and the project invites contributions from the community for ongoing development and enhancement.

B Transport codes

B.1 CORSIKA

CORSIKA is a Monte Carlo code for simulating of extensive air showers. It was originally developed for the KASCADE experiment [159], but has found wide application in many astroparticle physics experiments [54]. CORSIKA is a monolithic Fortran code that exhibits excellent performance but incurs limitations, such as limited parallelization possibilities and increasingly difficult maintenance. To address these issues and take advantage of modern software engineering possibilities, a rewrite of CORSIKA in modern C++17 has been underway since 2018, focusing on modularity and the needs and capabilities of modern supercomputing [124, 160]. This version, called CORSIKA 8, is now physics-complete and offers unprecedented flexibility in air shower simulations [143], including

¹⁰Available at www.fluka.eu.

¹¹<https://gitlab.iap.kit.edu/AirShowerPhysics/crmc>

¹²<https://github.com/impj-project/chromo>

radio and Cherenkov emission. Although it is slower by a factor of 3–5 compared to the highly-optimized but more specialised preceding Fortran versions, CORSIKA offers new possibilities, such as the complete genealogy of air shower particles, showers in different media (including e.g. the crossing from the atmosphere into ice or rock), multithreaded radio emission calculation, and GPU-parallelized calculation of the Cherenkov emission of air showers.

One of the main applications of CORSIKA concerns simulating EAS and comparing them with observations. In particular, measurements of the muon content of ultra-high energy cosmic ray-induced EAS, notably by the Pierre Auger Observatory, show that hadronic multi-particle production in EAS is not yet fully understood [161, 162]. Examining the genealogical information of particles in EAS simulations, such as generation number and the particle species of preceding generations, can provide valuable insight e.g. into the production mechanism of muons and the gradual decoupling and evolution of the electromagnetic cascade. Furthermore, quantitative statements can be compared with Heitler-Matthews-like toy models [163] that qualitatively describe EAS observables. The number of hadron generations preceding decay into a muon has been studied as a function of primary energy, zenith angle and lateral distance. Additionally, muon production depth profiles have been studied as a function of hadron generation [164]. Furthermore, EM profiles as a function of hadron generation have been investigated and it has been analyzed to what extent X_{max} is already determined by the primary interaction alone and which influence later hadron generations exert [62].

Both the original CORSIKA and CORSIKA 8 use external event generators to simulate hadronic interactions. For CORSIKA, these are EPOS, SIBYLL, QGSJET and DPMJET [165] for high-energy interactions, and UrQMD or FLUKA for low-energy interactions. In the case of CORSIKA 8 the available models are EPOS, SIBYLL, QGSJET and PYTHIA for high energies and UrQMD and FLUKA for low energies.

B.2 CONEX

CONEX [58] is a Fortran code which was designed to realistically simulate the longitudinal air shower development for experiments observing air showers with fluorescence or air-Cherenkov telescopes. CONEX can simulate the longitudinal profile much faster than a full Monte Carlo approach, and does so without using the thinning technique that is mandatory for simulating ultra-high energy air showers. It is also commonly used in studies that explore the impact of modified hadronic interactions on air shower observables.

CONEX uses a hybrid approach. The initial stages of the hadronic cascade, which dominate its shower-to-shower fluctuations, are computed using the Monte Carlo technique. Then, particles are binned and the cascade equations are solved numerically. This allows CONEX to simulate observables related to shower-to-shower fluctuations of the depth of the shower maximum, X_{max} , or the muon number, N_{μ} . CONEX was later integrated in CORSIKA 7 [166], which enables 3D hybrid calculations, where the final stage of the air shower is again simulated using the Monte Carlo technique. This speeds up air shower simulations by a factor of five compared to the full Monte Carlo approaches with thinning at high energies. However, in most studies, CONEX is used in its original mode. In principle, any event generator capable of generating hadron-nucleus interactions at arbitrary energies can be used with CONEX. In practice, however, only interfaces for EPOS LHC, SIBYLL and QGSJET are provided.

B.3 MCEq

MCEq [59] is an open-source Python-based numerical cascade equation solver that has been developed and optimized for calculating atmospheric lepton fluxes. It is conceptually similar to CONEX,

but it does not use Monte Carlo simulation in the initial stages of the shower. It allows one to use various hadronic interaction models, including SIBYLL, EPOS LHC, QGSJET, DPMJET and PYTHIA. For underground transport the PROPOSAL code has been established. Results obtained with CONEX and MCEQ are numerically similar if the same event generators are used. Although MCEQ is written in Python, it is much faster than CONEX (a few seconds versus tens of minutes), because the numerical heavy-lifting is done by fast third-party libraries that allow one to exploit the sparsity in the system of equations.

Atmospheric neutrino fluxes are of particular interest to neutrino experiments such as IceCube because they represent a foreground to the astrophysical neutrino fluxes. Atmospheric neutrino fluxes are divided into a conventional component resulting from the decay of pions and kaons, and a so-called prompt component resulting from the decay of heavy mesons and other hadrons. The largest contribution to the prompt flux stems from the decay of D mesons. Due to the time dilatation of long-lived light mesons in the relativistic regime, the spectrum of the conventional neutrinos is steeper than the primary cosmic ray flux by about $1/E$. In contrast, the prompt neutrinos roughly follow the primary fluxes. Due to the difference in spectral slopes, the prompt component begins to dominate the atmospheric lepton flux above 10 PeV.

B.4 CRPropa

CRPROPA is designed to model the transport of high-energy particles over galactic, intergalactic, and cosmological distances. It focuses on cosmic ray propagation in coherent and turbulent magnetic fields, and on photo-nuclear interactions with cosmic photon background fields. The recently released version CRPROPA 3.2 [56] is the latest update in an ongoing effort to maintain and extend this open-source code, which is well established in the cosmic-ray community. Originally intended to simulate the ballistic propagation and interactions of Ultra-High Energy Cosmic Rays [167, 168], it can now also handle the diffusive propagation of cosmic rays in various magnetic fields [169], address stochastic cosmic ray acceleration, and model electromagnetic cascades for gamma-ray emission and transport, among other capabilities.

Currently, it is not expected that CRPROPA will be used for event generator tuning. However, this may change in the future, as the latest version has implemented hadronic interactions either by directly calling event generators or by using precomputed tables [170]. This is motivated by enabling in-source interactions for multi-messenger analyses of cosmic rays, gamma rays, and neutrinos. A recent study [171] showed that uncertainties in hadronic interaction models result in flux differences up to a factor of two for high-energy neutrinos and photons from molecular clouds. Thus, it may be possible to use neutrino and gamma emissions from strong sources for tuning because neutrinos are produced by decays of charged pions and gamma rays are produced by decay of neutral pions.

The mathematical and technological approaches used in CRPROPA are noteworthy. They have inspired other transport codes, particularly CORSIKA 8. CRPROPA is written in a mix of C++ and Python, uses a modern modular design, and features sophisticated parallelization techniques. In CRPROPA, each step in the simulation is handled by a module that implements a physical process. Each module processes a stack of (pseudo)particles simultaneously, allowing one to leverage vectorization capabilities of modern CPUs and GPUs. CRPROPA's design offers a great deal of flexibility for debugging, prototyping, and experimentation. Modules can be written in either pure Python or in C++. In most frameworks, the main loop that passes the particle stack from module to module is written in C++ and cannot be directly accessed from the Python layer. In CRPROPA, one can replace the standard loop completely with a plain Python loop, providing maximum control for experts and enabling introspection. The latency of executing Python calls is not an issue with this approach if there are enough particles on the stack. In this case, the overall computation time

is still dominated by the time spent in each module, making this approach feasible.

B.5 Z-moment method

Atmospheric lepton fluxes can be computed to good approximation with the semi-analytical Z-moment method (see e.g. [60]). In this approach, the cascade equations are solved for a continuous power-law energy spectrum of cosmic rays under several assumptions, for example, superposition for the projectile (as far as forward production is concerned, a projectile nucleus can be treated like a superposition of its nucleons, each with the same fraction of the total energy). A Z-moment is the result of the integral over the input nucleon spectrum and the (energy-)differential cross section for the production of the desired lepton. Although this method introduces approximations that must be verified using numerical codes, it is very transparent making it useful for studying the impact of cross section uncertainties on atmospheric lepton fluxes. Another advantage is that only differential cross sections are needed as input. These can come from any source: an event generator (e.g. PYTHIA, SIBYLL), an analytical calculation in pQCD (e.g. for D-mesons [172, 173]), or even parameterizations of suitable data [174, 175]. However, it cannot be used to simulate monoenergetic air showers since the method assumes a continuous input spectrum.

Recent works have studied the theoretical uncertainty of the prompt atmospheric neutrino flux with Z-moments [173, 176–179]. The dominant contribution to this flux involves Z-moments over production cross sections for charmed hadrons. In the collinear factorization framework, these cross sections depend on partonic charm production cross sections, which can be computed in pQCD, and the non-perturbative parton distribution functions (PDF) and fragmentation functions (FF) which in turn depend on the factorization scale. The partonic cross sections depend on the charm quark (pole) mass and the factorization and renormalization scales. The goal is to fit the non-perturbative components of the PDFs and FFs to as many accelerator-based measurements as possible to minimize uncertainties when extrapolating to energies and phase space that are inaccessible to direct experiments, yet relevant to cosmic ray physics.

The resulting uncertainties of prompt neutrino fluxes are relatively large, up to a factor of about 5 [177–179]. At neutrino energies below ~ 1 PeV in the laboratory frame, uncertainties from QCD dominate, with uncertainties from renormalization and factorization scales playing the largest role. PDF uncertainties increase with neutrino energy due to increasing sensitivity to the gluon PDF in the target at very small momentum fraction, where the gluon density rises rapidly and may experience saturation. Above ~ 1 PeV, uncertainties in the all-nucleon flux progressively become comparable to the QCD uncertainties. The former largely derive from theoretical uncertainties in the elemental composition of cosmic rays, and to a lesser extent, from inconsistencies between air shower measurements.

The composition uncertainties are dominated by theoretical uncertainties in the event generators that are used to interpret air shower data. Therefore, the accuracy of these calculations above 1 PeV will indirectly benefit from the global tuning of event generators. However, one can also exploit this sensitivity for tuning by using the atmospheric muon flux as input. Unlike the neutrino flux, the atmospheric muon flux is purely of atmospheric origin and can be measured by neutrino observatories like IceCube.

C Details on experiments

C.1 Accelerator: ALICE

ALICE [74] is a general-purpose detector for QCD and heavy-ion collision studies at the LHC. It was designed to study strongly interacting matter at high temperatures and energy densities in order to investigate the properties of the so-called Quark-Gluon Plasma (QGP). The ALICE detector consists of two main parts. The first component relies on a central tracking and particle identification system that uses energy-loss, transition-radiation, time-of-flight, calorimeter, and other information to track and identify hadrons. This system covers the range $|\eta| < 0.9$ and transverse momentum from 0.1 to tens of GeV/c. The ALICE tracker was designed to handle collisions involving thousands of particles. In addition to the mid-rapidity region, ALICE has a forward single-arm muon spectrometer that covers the range of $-4.0 < \eta < -2.5$, and particle counters that trigger the detector and measure event activities of the collision (centrality in heavy-ion collisions). These counters cover the range $-3.7 < \eta < -1.7$, and $2.8 < \eta < 5.1$. A system of zero-degree calorimeters measures protons and neutrons scattered at small angles (with $|\eta| > 7.0$ typically).

Thanks to its sensitivity down to almost zero transverse momentum, where non-perturbative effects dominate, its coverage of ppColl, pPbColl, and PbPbColl collisions, and its particle identification capabilities, ALICE has already provided unique measurements for the study of QCD and the tuning of event generators at the LHC in its configuration of LHC Run 1 (2009-2013) and Run 2 (2015-2018). Many of these results were recently summarized in Ref. [180]. For this context, important results include the production cross sections for charged particles up to $\eta \sim 5$, and measurements of the hadron composition in multiple systems and as a function of charged-particle multiplicity. Notably, the enhancement of strangeness production is a relevant trait for explaining the muon puzzle in air showers.

ALICE discovered multiplicity-dependent strangeness enhancement in p+p and p+Pb collisions, where it was not expected [11]. These measurements showed that production and hadronization in dense final states are modified, and that the classic assumption of universal fragmentation breaks down. However, this modification was found to largely depend on the charged-particle multiplicity of the event, i.e. to be largely independent of the collision system, meaning that a modified form of universality still holds. Not only is strangeness affected; hadron composition generally changes in high-multiplicity events. In the light flavor sector, the production of stable baryons (protons) as well as short-lived resonances (with lifetimes below 10 fm/c, e.g. ρ and $K(892)^0$) is reduced while the formation of light nuclei (d, t, and ^3He) is enhanced. These three aspects strongly suggest the existence of interactions in the late hadronic stage of the collision with a significant impact on the collision outcome. In the heavy-flavor sector, *open* charm production (D^0 , Λ_c^+ , ...) is enhanced as well, but effect appears to be dependent more on the collision system here. Despite these effects, the relative composition of light particles (π , K , p) remains fairly constant at mid-rapidity in average events. The strangeness enhancement for the lightest hadrons with one strange quark (K_s^0 , Λ) is mild.

Of interest to us here, ALICE recently conducted a series of studies correlating the energy flux in the very forward region, as measured with the zero-degree calorimeter (ZDC)[181], with the event activity in the mid-rapidity region. Notably, these studies were carried out in p+p and p+Pb systems. A first study examined the relationship between the leading energy in the very forward region and the multiplicity of unidentified charged particles in the mid-rapidity vicinity [182]. Another study investigated the relationship between the leading energy in the very forward region and the multiplicity of strange baryons present at mid-rapidity, as most sensitive particles to strangeness enhancement (Λ , Ξ , Ω)[183]. At a fixed multiplicity in the mid-rapidity region,

strangeness enhancement shows a prevailing correlation with the effective energy available outside the ZDC. This reveals the strong influence of the initial stage of the collision, to be compared to the impact of the final-state situation.

C.2 Accelerator: LHCb

The LHCb detector [184] is a general-purpose single-arm forward spectrometer at the LHC. It covers the range $2 < \eta < 5$ and transverse momentum from 0.1 to tens of GeV/ c . The detector was designed to study the decays of hadrons containing heavy quarks produced in high-energy proton-proton collisions and consists of a high-precision tracking system for charged particles with a high-resolution vertex detector located close to the interaction point for reconstructing decay chains of short-lived hadrons, and several sub-detectors for particle identification. These include two ring-imaging Cherenkov detectors that separate charged pions, kaons, and protons, a calorimeter system that separates electrons/photons and electrons/pions, and a muon system. The electromagnetic calorimeter is finely segmented with good energy resolution which allows for the study of photons and neutral pion decays. The LHCb detector is the only detector at the LHC with these identification capabilities over its entire acceptance.

LHCb provides unique input for tuning event generators by making precise measurements in the forward region. Its measurements of D and B meson production constrain parton distribution functions (PDFs) in proton and in lead nuclei: LHCb can probe gluon PDFs down to a momentum fraction of $\sim 10^{-6}$ providing strong constraints for simulations of the atmospheric lepton flux observed by neutrino observatories [145, 177]. Regarding soft-QCD, LHCb has recently measured the production cross section for prompt long-lived charged particles in p+p and p+Pb collisions [185, 186] to an accuracy of a few percent and has measured neutral pion production in p+p and p+Pb collisions [187]. The ratios of pions, kaons, and protons have been studied in p+p collisions up to 7 TeV [188], and an ongoing analysis studies this ratios in p+p at 13 TeV and in p+Pb at 8.16 TeV. Following the discovery of a multiplicity-dependent strangeness enhancement in p+p collisions by ALICE, LHCb found evidence for a multiplicity-dependent increase in the B_s^0/B^0 ratio [189], and in the D_s^+/D^+ [190] ratio.

The LHCb experiment is in a unique position because it can collect data in both collider and fixed-target modes. This is possible thanks to LHCb's fixed-target system, called SMOG (System for Measuring Overlap with Gas) [191]. The SMOG system was originally designed to precisely calibrate the luminosity of colliding proton beams [192]. By injecting small amounts of noble gases directly into the primary LHC vacuum around the vertex detector, LHCb can study interactions of the LHC beams and gas in collisions with center-of-mass energies up to 113 GeV, the highest achieved so far in a fixed-target experiment. This capability has been used to measure the anti-proton production cross section in proton-helium collisions [193, 194], and charm production in proton-neon and lead-neon collisions [195, 196], which constrain a potential intrinsic charm component in the proton with implications for the prompt atmospheric lepton flux.

In recent years, the LHCb detector underwent a major upgrade in preparation for the current data-taking period [197], including a new SMOG2 system [77]. Gas is now injected into an open storage cell located upstream of the LHCb collision point, and is suppressed outside the cell by vacuum pumps. This new system enables the study of collisions involving non-noble gases, such as hydrogen and deuterium, and possibly oxygen and nitrogen, and at higher gas pressures. This increases the luminosity by two orders of magnitude compared to before [77, 198]. Proton-oxygen and proton-nitrogen collisions, in particular, will be of great interest for air showers. The increased luminosity will also enable precision measurements of D and B meson production. During the recent run with oxygen beam in 2025, collisions on a hydrogen target gave access to proton-oxygen collisions

in the forward hemisphere.

C.3 Accelerator: LHCf

The LHC forward (LHCf) experiment [81] is designed to study the production of energetic neutral particles, such as γ , π^0 , and neutrons, emitted in the very forward region at pseudorapidity $\eta > 8.4$, which significantly contributes to the air shower development induced by high-energy cosmic rays. LHCf comprises two independent subdetectors, Arm1 and Arm2, installed in the instrumental slots of the TANs (Neutral Target Absorbers), located ± 140 m from the ATLAS interaction point. Each LHCf detector consists of two sampling and position-sensitive calorimeter towers. Above the design threshold of 100 GeV, the energy resolution is better than 5% for photons and 40% for neutrons.

Since the start of the LHC, LHCf has carried out a number of operations at various collision energies ranging from 0.9 to 13.6 TeV with p+p and p+Pb. The measured inclusive differential cross sections of γ , π^0 , and neutron [83–85, 142, 199, 200], mainly originating from the proton fragments, were used to test and tune the hadronic interaction models. The most recent operation in 2022 with p+p collisions at $\sqrt{s} = 13.6$ TeV focused on increasing statistics to study strange hadron production by measuring the following: η ($\eta \rightarrow 2\gamma$), K_s^0 ($K_s^0 \rightarrow 2\pi^0 \rightarrow 4\gamma$), and Λ ($\Lambda \rightarrow n + \pi \rightarrow n + 2\gamma$). This is important for solving the muon puzzle, since strangeness enhancement in the forward region increases the muon yield in air shower simulations.

Furthermore, joint analyses with the ATLAS experiment are conducted to study details of forward particle production, such as diffractive processes. LHCf events originating from low-mass diffractive collisions are easily selected because no particle detection in the ATLAS inner tracker is required for the pseudo-rapidity range of $|\eta| < 2.5$ [201]. During the 2022 operation, LHCf performed a joint analysis with ATLAS, incorporating the ATLAS zero-degree calorimeter (ZDC) and Roman-pot detectors (AFP and ALFA). Combining data from these ATLAS forward detectors allowed to study various physics processes, such as $p - \pi$ interaction via the one-pion-exchange process and low-mass resonance production [202]. These results will be important for tuning hadronic interaction models.

C.4 Accelerator: TOTEM

The TOTEM experiment (Total Cross Section, Elastic Scattering and Diffraction Dissociation) at the Large Hadron Collider (LHC) was dedicated to studying proton-proton interactions at very small angles and large distances from the collision point [78]. Its primary goals included precise measurements of the total proton-proton cross-section, elastic scattering, and diffractive processes, which are key to understanding the strong interaction in the non-perturbative regime of QCD and the tuning of event generators. TOTEM employs specialized Roman Pot detectors placed along the LHC beamline to detect particles scattered at extremely small angles relative to the beam axis. These detectors allow TOTEM to probe phenomena such as diffraction and soft processes that are complementary to high-energy studies performed by other LHC experiments like ATLAS and CMS. By combining its results with data from these experiments, TOTEM contributes significantly to a comprehensive understanding of proton structure and fundamental QCD dynamics.

C.5 Accelerator: FASER/SND and the Forward Physics Facility

The FASER experiment (Forward Search Experiment) [82] at the LHC is designed to search for new, very light and weakly interacting particles that may be produced in high-energy proton-proton collisions but travel in the forward direction. In contrast to the general purpose experiments ATLAS and CMS, that focus on particles emitted at large angles, FASER being located hundreds of meters

downstream from the ATLAS collision point, focuses on the forward produced particles that may have gone unnoticed by ATLAS. Its main goal is the search for the hypothetical particles such as dark photons, axion-like particles, and other light dark matter candidates.

SND@LHC (Scattering and Neutrino Detector) [120] is a detector complementary to FASER located off-axis from the ATLAS interaction point. It is aimed at detecting all three neutrino flavors from LHC collisions and probing feebly interacting particles. It covers a different angular region than FASER, providing broader neutrino measurements.

The Forward Physics Facility (FPF) is a proposed experimental site at the LHC designed to study particles produced in the very forward region of high-energy collisions [90]. Located several hundred meters downstream from the ATLAS interaction point, the FPF is planned to house scaled up and extended versions of the FASER and SND detectors. The FPF aims to explore phenomena beyond the Standard Model, such as searches for dark matter candidates or rare processes, while also improving our understanding of QCD and particle production mechanisms in extreme kinematic regions.

C.6 Accelerator: NA61/SHINE

NA61/SHINE (SPS Heavy Ion and Neutrino Experiment) [69] is a multipurpose fixed-target experiment designed to study hadron production in hadron-nucleus and nucleus-nucleus collisions at the CERN SPS. The core component of the detector is a set of large-acceptance Time Projection Chambers (TPCs) and two superconducting magnets with a combined bending power of 9 Tm. This setup enables precise measurements of particle momenta ($\sigma(p)/p^2 \approx (0.3-7) \times 10^{-4}$ GeV/c) and provides excellent particle identification capabilities via the specific energy loss in the TPC volumes.

The experiment began operations in 2007 and has since collected hadroproduction data using various projectiles, beam energies, and target materials. NA61/SHINE has conducted detailed measurements of particle production in p+C interactions at 31 GeV/c [203–205] and π^+ +C at 60 GeV/c to determine the beam properties for accelerator-based neutrino experiments [206]. Since carbon is a good proxy for nitrogen interactions in air, the measured spectra in these reactions are also highly relevant for modeling low-energy interactions in air showers. Particle production measurements in negatively charged pions with carbon at 158 and 350 GeV/c are of particular interest for air shower physics [71, 207]. Spectra of π^\pm , K^\pm , p, \bar{p} , ρ^0 , ω , K^{*0} , K_S^0 , Λ , $\bar{\Lambda}$ were measured in a wide range of longitudinal and transverse momentum.

Furthermore, p+p interactions were studied in a wide range of beam momenta (20, 31, 40, 80 and 158 GeV/c) [208, 209] to create a reference dataset for the heavy ion physics program of NA61/SHINE. This dataset is also instrumental in studying the secondary production of antiprotons and antinuclei in collisions of cosmic-ray protons with the interstellar medium in the Galaxy.

Finally, after a successful pilot run in 2018 [210, 211], the collaboration plans to take substantial data on nuclear fragmentation cross sections. These data are essential for interpreting recent high-precision cosmic-ray data on secondary Galactic nuclei, see e.g. Ref. [212, 213] and will also help refine the fragmentation models of hadronic interaction models, thereby improving the modeling of air shower fluctuations.

C.7 Astroparticle: Pierre Auger Observatory

The Pierre Auger Observatory [5] is located in Malargüe, Argentina, at an atmospheric depth of 880 g/cm². It is the world’s largest observatory for detecting ultra-high-energy cosmic rays and has been operating successfully for 20 years. Its hybrid design consists of a Surface Detector (SD) array of 1660 water Cherenkov tanks arranged in a triangular grid with a baseline of 1.5 km, covering

an area of 3000 km^2 . The Fluorescence Detector (FD) [214] complementing the SD consists of four telescope sites, each with 6 telescopes, at the periphery of the Observatory overlooking the SD at elevation angles ranging from 0° to 30° . Another set of three telescopes (High Elevation Telescopes; HEAT) extends the elevation range to 60° above the horizon. Buried muon detectors made of plastic scintillator slabs provide additional clean information about air-shower muons.

A fraction of the events (called hybrid events) are observed in both the SD and FD. As shown in [162], the combination of signals from the surface and fluorescence detectors is a powerful tool for examining current models of hadronic interactions. Five two-dimensional distributions, corresponding to different cosmic ray mass hypotheses were simultaneously fitted with Monte Carlo templates for the ground signal at 1000 m from the shower core and the depth of the shower maximum. Surprisingly, the predicted X_{max} scale for the models EPOS-LHC, QGSJET-II-04, and SIBYLL 2.3d models describes the Auger data better when assuming a depth in the atmosphere that is about 20 to 50 g/cm^2 deeper. This results in a heavier mixed mass composition of primary particles than that obtained for unmodified X_{max} scales of the models. The predicted hadronic signal should increase by about 15-25%, alleviating the muon puzzle for unmodified X_{max} scales. The improvement in describing measured data with the assumed modifications to the model predictions is significant, exceeding 5σ for any linear combination of experimental systematic uncertainties. In Ref. [62] (*cf.* Figure 2), the impact of modifying basic parameters of hadronic interactions was studied in detail using the 1-D simulation package CONEX. In particular, the study examined multiplicity, elasticity, and cross section. The same approach can be applied to study general 3-D observables by applying different ranges and thresholds to the modifications of individual parameters based on existing experimental constraints, which allows for modifications of all three parameters at once [215–217]. Due to the general anticorrelation between the change of the muon signal at 1000 m, $R_\mu(1000)$, and X_{max} , only a specific combination the considered modifications (decreased cross section, and increased elasticity and multiplicity) fits the Auger results in the $R_\mu(1000)$ – X_{max} plane [162]. However, such modifications conflict with the Auger measurements of the proton-air cross section [93] and potentially with higher moments of the observed X_{max} distributions.

Following a significant upgrade, the Pierre Auger Observatory has entered its second phase of operation, known as AugerPrime [218]. The upgrade enhances the particle physics capabilities of the Observatory and increases its sensitivity to the primary mass. This is accomplished by adding scintillation and radio detectors to each surface detector station, tripling the sampling rate of the readout electronics, expanding the dynamic range of the signals, adding new event triggers, and installing an Underground Muon Detector (UMD) in the low-energy extension of the surface detector array. The latter is centered 6 km away from the HEAT telescopes and consists of a denser array with 750 m spacing nested within the 1500 m array. Each UMD consists of a 30 m^2 array of plastic scintillator muon counters buried 2.3 m underground near the water-Cherenkov detectors of the nested infill array. It will provide a direct measurement of the muon component of air showers in the energy range $3 \times 10^{16} \text{ eV}$ to $1 \times 10^{19} \text{ eV}$. This will significantly contribute to discriminating the primary mass and testing hadronic interaction models. The soil above each UMD detector absorbs the electromagnetic component of air showers and imposes an energy cut of about 1 GeV for vertical muons. The muon counts are used to fit a lateral distribution function and the resulting muon density at a reference distance of 450 m to be compared with EAS simulations. Preliminary data from a subset of stations equipped with PMTs were used to quantify a muon deficit of about 35-50% compared to data of corresponding X_{max} measurements [219].

As part of the AugerPrime upgrade, each of the surface detector stations of the Pierre Auger Observatory was equipped each with a dual-polarized Short Aperiodic Loaded Loop Antenna (SALLA), which measures the radio signals from EAS in the 30–80 MHz band. This enables the measurement of the energy in the electromagnetic cascade of inclined air showers with zenith angles above around

65° with a resolution below 10% [220]. Combining measurements of this electromagnetic energy with the pure measurements of the muon content of inclined air showers by the water-Cherenkov detectors enables precise studies of muon numbers and their fluctuations at energies beyond $10^{18.4}$ eV, with much larger statistics than could be achieved previously by combining of water-Cherenkov and fluorescence detector data. Furthermore, the radio detector will allow to cross-check the energy scale of cosmic-ray measurements using an independent approach based on the first-principles classical electrodynamics calculation of radio signals from EAS [221].

C.8 Astroparticle: IceCube Neutrino Observatory

The IceCube Neutrino Observatory [47] (IceCube) is a cubic-kilometer detector deployed deep in the ice at the geographic South Pole, at depths between 1450 m and 2450 m. It is accompanied by an array of surface detectors, IceTop [222]. The in-ice detector measures high-energy muons, above a few 100 GeV, from EAS that penetrate the Antarctic ice, as well as charged secondaries induced by neutrino interactions. In addition, IceTop [222] measures EAS resulting from cosmic-ray interactions ranging from PeV to EeV energies at an atmospheric depth of approximately 690 g/cm^2 . This hybrid detector setup provides a unique opportunity to study hadronic interactions in EAS in great detail. New surface detectors, including scintillator detectors and radio antennas, are under development for IceTop [223] and IceCube-Gen2 [224]. They will further enhance the capability to study hadronic interaction models in the future.

IceTop has recently reported measurements of muon densities in EAS as a function of energy at reference distances of 600 m and 800 m for primary energies between 2.5–40 PeV and 9–120 PeV, respectively [225]. These measurements are consistent within uncertainties with predictions using the pre-LHC model SIBYLL 2.1. However, comparisons to simulations using the post-LHC models EPOS LHC and QGSJET-II-04 yield higher muon densities than observed. Interestingly, preliminary results of a recent measurement of the multiplicity of TeV muons in EAS, measured in the deep ice with IceCube [226], show agreement within uncertainties with all hadronic interaction models considered. Therefore, these two measurements indicate inconsistencies in the modeling of GeV and TeV muons within the post-LHC models. To further study these inconsistencies, efforts are ongoing to simultaneously measure GeV and TeV muons from the same air shower on an event-by-event basis [227, 228]. These measurements will provide important information about energy sharing between low- and high-energy interactions during the EAS development and will constrain hadronic interaction models [20].

IceCube’s deep-ice detector also allows for the measurement of the atmospheric neutrino spectrum [229–232], as well as the muon energy spectrum at very high energies (above a few 10 TeV) [233–235]. Combining these two channels provides valuable input for hadronic interaction models, such as the kaon-to-pion ratio or the contribution from the prompt atmospheric lepton flux [145]. Current efforts are underway to update these measurements and utilize their synergies to constrain hadronic interaction models and measure the relative contributions from the decay of unflavored and charmed mesons. Additionally, measurements of the seasonal variations in high-energy muon [236, 237] and neutrino fluxes [238] provide information on the kaon-to-pion ratio [239, 240], which further constrains hadronic interaction models.

C.9 Astroparticle: KASCADE

The cosmic-ray air-shower experiments KASCADE [159] and KASCADE-Grande [241] were located at the Karlsruhe Institute of Technology in Germany, at an atmospheric depth of 1022 g/cm^2 . KASCADE took data from 1996 to 2003, after which it was superseded by the KASCADE-Grande

experiment which took data until 2012. In addition to its array of electron and muon counters, KASCADE operated a 320 m^2 highly segmented hadronic calorimeter to test hadronic interaction models. One inclusive test compared the detected rates of high-energy hadrons in the calorimeter with CORSIKA simulations that employed the high-energy hadronic interaction models available at that time (QGSJET, DPMJET, HDPM, SIBYLL, VENUS, and NeXus 2). Using data from the PeV region, it was concluded that the contribution of diffraction dissociation should be reduced for all models, for QGSJET, for example, by about 5–7 % of the inelastic cross section [242]. Other tests examined the number of hadrons with $E > 50\text{ GeV}$ in relation on the number of electrons and muons ($E > 200\text{ MeV}$) in EAS.

The KASCADE-Grande detector arrays measured the energy spectrum and mass composition of cosmic rays within the primary energy range of PeV to EeV [243–245]. The results were compared to predictions of various hadronic interaction models [246]. Generally, the models agree better on the all-particle cosmic ray flux than on its composition. Interestingly, post-LHC models predict a lower all-particle flux than the pre-LHC models at energies of around PeV.

The special configuration of the experiments allows one to combine the KASCADE and KASCADE-Grande data, making it possible to investigate and compare the muon content close to and far from the core [247]. A combined analysis shows that the hadronic interaction models QGSJET-II-04, EPOS LHC, and SIBYLL 2.3 systematically underpredict the muon content of the showers.

In addition, an analysis was performed to estimate the muon content in cosmic-ray induced air showers as a function of the primary energy [248]. These measurements were compared to predictions of the event generators QGSJET-II-04, EPOS LHC, and SIBYLL 2.3, which were unable to consistently describe the KASCADE-Grande data for all zenith angles and energies. This suggests that the attenuation of the muon number with the zenith angle is smaller in the data than in the simulations. The observed anomalies could imply that the energy spectrum of muons from real EAS at the production site, for a given primary energy, is harder than the respective model predictions. Further investigations are ongoing using data available through the KASCADE Cosmic Ray Data Centre (KCDC) [110].

The importance of improving hadronic interaction models was already underlined in the most cited KASCADE paper [243] where it was concluded that: *“At present, the limiting factors of the analysis are the properties of the high energy interaction models used and not the quality or the understanding of the KASCADE data. The observed discrepancies between simulations and data have to be attributed to the models and may give valuable information for their further improvements.”*

C.10 The muon puzzle in EAS

To further investigate the muon deficit reported by Auger and other experiments, the Working Group for Hadronic Interactions and Shower Physics (WHISP) [98–101] has performed a meta-analysis of muon number measurements from different air shower observatories. The group comprises members of the EAS-MSU, IceCube, KASCADE-Grande, NEVOD-DECOR, Pierre Auger, SUGAR, Telescope Array (TA), and Yakutsk EAS Array collaborations and combined published data from a variety of muon detection methods, including the ice-Cherenkov stations of IceTop [225], the KASCADE-Grande shielded scintillation detectors [249], the Yakutsk underground scintillation detectors [250], the underground Geiger-Mueller counters of EAS-MSU [251], the tracking detector and water-Cherenkov calorimeter of NEVOD-DECOR [252, 253], the underground liquid scintillator tanks of SUGAR [254, 255], the buried scintillator counters of HiRes-MIA [256], the scintillator modules of TA [257], the water-Cherenkov array of Auger [94, 95, 161], and the underground scintillator modules of Auger [219], as well as the shielded scintillator array of AGASA [258], alongside previously unconsidered data from Haverah Park [259] and new estimates from an analysis

of KASCADE-Grande data [260] that uses the energy scale of the Pierre Auger Observatory for calibration.

The diversity of these measurements make a direct comparison difficult. Apart from the cosmic ray energy, E , the observed muon density at ground level depends on the atmospheric depth of the ground array, the lateral distance at which the muon density is measured, the zenith angle of the considered showers, and the effective energy cutoff introduced by the shielding of the detectors. Furthermore, the muon number, N_μ , is measured in many different ways. The standard method uses shielded detectors to isolate the muon signal from other particles produced in the air shower. However, experiments without such shielded detectors use different techniques; some use the atmosphere itself as a shield by analyzing highly inclined showers. Others discriminate muon hits in ground detectors from hits of other particles based on the characteristic energy deposit of muons, which peaks around a value dependend on the muon inclination. Therefore, the comparison of experimental data and model expectations was done by introducing a metavariable, z , which compares respective measurements with expectations from simulated air showers. It is defined as

$$z = \frac{\ln\langle N_\mu^{\text{det}} \rangle(E) - \ln\langle N_{\mu,p}^{\text{det}} \rangle(E)}{\ln\langle N_{\mu,\text{Fe}}^{\text{det}} \rangle(E) - \ln\langle N_{\mu,p}^{\text{det}} \rangle(E)}, \quad (1)$$

where $\langle N_\mu^{\text{det}} \rangle$ is the mean value of the measured muon density under the specific conditions of the experiment, and $\langle N_{\mu,p}^{\text{det}} \rangle$ and $\langle N_{\mu,\text{Fe}}^{\text{det}} \rangle$ are the corresponding predicted average muon densities for proton and iron showers, respectively, under the same conditions.

The method used to estimate the shower energy, E , is important for the z -scale, since N_μ is nearly proportional to E . Systematic shifts in the energy scale lead to apparent shifts in the z -values. To address this issue, WHISP adjusted the energy scales of the experiments to align them with a common reference spectrum at a given energy [99]. This greatly improved the consistency of the measurements.

Furthermore, correlations between the estimation of the muon density, N_μ , and the energy, E , can distort the measurement and should ideally be negligible. Ideally, the cosmic ray energy is estimated by integrating the longitudinal energy loss profile observed in the atmosphere with fluorescence or Cherenkov telescopes. Experiments without telescopes instead use the charged particle density measured by surface detector arrays, which includes a contribution from muons. In the latter case, the energy estimate always exhibits some degree of cross-contamination from N_μ , resulting in positive correlations on event-by-event basis. Finally, some experiments measure only the muon number and obtain a muon multiplicity distribution. This distribution can be compared with predictions based on the cosmic ray flux obtained from another experiment using the FD technique to infer z -values (sometimes referred to as *intensity based* z -values).

In addition to an uncorrelated energy estimation method, which is ideal for muon measurements with small systematic uncertainties, a full detector simulation is required to account for potential detector biases and a small atmospheric overburden. While large atmospheric overburden is irrelevant for an FD-based energy estimation, it increases the uncertainties for a ground-based energy estimation.

The results of the cross-calibrated z values are shown in Figure 6. By construction, the z -values depend on the event generator used in the air shower simulations. The WHISP group uses published simulations that employed the event generators that were available at the time of publication. Therefore, not all data points are available for each event generator. At first glance, there is no coherent global picture from 1 PeV to 10 EeV. Considering the various conditions under which the experiments were conducted, such as distance to the shower core, zenith angle, and muon energy, does not solve the problem [100]. However, two groups can be identified. Experiments that directly

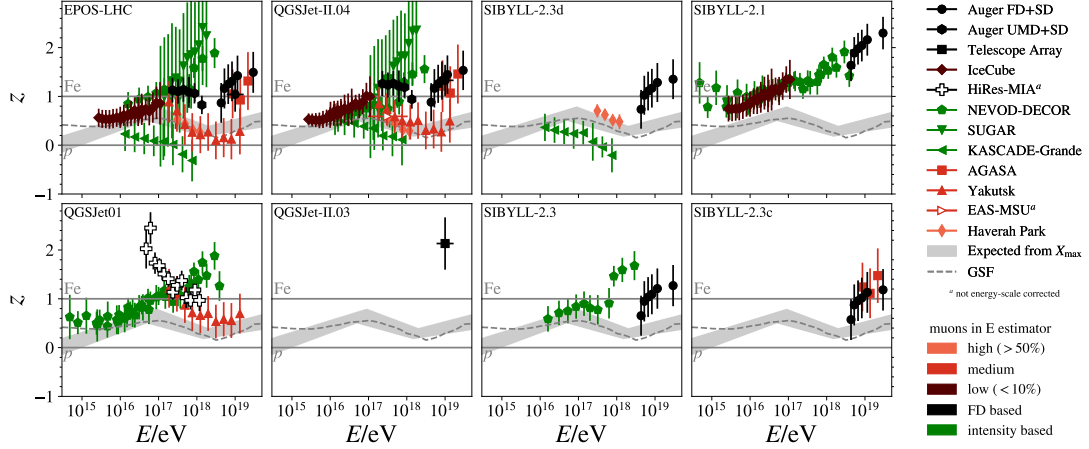


Figure 6: Muon content of air showers encoded in z -values (see text) as a function of the shower energy, E , from different experiments. The event generator used to compute the predicted muon content is shown in the upper left corner of each plot. The colors indicate the contribution of muons to the estimate of the shower energy, and the dashed line shows the expected z -value based on the GSF model [97], while the gray band shows the expectation from Auger X_{max} measurements. The error bars show statistical and systematic uncertainties added in quadrature. Figure taken from Ref. [98].

measure the shower energy with little (red brown markers) or no muon contribution (black markers), such as IceCube and Auger, show a muon deficit in the simulations that grows at a constant rate with increasing energy. It appears as an increase in z over the expectation from the cosmic ray composition. Experiments with a medium (red) or high muon contribution (orange) to the estimator of the shower energy, or intensity based experiments (green) where the energy scale is inferred from the muon content itself, show no consistent picture. This is presumably because the strong dependence of the number of muons on the shower energy masks the deficit.

D Details on tuning

There are two practical approaches commonly used in automatic tuning to find an optimal description of the data: One approach is to minimize the least-squares-type cost function via gradient descent. The other approach is to compute the posterior probability density of the parameters from the likelihood function and priors in a Bayesian framework.

The largest PYTHIA 8 tuning campaigns, such as the ATLAS A14 [279] and CMS CUETP8M1 [280] tunes, have simultaneously floated $\mathcal{O}(40\text{--}60)$ parameters, covering MPI, ISR and FSR, color reconnection, and hadronization settings. Another well-known PYTHIA 8 tune is the Monash 2013 tune [116], which floated $\mathcal{O}(20\text{--}30)$ parameters, covering key aspects of the parton shower, MPI, hadronization, and baryon/strangeness production. This tune has become a widely used baseline for collider physics. Monash-2013-type tunes appear only every five to ten years, whereas experiment-specific tunes (e.g. ATLAS A14 and CMS CUETP8M1) are produced more frequently, approximately every two to four years, often in conjunction with new LHC data releases. These tunes are based ex-

Table 6: RIVET plugins and HEPData entries used in the forward tuning of PYTHIA, along with the ongoing RIVET-ization efforts toward a tune for air showers, as discussed in Subsection 5.2. The third column specifies whether the analysis has an entry in the HEPData database. The fourth column indicates whether the plugin is included in the public RIVET repository. Columns five and six define the collision system. The CM energy denoted by $\sqrt{s_{\text{NN}}}$ is per-nucleon. The second half of the table focuses on fixed-target experiments, organized by beam momentum. The final column lists the extracted final states used for tuning.

RIVET plugin	Ref.	HEPData	Published	$\sqrt{s}, \sqrt{s_{\text{NN}}} \text{ (TeV)}$	Collision system	Final state / Observable
LHCF_2015_I1351909	[84]	✓	✓	7	pp	neutral $d\sigma/dx_F$
LHCF_2016_I1385877	[85]	✓	✓	2.76, 7, 5.02	pp, pPb	neutral $d\sigma/dx_F$
LHCF_2018_I1692008	[200]	✓	✓	13	pp	neutral $d\sigma/dx_F$
LHCF_2018_I1518782	[83]	✓	✓	13	pp	neutral $d\sigma/dx_F$
LHCF_2023_I2658888	[261]	✓	✓	13	pp	neutral $d\sigma/dx_F$
LHCB_2013_I1251899	[262]	✓	✓	5	pPb	$d\sigma/dp_T dy$
LHCB_2016_I1504058	[263]	✓	✓	7, 13	pp	$d\sigma/d\eta$
LHCB_2019_I1720413	[264]	✓	✓	8.16	pPb	$d\sigma/dp_T dy$
LHCB_2021_I1889335	[186]	✓	✓	13	pp	charged $d\sigma/dp_T d\eta$
LHCB_2021_I1913240	[185]	✓	✓	5	pp, pPb	charged $d\sigma/dp_T d\eta$
LHCB_2022_I2694685	[265]	✓	✓	8.16	pPb	$d\sigma/dp_T dy$
$p_{\text{beam}} \text{ (GeV/c)}$						
E104_1976_I98502	[266]	✓		[23 - 280]	$\pi^\pm p, K^\pm p, pp, p\bar{p}$	σ^{tot}
E104_1979_I132765	[267]	✓		[200 - 370]	$\pi^\pm p, K^\pm p, pp, p\bar{p}$	σ^{tot}
E104_1979_I132133	[268]	✓		[60 - 280]	$\pi^\pm p, K^\pm p, pp, p\bar{p}$	σ^{prod}
NA8_1983_I182455	[269]	✓		[30 - 345]	$\pi^- p, pp$	elastic $d\sigma/dt$
NA22_1986_I18431	[270]	✓	✓	250	$\pi^+ p, K^+ p, pp$	P_n
NA22_1987_I246909	[271]	✓		250	$\pi^+ p, K^+ p$	elastic $d\sigma/dt$
NA22_1988_I265504	[272]	✓	✓	250	$\pi^+ p, K^+ p, pp$	$d\sigma/dx_F dp_T dy$
NA22_1990_I301243	[273]	✓		250	$\pi^+ p$	$d\sigma/dx_F, d\sigma/dp_T^2$
NA22_1992_I322980	[274]	✓		250	$\pi^+ p, K^+ p$	$d\sigma/dx_F, d\sigma/dp_T^2$
NA49_2006_I694016	[275]	✓	✓	158	pp	$E d\sigma/dx_F dp_T^2$
NA49_2009_I818217	[141]		✓	158	pp	$E d\sigma/dx_F dp_T^2$
NA61_2017_I1598505	[276]	✓		[20 - 158]	pp	$d^2n/dy dp_T$
NA61_2017_I1600971	[207]			158, 350	$\pi^- C$	$x_F dn/dx_F$
NA61_2019_I1753094	[277]	✓		60, 120	pC, pBe, pAl	$\sigma^{\text{prod}}, \sigma^{\text{inel}}$
NA61_2022_I1868367	[278]			158	pp	$d^2n/dy dp_T, dn/dy$
NA61_2023_I2155140	[71]			158, 350	$\pi^- C$	$\sigma^{\text{prod}}, d^2n/dp dp_T$

clusively on high-energy accelerator measurements, primarily from the LHC and LEP experiments. No astroparticle data are included.

Gradient-based tuning A least-squares-type cost function quantifies the agreement between the event generator and the measurements. This function can be optimized using local gradient descent to determine the optimal set of tuning parameters. To enable analytical computation of the gradient, the event generator is replaced by a surrogate model.

Gradient-based automatic tuning first emerged in particle physics with the PROFESSOR [281] software package, which employs a high-dimensional polynomial as a surrogate model. This inspired the development of APPRENTICE [122], which offers several improvements. It supports the use of Padé approximants (ratios of polynomials) to construct the surrogate model, providing more flexibility. It also provides algorithms to avoid unwanted poles in their construction.

Bayesian tuning Bayesian tuning also starts with a weighted least-squares-type cost function and the construction of a surrogate model that replaces the event generator. Then, a Markov-Chain Monte Carlo method is used to sample points from the posterior distribution to find the best set of parameters, including uncertainties and their correlations. The posterior distribution can be used to determine the optimal parameters and study their uncertainties of the parameters and their correlations. The effectiveness of the Bayesian tuning approach was demonstrated using collider data from LEP experiments [125, 126].

A crucial initial step in achieving global tuning to both particle and astroparticle data is to establish the feasibility of tuning to air shower data. To explore this, a study was conducted using the event generator PYTHIA 8 and the air shower simulation framework CORSIKA 8. Mock air shower data were generated using the default PYTHIA 8 settings and were then used in Bayesian tuning to determine if these default values could be recovered. In a first scenario, the number of muons produced in the shower, N_μ , was chosen as the tuning observable, and the strong coupling constant, α_s , was chosen as the tuning parameter. In a second scenario, both N_μ and the depth of the shower maximum, X_{\max} , were used as observables, and two parameters related to Lund string fragmentation (and thus hadron multiplicity) were tuned. Tuning was then performed as described above. A surrogate model was constructed by running multiple sets of 10 PeV protons air shower simulations with different tuning parameter values. In both scenarios, the Bayesian method successfully generated posterior distributions centered on the input values. This study demonstrates that tuning to air shower observables is possible in principle and that the Bayesian tuning approach is a promising method for global tuning to particle and astroparticle data. The experiment also highlights the necessity for fast air shower simulations. The next step is to perform an initial tuning to the data.

Table 6 provides a summary of the RIVET plugins and HEPData entries used in the “forward physics” tune of PYTHIA 8, along with the ongoing efforts toward an air showers tune discussed in Subsection 5.2. The latter tune is intended primarily for EAS experiments, but is still based solely on HEP data. This work involves creating new RIVET plugins from available HepData entries for fixed-target measurements, as well as advocating for the inclusion of the most recent measurements in HepData.

D.1 Tuning without a surrogate model

One limitation of established automatic tuning methods is the requirement of construct a surrogate model. This step adds complexity because the parameter space must be sampled efficiently. Ad-

ditionally, the approach suffers from the curse of dimensionality: constructing a surrogate model requires grid-like sampling of a high-dimensional parameter space. The number of required grid points increases exponentially with each additional dimension.

Direct tuning of the event generator via stochastic gradient descent (SGD) could eliminate the need for a surrogate model, and significantly reduce the computational effort required for tuning multi-parameters simultaneously. SGD algorithms, such as ADAM [282], can successfully train neural networks with large parameter spaces at a fraction of the computational cost of traditional methods. These algorithms avoid the curse of dimensionality, because the cost of computing the gradient increases only linearly with the number of dimensions.

Gradient formulas are exact when training neural networks. However, they are computed over a random subset of the full data sample. This introduces random fluctuations into the gradient, similar to those introduced by a Monte Carlo simulation in an event generator. Although SGD algorithms are designed to handle these fluctuations, exploding gradients are still a problem. In the tuning application, the gradients must be calculated using a finite-difference formula using an automatically chosen step size that is large enough to prevent gradient explosion. The ADAM algorithm already automatically determines the learning rate for each parameter based on previous results. Therefore, it seems plausible that the step size for the finite-difference computation of the gradient could be determined similarly. Future research could explore this possibility.

References

- [1] S. Navas et al. “Review of particle physics”. In: *Phys. Rev. D* 110.3 (2024), p. 030001. DOI: 10.1103/PhysRevD.110.030001.
- [2] Gaetano Barone et al. “Higgs production via vector-boson fusion at the LHC”. In: (July 2025). arXiv: 2507.22574 [hep-ph].
- [3] Johannes Blumer, Ralph Engel, and Jorg R. Horandel. “Cosmic Rays from the Knee to the Highest Energies”. In: *Prog. Part. Nucl. Phys.* 63 (2009), pp. 293–338. DOI: 10.1016/j.pnpnp.2009.05.002. arXiv: 0904.0725 [astro-ph.HE].
- [4] Karl-Heinz Kampert and Michael Unger. “Measurements of the Cosmic Ray Composition with Air Shower Experiments”. In: *Astropart. Phys.* 35 (2012), pp. 660–678. DOI: 10.1016/j.astropartphys.2012.02.004. arXiv: 1201.0018 [astro-ph.HE].
- [5] Alexander Aab et al. “The Pierre Auger Cosmic Ray Observatory”. In: *Nucl. Instrum. Meth. A* 798 (2015), pp. 172–213. DOI: 10.1016/j.nima.2015.06.058. arXiv: 1502.01323 [astro-ph.IM].
- [6] D. Bastieri et al. “Using the photons from the Crab nebula seen by GLAST to calibrate MAGIC and the imaging air Cerenkov telescopes”. In: *Astropart. Phys.* 23 (2005), pp. 572–576. DOI: 10.1016/j.astropartphys.2005.05.002. arXiv: astro-ph/0504301.
- [7] M. Meyer, D. Horns, and H. -S. Zechlin. “The Crab Nebula as a standard candle in very high-energy astrophysics”. In: *Astron. Astrophys.* 523 (2010), A2. DOI: 10.1051/0004-6361/201014108. arXiv: 1008.4524 [astro-ph.HE].
- [8] Johannes Albrecht et al. “The Muon Puzzle in cosmic-ray induced air showers and its connection to the Large Hadron Collider”. In: *Astrophys. Space Sci.* 367.3 (2022), p. 27. DOI: 10.1007/s10509-022-04054-5. arXiv: 2105.06148 [astro-ph.HE].

- [9] George Sterman et al. “Handbook of perturbative QCD”. In: *Rev. Mod. Phys.* 67 (1 Jan. 1995), pp. 157–248. DOI: 10.1103/RevModPhys.67.157. URL: <https://link.aps.org/doi/10.1103/RevModPhys.67.157>.
- [10] Tigran Kalaydzhyan and Edward Shuryak. “Collective flow in high-multiplicity proton-proton collisions”. In: *Phys. Rev. C* 91.5 (2015), p. 054913. DOI: 10.1103/PhysRevC.91.054913. arXiv: 1503.05213 [hep-ph].
- [11] Jaroslav Adam et al. “Enhanced production of multi-strange hadrons in high-multiplicity proton-proton collisions”. In: *Nature Phys.* 13 (2017), pp. 535–539. DOI: 10.1038/nphys4111. arXiv: 1606.07424 [nucl-ex].
- [12] Sebastian Baur et al. “Combined analysis of accelerator and ultra-high energy cosmic ray data”. In: *PoS ICRC2015* (2016), p. 418. DOI: 10.22323/1.236.0418.
- [13] V. A. Petrov, R. A. Ryutin, and A. E. Sobol. “LHC as pi p and pi pi Collider”. In: *Eur. Phys. J. C* 65 (2010), pp. 637–647. DOI: 10.1140/epjc/s10052-009-1202-0. arXiv: 0906.5309 [hep-ph].
- [14] R. A. Ryutin, V. A. Petrov, and A. E. Sobol. “Towards Extraction of π^+p and $\pi^+\pi^+$ cross-sections from Charge Exchange Processes at the LHC”. In: *Eur. Phys. J. C* 71 (2011), p. 1667. DOI: 10.1140/epjc/s10052-011-1667-5. arXiv: 1101.0078 [hep-ph].
- [15] D. Maurin et al. “Precision cross-sections for advancing cosmic-ray physics and other applications: a comprehensive programme for the next decade”. In: (Mar. 2025). arXiv: 2503.16173 [astro-ph.HE].
- [16] Klaus Werner. “Revealing a deep connection between factorization and saturation: New insight into modeling high-energy proton-proton and nucleus-nucleus scattering in the EPOS4 framework”. In: *Phys. Rev. C* 108.6 (2023), p. 064903. DOI: 10.1103/PhysRevC.108.064903. arXiv: 2301.12517 [hep-ph].
- [17] Tanguy Pierog and Klaus Werner. “EPOS LHC-R : up-to-date hadronic model for EAS simulations”. In: *PoS ICRC2023* (2023), p. 230. DOI: 10.22323/1.444.0230.
- [18] Tanguy Pierog and Klaus Werner. “EPOS.LHC-R : a global approach to solve the muon puzzle”. In: Aug. 2025. arXiv: 2508.07105 [astro-ph.HE].
- [19] Sergey Ostapchenko. “QGSJET-III model of high energy hadronic interactions: II. Particle production and extensive air shower characteristics”. In: (Mar. 2024). arXiv: 2403.16106 [hep-ph].
- [20] Felix Riehn et al. “Hadronic interaction model Sibyll 2.3d and extensive air showers”. In: *Phys. Rev. D* 102.6 (2020), p. 063002. DOI: 10.1103/PhysRevD.102.063002. arXiv: 1912.03300 [hep-ph].
- [21] Christian Bierlich et al. “A comprehensive guide to the physics and usage of PYTHIA 8.3”. In: *SciPost Phys. Codeb.* 2022 (2022), p. 8. DOI: 10.21468/SciPostPhysCodeb.8. arXiv: 2203.11601 [hep-ph].
- [22] Torbjörn Sjöstrand and Marius Uthm. “Hadron interactions for arbitrary energies and species, with applications to cosmic rays”. In: *Eur. Phys. J. C* 82.1 (2022), p. 21. DOI: 10.1140/epjc/s10052-021-09953-5. arXiv: 2108.03481 [hep-ph].
- [23] S. A. Bass et al. “Microscopic models for ultrarelativistic heavy ion collisions”. In: *Prog. Part. Nucl. Phys.* 41 (1998), pp. 255–369. DOI: 10.1016/S0146-6410(98)00058-1. arXiv: nucl-th/9803035.

- [24] Ioana C. Maris et al. “Influence of Low Energy Hadronic Interactions on Air-shower Simulations”. In: *Nucl. Phys. B Proc. Suppl.* 196 (2009). Ed. by Jean-Noël Capdevielle, Ralph Engel, and Bryan Pattison, pp. 86–89. DOI: 10.1016/j.nuclphysbps.2009.09.013. arXiv: 0907.0409 [astro-ph.CO].
- [25] Bo Nilsson-Almqvist and Evert Stenlund. “Interactions Between Hadrons and Nuclei: The Lund Monte Carlo, Fritiof Version 1.6”. In: *Comput. Phys. Commun.* 43 (1987), p. 387. DOI: 10.1016/0010-4655(87)90056-7.
- [26] S. Agostinelli et al. “GEANT4—a simulation toolkit”. In: *Nucl. Instrum. Meth. A* 506 (2003), pp. 250–303. DOI: 10.1016/S0168-9002(03)01368-8.
- [27] L. V. Gribov, E. M. Levin, and M. G. Ryskin. “Semihard Processes in QCD”. In: *Phys. Rept.* 100 (1983), pp. 1–150. DOI: 10.1016/0370-1573(83)90022-4.
- [28] H. J. Drescher et al. “Parton based Gribov-Regge theory”. In: *Phys. Rept.* 350 (2001), pp. 93–289. DOI: 10.1016/S0370-1573(00)00122-8. arXiv: hep-ph/0007198.
- [29] M. L. Good and W. D. Walker. “Diffraction disscociation of beam particles”. In: *Phys. Rev.* 120 (1960), pp. 1857–1860. DOI: 10.1103/PhysRev.120.1857.
- [30] R. J. Glauber and G. Matthiae. “High-energy scattering of protons by nuclei”. In: *Nucl. Phys. B* 21 (1970), pp. 135–157. DOI: 10.1016/0550-3213(70)90511-0.
- [31] J. Engel et al. “Nucleus-nucleus collisions and interpretation of cosmic ray cascades”. In: *Phys. Rev. D* 46 (1992), pp. 5013–5025. DOI: 10.1103/PhysRevD.46.5013.
- [32] Christian Bierlich et al. “The Angantyr model for Heavy-Ion Collisions in PYTHIA8”. In: *JHEP* 10 (2018), p. 134. DOI: 10.1007/JHEP10(2018)134. arXiv: 1806.10820 [hep-ph].
- [33] Maximilian Reininghaus. “Air showers and hadronic interactions with CORSIKA 8”. In: *SciPost Phys. Proc.* 15 (2024), p. 019. DOI: 10.21468/SciPostPhysProc.15.019. arXiv: 2210.07797 [astro-ph.HE].
- [34] K. J. Eskola, H. Paukkunen, and C. A. Salgado. “EPS09: A New Generation of NLO and LO Nuclear Parton Distribution Functions”. In: *JHEP* 04 (2009), p. 065. DOI: 10.1088/1126-6708/2009/04/065. arXiv: 0902.4154 [hep-ph].
- [35] Kari J. Eskola et al. “EPPS16: Nuclear parton distributions with LHC data”. In: *Eur. Phys. J. C* 77.3 (2017), p. 163. DOI: 10.1140/epjc/s10052-017-4725-9. arXiv: 1612.05741 [hep-ph].
- [36] Bo Andersson et al. “Parton Fragmentation and String Dynamics”. In: *Phys. Rept.* 97 (1983), pp. 31–145. DOI: 10.1016/0370-1573(83)90080-7.
- [37] Jesper R. Christiansen and Peter Z. Skands. “String Formation Beyond Leading Colour”. In: *JHEP* 08 (2015), p. 003. DOI: 10.1007/JHEP08(2015)003. arXiv: 1505.01681 [hep-ph].
- [38] Christian Bierlich et al. “Effects of Overlapping Strings in pp Collisions”. In: *JHEP* 03 (2015), p. 148. DOI: 10.1007/JHEP03(2015)148. arXiv: 1412.6259 [hep-ph].
- [39] Christian Bierlich, Gösta Gustafson, and Leif Lönnblad. “A shoving model for collectivity in hadronic collisions”. In: (Dec. 2016). arXiv: 1612.05132 [hep-ph].
- [40] Philip Ilten and Marius Uthm. “Forming molecular states with hadronic rescattering”. In: *Eur. Phys. J. A* 58.1 (2022), p. 1. DOI: 10.1140/epja/s10050-021-00650-1. arXiv: 2108.03479 [hep-ph].

- [41] Xin-Nian Wang and Miklos Gyulassy. “HIJING: A Monte Carlo model for multiple jet production in p p, p A and A A collisions”. In: *Phys. Rev. D* 44 (1991), pp. 3501–3516. DOI: 10.1103/PhysRevD.44.3501.
- [42] Wei-Tian Deng, Xin-Nian Wang, and Rong Xu. “Hadron production in p+p, p+Pb, and Pb+Pb collisions with the HIJING 2.0 model at energies available at the CERN Large Hadron Collider”. In: *Phys. Rev. C* 83 (2011), p. 014915. DOI: 10.1103/PhysRevC.83.014915. arXiv: 1008.1841 [hep-ph].
- [43] N. N. Kalmykov et al. “The Predictions of Quark-Gluon String Model and the Data of Air Showers at Ultra High Energies”. In: International Cosmic Ray Conference 1 (Jan. 1995), p. 123.
- [44] Lilly Pyras et al. “Atmospheric muons at PeV energies in radio neutrino detectors”. In: *JCAP* 10 (2023), p. 043. DOI: 10.1088/1475-7516/2023/10/043. arXiv: 2307.04736 [astro-ph.HE].
- [45] Ralf Ulrich, Tanguy Pierog, and Colin Baus. *Cosmic Ray Monte Carlo Package, CRMC*. Version 2.0.1. Aug. 2021. DOI: 10.5281/zenodo.5270381.
- [46] Hans Dembinski, Anatoli Fedynitch, and Anton Prosekin. “Chromo: An event generator frontend for particle and astroparticle physics”. In: *PoS ICRC2023* (2023), p. 189. DOI: 10.22323/1.444.0189.
- [47] M. G. Aartsen et al. “The IceCube Neutrino Observatory: Instrumentation and Online Systems”. In: *JINST* 12.03 (2017), P03012. DOI: 10.1088/1748-0221/12/03/P03012.
- [48] J. H. Koehne et al. “PROPOSAL: A tool for propagation of charged leptons”. In: *Comput. Phys. Commun.* 184 (2013), pp. 2070–2090. DOI: 10.1016/j.cpc.2013.04.001.
- [49] Alfredo Ferrari et al. “FLUKA: A multi-particle transport code (Program version 2005)”. In: (Oct. 2005). DOI: 10.2172/877507.
- [50] Pedro Abreu et al. “Techniques for Measuring Aerosol Attenuation using the Central Laser Facility at the Pierre Auger Observatory”. In: *JINST* 8 (2013), P04009. DOI: 10.1088/1748-0221/8/04/P04009. arXiv: 1303.5576 [astro-ph.IM].
- [51] T. Shibata et al. “Absolute energy calibration of the Telescope Array fluorescence detector with an electron linear accelerator”. In: *EPJ Web Conf.* 53 (2013). Ed. by K. -H. Kampert et al., p. 10004. DOI: 10.1051/epjconf/20135310004.
- [52] Bianca Keilhauer. “The Balloon-the-Shower programme of the Pierre Auger Observatory”. In: *Astrophys. Space Sci. Trans.* 6 (2010). Ed. by K. Scherer et al., pp. 27–30. DOI: 10.5194/astra-6-27-2010.
- [53] P. Abreu et al. “Description of Atmospheric Conditions at the Pierre Auger Observatory using the Global Data Assimilation System (GDAS)”. In: *Astropart. Phys.* 35 (2012), pp. 591–607. DOI: 10.1016/j.astropartphys.2011.12.002. arXiv: 1201.2276 [astro-ph.HE].
- [54] D. Heck et al. “CORSIKA: A Monte Carlo code to simulate extensive air showers”. In: (Feb. 1998).
- [55] S. J. Sciutto. “AIRES: A system for air shower simulations”. In: (Nov. 1999). DOI: 10.13140/RG.2.2.12566.40002. arXiv: astro-ph/9911331.
- [56] Rafael Alves Batista et al. “CRPropa 3.2 — an advanced framework for high-energy particle propagation in extragalactic and galactic spaces”. In: *JCAP* 09 (2022), p. 035. DOI: 10.1088/1475-7516/2022/09/035. arXiv: 2208.00107 [astro-ph.HE].

- [57] A. M. Hillas. “Shower simulation: Lessons from MOCCA”. In: *Nucl. Phys. B Proc. Suppl.* 52 (1997). Ed. by H. Rebel, G. Schatz, and J. Knapp, pp. 29–42. DOI: 10.1016/S0920-5632(96)00847-X.
- [58] Till Bergmann et al. “One-dimensional Hybrid Approach to Extensive Air Shower Simulation”. In: *Astropart. Phys.* 26 (2007), pp. 420–432. DOI: 10.1016/j.astropartphys.2006.08.005. arXiv: astro-ph/0606564.
- [59] Tetiana Kozynets, Anatoli Fedynitch, and D. Jason Koskinen. “Atmospheric lepton fluxes via two-dimensional matrix cascade equations”. In: *Phys. Rev. D* 108.10 (2023), p. 103040. DOI: 10.1103/PhysRevD.108.103040. arXiv: 2306.15263 [astro-ph.HE].
- [60] Thomas K. Gaisser, Ralph Engel, and Elisa Resconi. *Cosmic Rays and Particle Physics: 2nd Edition*. Cambridge University Press, June 2016. ISBN: 978-0-521-01646-9.
- [61] Jeferson A. Ortiz, Gustavo A. Medina Tanco, and V. de Souza. “Longitudinal development of extensive air showers: Hybrid code SENECA and full Monte Carlo”. In: *Astropart. Phys.* 23 (2005), pp. 463–476. DOI: 10.1016/j.astropartphys.2005.02.007. arXiv: astro-ph/0411421.
- [62] Ralf Ulrich, Ralph Engel, and Michael Unger. “Hadronic Multiparticle Production at Ultra-High Energies and Extensive Air Showers”. In: *Phys. Rev. D* 83 (2011), p. 054026. DOI: 10.1103/PhysRevD.83.054026. arXiv: 1010.4310 [hep-ph].
- [63] Sebastian Baur et al. “Core-corona effect in hadron collisions and muon production in air showers”. In: *Phys. Rev. D* 107.9 (2023), p. 094031. DOI: 10.1103/PhysRevD.107.094031. arXiv: 1902.09265 [hep-ph].
- [64] Christian Bierlich et al. “Reweight Monte Carlo predictions and automated fragmentation variations in Pythia 8”. In: *SciPost Phys.* 16.5 (2024), p. 134. DOI: 10.21468/SciPostPhys.16.5.134. arXiv: 2308.13459 [hep-ph].
- [65] T. Pierog et al. “EPOS LHC: Test of collective hadronization with data measured at the CERN Large Hadron Collider”. In: *Phys. Rev. C* 92.3 (2015), p. 034906. DOI: 10.1103/PhysRevC.92.034906. arXiv: 1306.0121 [hep-ph].
- [66] S. Bailey et al. “Parton distributions from LHC, HERA, Tevatron and fixed target data: MSHT20 PDFs”. In: *Eur. Phys. J. C* 81.4 (2021), p. 341. DOI: 10.1140/epjc/s10052-021-09057-0. arXiv: 2012.04684 [hep-ph].
- [67] R. Abdul Khalek et al. “Science Requirements and Detector Concepts for the Electron-Ion Collider: EIC Yellow Report”. In: *Nucl. Phys. A* 1026 (2022), p. 122447. DOI: 10.1016/j.nuclphysa.2022.122447. arXiv: 2103.05419 [physics.ins-det].
- [68] Michael Benedikt et al. *Future Circular Collider Feasibility Study Report Volume 1: Physics and Experiments*. Tech. rep. Geneva: CERN, 2025. DOI: 10.17181/CERN.9DKX.TDH9. URL: <https://cds.cern.ch/record/2928193>.
- [69] N. Abgrall et al. “NA61/SHINE facility at the CERN SPS: beams and detector system”. In: *JINST* 9 (2014), P06005. DOI: 10.1088/1748-0221/9/06/P06005. arXiv: 1401.4699 [physics.ins-det].
- [70] Jaroslav Adam et al. “Pseudorapidity and transverse-momentum distributions of charged particles in proton–proton collisions at $\sqrt{s} = 13$ TeV”. In: *Phys. Lett. B* 753 (2016), pp. 319–329. DOI: 10.1016/j.physletb.2015.12.030. arXiv: 1509.08734 [nucl-ex].

- [71] H. Adhikary et al. “Measurement of hadron production in π -C interactions at 158 and 350 GeV/c with NA61/SHINE at the CERN SPS”. In: *Phys. Rev. D* 107.6 (2023), p. 062004. DOI: 10.1103/PhysRevD.107.062004. arXiv: 2209.10561 [nucl-ex].
- [72] G. Aad et al. “The ATLAS Experiment at the CERN Large Hadron Collider”. In: *JINST* 3 (2008), S08003. DOI: 10.1088/1748-0221/3/08/S08003.
- [73] S. Chatrchyan et al. “The CMS Experiment at the CERN LHC”. In: *JINST* 3 (2008), S08004. DOI: 10.1088/1748-0221/3/08/S08004.
- [74] K. Aamodt et al. “The ALICE experiment at the CERN LHC”. In: *JINST* 3 (2008), S08002. DOI: 10.1088/1748-0221/3/08/S08002.
- [75] A. Augusto Alves Jr. et al. “The LHCb Detector at the LHC”. In: *JINST* 3 (2008), S08005. DOI: 10.1088/1748-0221/3/08/S08005.
- [76] LHCb collaboration. “Precision luminosity measurements at LHCb”. In: *JINST* 9 (2014), P12005. DOI: 10.1088/1748-0221/9/12/P12005. arXiv: 1410.0149 [hep-ex].
- [77] *LHCb SMOG Upgrade*. Tech. rep. Geneva: CERN, 2019. DOI: 10.17181/CERN.SAQC.EOWH. URL: <https://cds.cern.ch/record/2673690>.
- [78] G. Anelli et al. “The TOTEM experiment at the CERN Large Hadron Collider”. In: *JINST* 3 (2008), S08007. DOI: 10.1088/1748-0221/3/08/S08007.
- [79] Serguei Chatrchyan et al. “Measurement of pseudorapidity distributions of charged particles in proton-proton collisions at $\sqrt{s} = 8$ TeV by the CMS and TOTEM experiments”. In: *Eur. Phys. J. C* 74.10 (2014), p. 3053. DOI: 10.1140/epjc/s10052-014-3053-6. arXiv: 1405.0722 [hep-ex].
- [80] Albert M Sirunyan et al. “Measurement of the average very forward energy as a function of the track multiplicity at central pseudorapidities in proton-proton collisions at $\sqrt{s} = 13$ TeV”. In: *Eur. Phys. J. C* 79.11 (2019), p. 893. DOI: 10.1140/epjc/s10052-019-7402-3. arXiv: 1908.01750 [hep-ex].
- [81] O. Adriani et al. “The LHCf detector at the CERN Large Hadron Collider”. In: *JINST* 3 (2008), S08006. DOI: 10.1088/1748-0221/3/08/S08006.
- [82] Henso Abreu et al. “The FASER detector”. In: *JINST* 19.05 (2024), P05066. DOI: 10.1088/1748-0221/19/05/P05066. arXiv: 2207.11427 [physics.ins-det].
- [83] O. Adriani et al. “Measurement of forward photon production cross-section in proton-proton collisions at $\sqrt{s} = 13$ TeV with the LHCf detector”. In: *Phys. Lett. B* 780 (2018), pp. 233–239. DOI: 10.1016/j.physletb.2017.12.050. arXiv: 1703.07678 [hep-ex].
- [84] O. Adriani et al. “Measurement of very forward neutron energy spectra for 7 TeV proton-proton collisions at the Large Hadron Collider”. In: *Phys. Lett. B* 750 (2015), pp. 360–366. DOI: 10.1016/j.physletb.2015.09.041. arXiv: 1503.03505 [hep-ex].
- [85] O. Adriani et al. “Measurements of longitudinal and transverse momentum distributions for neutral pions in the forward-rapidity region with the LHCf detector”. In: *Phys. Rev. D* 94.3 (2016), p. 032007. DOI: 10.1103/PhysRevD.94.032007. arXiv: 1507.08764 [hep-ex].
- [86] Roshan Mammen Abraham et al. “First Measurement of the Muon Neutrino Interaction Cross Section and Flux as a Function of Energy at the LHC with FASER”. In: *Phys. Rev. Lett.* 134.21 (2025), p. 211801. DOI: 10.1103/PhysRevLett.134.211801. arXiv: 2412.03186 [hep-ex].

- [87] CERN. *For one day only LHC collides xenon beams*. 2017. URL: <https://home.cern/news/news/accelerators/one-day-only-lhc-collides-xenon-beams> (visited on 10/12/2017).
- [88] Jasmine Brewer, Aleksas Mazeliauskas, and Wilke van der Schee. “Opportunities of OO and pO collisions at the LHC”. In: *Opportunities of OO and pO collisions at the LHC*. Mar. 2021. arXiv: 2103.01939 [hep-ph].
- [89] CERN. *First-ever collisions of oxygen at the LHC*. 2025. URL: <https://home.web.cern.ch/news/news/accelerators/first-ever-collisions-oxygen-lhc> (visited on 08/12/2025).
- [90] Luis A. Anchordoqui et al. “The Forward Physics Facility: Sites, experiments, and physics potential”. In: *Phys. Rept.* 968 (2022), pp. 1–50. DOI: 10.1016/j.physrep.2022.04.004. arXiv: 2109.10905 [hep-ph].
- [91] T Antoni et al. “Electron, muon, and hadron lateral distributions measured in air-showers by the KASCADE experiment”. In: *Astropart. Phys.* 14 (2001), pp. 245–260. DOI: 10.1016/S0927-6505(00)00125-0. arXiv: astro-ph/0004233.
- [92] Lorenzo Cazon et al. “Time structure of muonic showers”. In: *Astropart. Phys.* 21 (2004), pp. 71–86. DOI: 10.1016/j.astropartphys.2003.12.009. arXiv: astro-ph/0311223.
- [93] Pedro Abreu et al. “Measurement of the proton-air cross-section at $\sqrt{s} = 57$ TeV with the Pierre Auger Observatory”. In: *Phys. Rev. Lett.* 109 (2012), p. 062002. DOI: 10.1103/PhysRevLett.109.062002. arXiv: 1208.1520 [hep-ex].
- [94] Alexander Aab et al. “Muons in Air Showers at the Pierre Auger Observatory: Mean Number in Highly Inclined Events”. In: *Phys. Rev. D* 91.3 (2015). [Erratum: Phys.Rev.D 91, 059901 (2015)], p. 032003. DOI: 10.1103/PhysRevD.91.032003. arXiv: 1408.1421 [astro-ph.HE].
- [95] Alexander Aab et al. “Measurement of the Fluctuations in the Number of Muons in Extensive Air Showers with the Pierre Auger Observatory”. In: *Phys. Rev. Lett.* 126.15 (2021), p. 152002. DOI: 10.1103/PhysRevLett.126.152002. arXiv: 2102.07797 [hep-ex].
- [96] R. Abbasi et al. “Improved Characterization of the Astrophysical Muon–neutrino Flux with 9.5 Years of IceCube Data”. In: *Astrophys. J.* 928.1 (2022), p. 50. DOI: 10.3847/1538-4357/ac4d29. arXiv: 2111.10299 [astro-ph.HE].
- [97] Hans Peter Dembinski et al. “Data-driven model of the cosmic-ray flux and mass composition from 10 GeV to 10^{11} GeV”. In: *PoS ICRC2017* (2018), p. 533. DOI: 10.22323/1.301.0533. arXiv: 1711.11432 [astro-ph.HE].
- [98] Juan Carlos Arteaga Velazquez. “A report by the WHISP working group on the combined analysis of muon data at cosmic-ray energies above 1 PeV”. In: *PoS ICRC2023* (2023), p. 466. DOI: 10.22323/1.444.0466.
- [99] H. P. Dembinski et al. “Report on Tests and Measurements of Hadronic Interaction Properties with Air Showers”. In: *EPJ Web Conf.* 210 (2019). Ed. by I. Lhenry-Yvon et al., p. 02004. DOI: 10.1051/epjconf/201921002004. arXiv: 1902.08124 [astro-ph.HE].
- [100] Lorenzo Cazon. “Working Group Report on the Combined Analysis of Muon Density Measurements from Eight Air Shower Experiments”. In: *PoS ICRC2019* (2020), p. 214. DOI: 10.22323/1.358.0214. arXiv: 2001.07508 [astro-ph.HE].
- [101] Dennis Soldin. “Update on the Combined Analysis of Muon Measurements from Nine Air Shower Experiments”. In: *PoS ICRC2021* (2021), p. 349. DOI: 10.22323/1.395.0349. arXiv: 2108.08341 [astro-ph.HE].

- [102] Alexander Aab et al. “Muons in Air Showers at the Pierre Auger Observatory: Measurement of Atmospheric Production Depth”. In: *Phys. Rev. D* 90.1 (2014). [Addendum: Phys.Rev.D 90, 039904 (2014), Erratum: Phys.Rev.D 92, 019903 (2015)], p. 012012. DOI: 10.1103/PhysRevD.90.012012. arXiv: 1407.5919 [hep-ex].
- [103] Sergey Ostapchenko and Günter Sigl. “On the model uncertainties for the predicted muon content of extensive air showers”. In: *Astropart. Phys.* 163 (2024), p. 103004. DOI: 10.1016/j.astropartphys.2024.103004. arXiv: 2404.02085 [hep-ph].
- [104] Felix Riehn, Ralph Engel, and Anatoli Fedynitch. “Sibyll★: ad-hoc modifications for an improved description of muon data in extensive air showers”. In: *PoS ICRC2023* (2023), p. 429. DOI: 10.22323/1.444.0429. arXiv: 2309.05390 [astro-ph.HE].
- [105] Julien Manshanden, Günter Sigl, and Maria V. Garzelli. “Modeling strangeness enhancements to resolve the muon excess in cosmic ray extensive air shower data”. In: *JCAP* 02 (2023), p. 017. DOI: 10.1088/1475-7516/2023/02/017. arXiv: 2208.04266 [hep-ph].
- [106] Luis A. Anchordoqui, Haim Goldberg, and Thomas J. Weiler. “Strange fireball as an explanation of the muon excess in Auger data”. In: *Phys. Rev. D* 95.6 (2017), p. 063005. DOI: 10.1103/PhysRevD.95.063005. arXiv: 1612.07328 [hep-ph].
- [107] Eamonn Maguire, Lukas Heinrich, and Graeme Watt. “HEPData: a repository for high energy physics data”. In: *J. Phys. Conf. Ser.* 898.10 (2017). Ed. by Richard Mount and Craig Tull, p. 102006. DOI: 10.1088/1742-6596/898/10/102006. arXiv: 1704.05473 [hep-ex].
- [108] David Maurin et al. “A cosmic-ray database update: CRDB v4.1”. In: *Eur. Phys. J. C* 83.10 (2023), p. 971. DOI: 10.1140/epjc/s10052-023-12092-8. arXiv: 2306.08901 [astro-ph.HE].
- [109] IceCube Collaboration. *IceCube data releases*. 2025. URL: <https://icecube.wisc.edu/science/data-releases/> (visited on 08/12/2025).
- [110] A. Haungs et al. “The KASCADE Cosmic-ray Data Centre KCDC: Granting Open Access to Astroparticle Physics Research Data”. In: *Eur. Phys. J. C* 78.9 (2018), p. 741. DOI: 10.1140/epjc/s10052-018-6221-2. arXiv: 1806.05493 [astro-ph.IM].
- [111] A. Abdul Halim et al. “The Pierre Auger Observatory open data”. In: *Eur. Phys. J. C* 85.1 (2025), p. 70. DOI: 10.1140/epjc/s10052-024-13560-5. arXiv: 2309.16294 [astro-ph.HE].
- [112] Sergey Ostapchenko. “QGSJET-III model of high energy hadronic interactions: The formalism”. In: *Phys. Rev. D* 109.3 (2024), p. 034002. DOI: 10.1103/PhysRevD.109.034002. arXiv: 2401.06202 [hep-ph].
- [113] Christian Bierlich et al. “Robust Independent Validation of Experiment and Theory: Rivet version 3”. In: *SciPost Phys.* 8 (2020), p. 026. DOI: 10.21468/SciPostPhys.8.2.026. arXiv: 1912.05451 [hep-ph].
- [114] Matt Dobbs and Jorgen Beck Hansen. “The HepMC C++ Monte Carlo event record for High Energy Physics”. In: *Comput. Phys. Commun.* 134 (2001), pp. 41–46. DOI: 10.1016/S0010-4655(00)00189-2.
- [115] Chloé Gaudu. “Pythia 8 and Air Shower Simulations: A Tuning Perspective”. In: *22nd International Symposium on Very High Energy Cosmic Ray Interactions*. Oct. 2024. arXiv: 2411.00111 [astro-ph.HE].
- [116] Peter Skands, Stefano Carrazza, and Juan Rojo. “Tuning PYTHIA 8.1: the Monash 2013 Tune”. In: *Eur. Phys. J. C* 74.8 (2014), p. 3024. DOI: 10.1140/epjc/s10052-014-3024-y. arXiv: 1404.5630 [hep-ph].

- [117] A. Karneyeu et al. “MCPLLOTS: a particle physics resource based on volunteer computing”. In: *Eur. Phys. J. C* 74 (2014), p. 2714. DOI: 10.1140/epjc/s10052-014-2714-9. arXiv: 1306.3436 [hep-ph].
- [118] Natalia Korneeva, Anton Karneyeu, and Peter Skands. “Event-generator validation with MC-PLOTS and LHC@home”. In: *Eur. Phys. J. Plus* 139.7 (2024), p. 653. DOI: 10.1140/epjp/s13360-024-05353-2. arXiv: 2401.10621 [hep-ph].
- [119] *LHC@home*. <https://lhathome.cern.ch/lhathome/index.php>. Accessed: 2025-06-22.
- [120] G. Acampora et al. “SND@LHC: the scattering and neutrino detector at the LHC”. In: *JINST* 19.05 (2024), P05067. DOI: 10.1088/1748-0221/19/05/P05067. arXiv: 2210.02784 [hep-ex].
- [121] Max Fieg et al. “Tuning pythia for forward physics experiments”. In: *Phys. Rev. D* 109.1 (2024), p. 016010. DOI: 10.1103/PhysRevD.109.016010. arXiv: 2309.08604 [hep-ph].
- [122] Mohan Krishnamoorthy et al. “Apprentice for Event Generator Tuning”. In: *EPJ Web Conf.* 251 (2021), p. 03060. DOI: 10.1051/epjconf/202125103060. arXiv: 2103.05748 [hep-ex].
- [123] Michael Windau et al. “Improving Air Shower Simulations by Tuning Pythia 8/Angantyr with Accelerator Data”. In: Aug. 2025. arXiv: 2508.11458 [astro-ph.HE].
- [124] Ralph Engel et al. “Towards a Next Generation of CORSIKA: A Framework for the Simulation of Particle Cascades in Astroparticle Physics”. In: *Comput. Softw. Big Sci.* 3.1 (2019), p. 2. DOI: 10.1007/s41781-018-0013-0. arXiv: 1808.08226 [astro-ph.IM].
- [125] Salvatore La Cagnina et al. “A Bayesian tune of the Herwig Monte Carlo event generator”. In: *JINST* 18.10 (2023), P10033. DOI: 10.1088/1748-0221/18/10/P10033. arXiv: 2302.01139 [hep-ph].
- [126] Oliver Schulz et al. “BAT.jl: A Julia-Based Tool for Bayesian Inference”. In: *SN Comput. Sci.* 2.3 (2021), pp. 1–17. DOI: 10.1007/s42979-021-00626-4. arXiv: 2008.03132 [stat.CO].
- [127] K. Werner and B. Guiot. “Perturbative QCD concerning light and heavy flavor in the EPOS4 framework”. In: *Phys. Rev. C* 108.3 (2023), p. 034904. DOI: 10.1103/PhysRevC.108.034904. arXiv: 2306.02396 [hep-ph].
- [128] K. Werner. “Parallel scattering, saturation, and generalized AGK theorem in the EPOS4 framework, with applications for heavy ion collisions at 5.02 ATeV and at 200 AGeV”. In: (Oct. 2023). arXiv: 2310.09380 [hep-ph].
- [129] K. Werner. “Core-corona procedure and microcanonical hadronization to understand strangeness enhancement in proton-proton and heavy ion collisions in the EPOS4 framework”. In: *Phys. Rev. C* 109.1 (2024), p. 014910. DOI: 10.1103/PhysRevC.109.014910. arXiv: 2306.10277 [hep-ph].
- [130] Klaus Werner, Fu-Ming Liu, and Tanguy Pierog. “Parton ladder splitting and the rapidity dependence of transverse momentum spectra in deuteron-gold collisions at RHIC”. In: *Phys. Rev. C* 74 (2006), p. 044902. DOI: 10.1103/PhysRevC.74.044902. arXiv: hep-ph/0506232.
- [131] V. A. Abramovsky, V. N. Gribov, and O. V. Kancheli. “Character of Inclusive Spectra and Fluctuations Produced in Inelastic Processes by Multi - Pomeron Exchange”. In: *Yad. Fiz.* 18 (1973), pp. 595–616.
- [132] Johannes Jahan, Klaus Werner, and Damien Vintache. “Integrating the Rivet analysis tool into EPOS 4”. In: *EPJ Web Conf.* 295 (2024), p. 05007. DOI: 10.1051/epjconf/202429505007.

- [133] M. Glück, E. Reya, and A. Vogt. “Dynamical parton distributions revisited”. In: *Eur. Phys. J. C* 5 (1998), pp. 461–470. DOI: 10.1007/s100520050289. arXiv: hep-ph/9806404.
- [134] Sergey Ostapchenko. “Monte Carlo treatment of hadronic interactions in enhanced Pomeron scheme: I. QGSJET-II model”. In: *Phys. Rev. D* 83 (2011), p. 014018. DOI: 10.1103/PhysRevD.83.014018. arXiv: 1010.1869 [hep-ph].
- [135] S. Ostapchenko. “QGSJET-II: physics, recent improvements, and results for air showers”. In: *EPJ Web Conf.* 52 (2013). Ed. by U. Gensh and M. Walter, p. 02001. DOI: 10.1051/epjconf/20125202001.
- [136] Guido Altarelli and G. Parisi. “Asymptotic Freedom in Parton Language”. In: *Nucl. Phys. B* 126 (1977), pp. 298–318. DOI: 10.1016/0550-3213(77)90384-4.
- [137] Yuri L. Dokshitzer. “Calculation of the Structure Functions for Deep Inelastic Scattering and e^+e^- Annihilation by Perturbation Theory in Quantum Chromodynamics.” In: *Sov. Phys. JETP* 46 (1977), pp. 641–653.
- [138] V. N. Gribov and L. N. Lipatov. “Deep inelastic $e p$ scattering in perturbation theory”. In: *Sov. J. Nucl. Phys.* 15 (1972), pp. 438–450.
- [139] Jian-wei Qiu and Ivan Vitev. “Resummed QCD power corrections to nuclear shadowing”. In: *Phys. Rev. Lett.* 93 (2004), p. 262301. DOI: 10.1103/PhysRevLett.93.262301. arXiv: hep-ph/0309094.
- [140] Jian-wei Qiu and Ivan Vitev. “Coherent QCD multiple scattering in proton-nucleus collisions”. In: *Phys. Lett. B* 632 (2006), pp. 507–511. DOI: 10.1016/j.physletb.2005.10.073. arXiv: hep-ph/0405068.
- [141] T. Anticic et al. “Inclusive production of protons, anti-protons and neutrons in $p+p$ collisions at 158-GeV/c beam momentum”. In: *Eur. Phys. J. C* 65 (2010), pp. 9–63. DOI: 10.1140/epjc/s10052-009-1172-2. arXiv: 0904.2708 [hep-ex].
- [142] O. Adriani et al. “Measurement of inclusive forward neutron production cross section in proton-proton collisions at $\sqrt{s} = 13$ TeV with the LHCf Arm2 detector”. In: *JHEP* 11 (2018), p. 073. DOI: 10.1007/JHEP11(2018)073. arXiv: 1808.09877 [hep-ex].
- [143] Jean-Marco Alameddine et al. “The particle-shower simulation code CORSIKA 8”. In: *PoS ICRC2023* (2023), p. 310. DOI: 10.22323/1.444.0310. arXiv: 2308.05475 [astro-ph.HE].
- [144] Eun-Joo Ahn et al. “Cosmic ray interaction event generator SIBYLL 2.1”. In: *Phys. Rev. D* 80 (2009), p. 094003. DOI: 10.1103/PhysRevD.80.094003. arXiv: 0906.4113 [hep-ph].
- [145] Anatoli Fedynitch et al. “Hadronic interaction model SIBYLL 2.3c and inclusive lepton fluxes”. In: *Phys. Rev. D* 100 (10 Nov. 2019), p. 103018. DOI: 10.1103/PhysRevD.100.103018. URL: <https://link.aps.org/doi/10.1103/PhysRevD.100.103018>.
- [146] A. Capella et al. “Dual parton model”. In: *Phys. Rept.* 236 (1994), pp. 225–329. DOI: 10.1016/0370-1573(94)90064-7.
- [147] Hans-Joachim Drescher. “Remnant Break-up and Muon Production in Cosmic Ray Air Showers”. In: *Phys. Rev. D* 77 (2008), p. 056003. DOI: 10.1103/PhysRevD.77.056003. arXiv: 0712.1517 [hep-ph].
- [148] A. Donnachie and P. V. Landshoff. “Total cross-sections”. In: *Phys. Lett. B* 296 (1992), pp. 227–232.
- [149] Hans-Uno Bengtsson and Torbjorn Sjostrand. “The Lund Monte Carlo for Hadronic Processes: Pythia Version 4.8”. In: *Comput. Phys. Commun.* 46 (1987), p. 43. DOI: 10.1016/0010-4655(87)90036-1.

- [150] Torbjorn Sjostrand. “Status of Fragmentation Models”. In: *Int. J. Mod. Phys. A* 3 (1988), p. 751. DOI: 10.1142/S0217751X88000345.
- [151] G. Ingelman and P. E. Schlein. “Jet Structure in High Mass Diffractive Scattering”. In: *Phys. Lett. B* 152 (1985), pp. 256–260. DOI: 10.1016/0370-2693(85)91181-5.
- [152] Torbjörn Sjöstrand and Marius Uthm. “A Framework for Hadronic Rescattering in pp Collisions”. In: *Eur. Phys. J. C* 80.10 (2020), p. 907. DOI: 10.1140/epjc/s10052-020-8399-3. arXiv: 2005.05658 [hep-ph].
- [153] Chloé Gaudu, Maximilian Reininghaus, and Felix Riehn. “CORSIKA 8 with Pythia 8/Angantyr: Simulating Inclined Proton Showers”. In: *PoS UHECR2024* (2025), p. 089. DOI: 10.22323/1.484.0089.
- [154] Chloé Gaudu, Maximilian Reininghaus, and Felix Riehn. “From collider to cosmic rays: Pythia 8/Angantyr for air shower simulations in CORSIKA 8”. In: Aug. 2025. arXiv: 2508.08793 [astro-ph.HE].
- [155] M. Bleicher et al. “Relativistic hadron hadron collisions in the ultrarelativistic quantum molecular dynamics model”. In: *J. Phys. G* 25 (1999), pp. 1859–1896. DOI: 10.1088/0954-3899/25/9/308. arXiv: hep-ph/9909407.
- [156] Paula Hillmann, Jan Steinheimer, and Marcus Bleicher. “Directed, elliptic and triangular flow of protons in Au+Au reactions at 1.23 A GeV: a theoretical analysis of the recent HADES data”. In: *J. Phys. G* 45.8 (2018), p. 085101. DOI: 10.1088/1361-6471/aac96f. arXiv: 1802.01951 [nucl-th].
- [157] Marcus Bleicher and Elena Bratkovskaya. “Modelling relativistic heavy-ion collisions with dynamical transport approaches”. In: *Prog. Part. Nucl. Phys.* 122 (2022), p. 103920. DOI: 10.1016/j.pnpnp.2021.103920.
- [158] T. T. Böhlen et al. “The FLUKA Code: Developments and Challenges for High Energy and Medical Applications”. In: *Nucl. Data Sheets* 120 (2014), pp. 211–214. DOI: 10.1016/j.nds.2014.07.049.
- [159] T Antoni et al. “The Cosmic ray experiment KASCADE”. In: *Nucl. Instrum. Meth. A* 513 (2003), pp. 490–510. DOI: 10.1016/S0168-9002(03)02076-X.
- [160] J. M. Alameddine et al. “Simulating radio emission from particle cascades with CORSIKA 8”. In: *Astropart. Phys.* 166 (2025), p. 103072. DOI: 10.1016/j.astropartphys.2024.103072. arXiv: 2409.15999 [astro-ph.HE].
- [161] Alexander Aab et al. “Testing Hadronic Interactions at Ultrahigh Energies with Air Showers Measured by the Pierre Auger Observatory”. In: *Phys. Rev. Lett.* 117.19 (2016), p. 192001. DOI: 10.1103/PhysRevLett.117.192001. arXiv: 1610.08509 [hep-ex].
- [162] A. Abdul Halim et al. “Testing hadronic-model predictions of depth of maximum of air-shower profiles and ground-particle signals using hybrid data of the Pierre Auger Observatory”. In: *Phys. Rev. D* 109 (10 May 2024), p. 102001. DOI: 10.1103/PhysRevD.109.102001. URL: <https://link.aps.org/doi/10.1103/PhysRevD.109.102001>.
- [163] J. Matthews. “A Heitler model of extensive air showers”. In: *Astropart. Phys.* 22 (2005), pp. 387–397. DOI: 10.1016/j.astropartphys.2004.09.003.
- [164] Maximilian Reininghaus, Ralf Ulrich, and Tanguy Pierog. “Air shower genealogy for muon production”. In: *PoS ICRC2021* (2021), p. 463. DOI: 10.22323/1.395.0463. arXiv: 2108.03266 [astro-ph.HE].

- [165] Stefan Roesler, Ralph Engel, and Johannes Ranft. “The Monte Carlo event generator DPMJET-III”. In: *International Conference on Advanced Monte Carlo for Radiation Physics, Particle Transport Simulation and Applications (MC 2000)*. Dec. 2000, pp. 1033–1038. DOI: 10.1007/978-3-642-18211-2_166. arXiv: hep-ph/0012252.
- [166] Tanguy Pierog et al. “3D Hybrid Air Shower Simulation in CORSIKA”. In: *32nd International Cosmic Ray Conference*. Vol. 2. 2011, p. 222. DOI: 10.7529/ICRC2011/V02/1170.
- [167] Eric Armengaud et al. “Crpropa: a numerical tool for the propagation of uhe cosmic rays, gamma-rays and neutrinos”. In: *Astropart. Phys.* 28 (2007), pp. 463–471. DOI: 10.1016/j.astropartphys.2007.09.004. arXiv: astro-ph/0603675.
- [168] Karl-Heinz Kampert et al. “CRPropa 2.0 – a Public Framework for Propagating High Energy Nuclei, Secondary Gamma Rays and Neutrinos”. In: *Astropart. Phys.* 42 (2013), pp. 41–51. DOI: 10.1016/j.astropartphys.2012.12.001. arXiv: 1206.3132 [astro-ph.IM].
- [169] Lukas Merten et al. “CRPropa 3.1—a low energy extension based on stochastic differential equations”. In: *JCAP* 06 (2017), p. 046. DOI: 10.1088/1475-7516/2017/06/046. arXiv: 1704.07484 [astro-ph.IM].
- [170] Leonel Morejon and Karl-Heinz Kampert. “Implementing hadronic interactions in CRPropa to study bursting sources of UHECRs”. In: *PoS ICRC2023* (2023), p. 285. DOI: 10.22323/1.444.0285.
- [171] Julien Dörner et al. “Uncertainties in astrophysical gamma-ray and neutrino fluxes from proton-proton cross-sections in the GeV to PeV range”. In: *JCAP* 04 (2025), p. 043. DOI: 10.1088/1475-7516/2025/04/043. arXiv: 2501.16967 [astro-ph.HE].
- [172] Rikard Enberg, Mary Hall Reno, and Ina Sarcevic. “Prompt neutrino fluxes from atmospheric charm”. In: *Phys. Rev. D* 78 (2008), p. 043005. DOI: 10.1103/PhysRevD.78.043005. arXiv: 0806.0418 [hep-ph].
- [173] M. Benzke et al. “Prompt neutrinos from atmospheric charm in the general-mass variable-flavor-number scheme”. In: *JHEP* 12 (2017), p. 021. DOI: 10.1007/JHEP12(2017)021. arXiv: 1705.10386 [hep-ph].
- [174] Anatoli Fedynitch and Juan Pablo Yanez. “daemonflux: Data-Driven Muon-Calibrated Neutrino Flux”. In: *PoS ICRC2023* (2023), p. 1215. DOI: 10.22323/1.444.1215.
- [175] Anatoli Fedynitch and Matthias Huber. “Data-driven hadronic interaction model for atmospheric lepton flux calculations”. In: *Phys. Rev. D* 106.8 (2022), p. 083018. DOI: 10.1103/PhysRevD.106.083018. arXiv: 2205.14766 [astro-ph.HE].
- [176] Atri Bhattacharya et al. “Prompt atmospheric neutrino fluxes: perturbative QCD models and nuclear effects”. In: *JHEP* 11 (2016), p. 167. DOI: 10.1007/JHEP11(2016)167. arXiv: 1607.00193 [hep-ph].
- [177] O. Zenaiev et al. “Improved constraints on parton distributions using LHCb, ALICE and HERA heavy-flavour measurements and implications for the predictions for prompt atmospheric neutrino fluxes”. In: *JHEP* 04 (2020), p. 118. DOI: 10.1007/JHEP04(2020)118. arXiv: 1911.13164 [hep-ph].
- [178] Yu Seon Jeong et al. “Neutrinos from charm: forward production at the LHC and in the atmosphere”. In: *PoS ICRC2021* (2021), p. 1218. DOI: 10.22323/1.395.1218. arXiv: 2107.01178 [hep-ph].

- [179] Weidong Bai et al. “Forward production of prompt neutrinos from charm in the atmosphere and at high energy colliders”. In: *JHEP* 10 (2023), p. 142. DOI: 10.1007/JHEP10(2023)142. arXiv: 2212.07865 [hep-ph].
- [180] K. Aamodt et al. “The ALICE experiment – A journey through QCD”. In: (Nov. 2022). arXiv: 2211.04384 [nucl-ex].
- [181] G. Dellacasa et al. “ALICE technical design report of the zero degree calorimeter (ZDC)”. In: (Mar. 1999).
- [182] Shreyasi Acharya et al. “Study of very forward energy and its correlation with particle production at midrapidity in pp and p-Pb collisions at the LHC”. In: *JHEP* 08 (2022), p. 086. DOI: 10.1007/JHEP08(2022)086. arXiv: 2107.10757 [nucl-ex].
- [183] Shreyasi Acharya et al. “First observation of strange baryon enhancement with effective energy in pp collisions at the LHC”. In: (Sept. 2024). arXiv: 2409.12702 [nucl-ex].
- [184] Roel Aaij et al. “LHCb Detector Performance”. In: *Int. J. Mod. Phys. A* 30.07 (2015), p. 1530022. DOI: 10.1142/S0217751X15300227. arXiv: 1412.6352 [hep-ex].
- [185] Roel Aaij et al. “Measurement of the Nuclear Modification Factor and Prompt Charged Particle Production in $p-Pb$ and pp Collisions at $\sqrt{s_{NN}}=5$ TeV”. In: *Phys. Rev. Lett.* 128.14 (2022), p. 142004. DOI: 10.1103/PhysRevLett.128.142004. arXiv: 2108.13115 [hep-ex].
- [186] Roel Aaij et al. “Measurement of prompt charged-particle production in pp collisions at $\sqrt{s} = 13$ TeV”. In: *JHEP* 01 (2022), p. 166. DOI: 10.1007/JHEP01(2022)166. arXiv: 2107.10090 [hep-ex].
- [187] Roel Aaij et al. “Nuclear Modification Factor of Neutral Pions in the Forward and Backward Regions in p-Pb Collisions”. In: *Phys. Rev. Lett.* 131.4 (2023), p. 042302. DOI: 10.1103/PhysRevLett.131.042302. arXiv: 2204.10608 [nucl-ex].
- [188] R Aaij et al. “Measurement of prompt hadron production ratios in pp collisions at $\sqrt{s} = 0.9$ and 7 TeV”. In: *Eur. Phys. J. C* 72 (2012), p. 2168. DOI: 10.1140/epjc/s10052-012-2168-x. arXiv: 1206.5160 [hep-ex].
- [189] Roel Aaij et al. “Evidence for modification of b quark hadronization in high-multiplicity pp collisions at $\sqrt{s} = 13$ TeV”. In: *Phys. Rev. Lett.* 131 (2023), p. 061901. DOI: 10.1103/PhysRevLett.131.061901. arXiv: 2204.13042 [hep-ex].
- [190] Roel Aaij et al. “Observation of strangeness enhancement with charmed mesons in high-multiplicity pPb collisions at $\sqrt{s_{NN}} = 8.16$ TeV”. In: (Nov. 2023). arXiv: 2311.08490 [hep-ex].
- [191] Colin Barschel. “Precision luminosity measurement at LHCb with beam-gas imaging”. Presented 05 Mar 2014. PhD thesis. RWTH Aachen U., 2014. URL: <https://cds.cern.ch/record/1693671>.
- [192] M. Ferro-Luzzi. “Proposal for an absolute luminosity determination in colliding beam experiments using vertex detection of beam-gas interactions”. In: *Nucl. Instrum. Meth.* A553 (2005), pp. 388–399. DOI: 10.1016/j.nima.2005.07.010.
- [193] Roel Aaij et al. “Measurement of Antiproton Production in pHe Collisions at $\sqrt{s_{NN}} = 110$ GeV”. In: *Phys. Rev. Lett.* 121.22 (2018), p. 222001. DOI: 10.1103/PhysRevLett.121.222001. arXiv: 1808.06127 [hep-ex].
- [194] R. Aaij et al. “Measurement of antiproton production from antihyperon decays in pHe collisions at $\sqrt{s_{NN}} = 110$ GeV”. In: *Eur. Phys. J. C* 83.6 (2023), p. 543. DOI: 10.1140/epjc/s10052-023-11673-x. arXiv: 2205.09009 [hep-ex].

- [195] LHCb collaboration. “ J/ψ and D^0 production in $\sqrt{s_{NN}} = 68.5$ GeV PbNe collisions”. In: *Eur. Phys. J. C* 83.7 (2023), p. 658. DOI: 10.1140/epjc/s10052-023-11674-w. arXiv: 2211.11652 [hep-ex].
- [196] LHCb collaboration. “Charmonium production in p Ne collisions at $\sqrt{s_{NN}} = 68.5$ GeV”. In: *Eur. Phys. J. C* 83.7 (2023), p. 625. DOI: 10.1140/epjc/s10052-023-11608-6. arXiv: 2211.11645 [hep-ex].
- [197] LHCb collaboration. “The LHCb Upgrade I”. In: *JINST* 19.05 (2024), P05065. DOI: 10.1088/1748-0221/19/05/P05065. arXiv: 2305.10515 [hep-ex].
- [198] Albert Bursche et al. *Physics opportunities with the fixed-target program of the LHCb experiment using an unpolarized gas target*. Tech. rep. Geneva: CERN, 2018. URL: <http://cds.cern.ch/record/2649878>.
- [199] O. Adriani et al. “Measurement of zero degree inclusive photon energy spectra for $\sqrt{s} = 900$ GeV proton-proton collisions at LHC”. In: *Phys. Lett. B* 715 (2012), pp. 298–303. DOI: 10.1016/j.physletb.2012.07.065. arXiv: 1207.7183 [hep-ex].
- [200] O. Adriani et al. “Measurement of energy flow, cross section and average inelasticity of forward neutrons produced in $\sqrt{s} = 13$ TeV proton-proton collisions with the LHCf Arm2 detector”. In: *JHEP* 07 (2020), p. 016. DOI: 10.1007/JHEP07(2020)016. arXiv: 2003.02192 [hep-ex].
- [201] “Measurement of contributions of diffractive processes to forward photon spectra in pp collisions at $\sqrt{s} = 13$ TeV”. In: (Nov. 2017). URL: <https://cds.cern.ch/record/2291387>.
- [202] ATLAS collaboration. “Physics potential of a combined data taking of the LHCf and ATLAS Roman Pot detectors”. In: (2023). ATL-PHYS-PUB-2023-024. URL: <https://cds.cern.ch/record/2871727>.
- [203] N. Abgrall et al. “Measurements of Cross Sections and Charged Pion Spectra in Proton-Carbon Interactions at 31 GeV/c”. In: *Phys. Rev. C* 84 (2011), p. 034604. DOI: 10.1103/PhysRevC.84.034604.
- [204] N. Abgrall et al. “Measurement of Production Properties of Positively Charged Kaons in Proton-Carbon Interactions at 31 GeV/c”. In: *Phys. Rev. C* 85 (2012), p. 035210. DOI: 10.1103/PhysRevC.85.035210.
- [205] N. Abgrall et al. “Measurements of π^\pm , K^\pm , K_S^0 , Λ and proton production in proton-carbon interactions at 31 GeV/c with the NA61/SHINE spectrometer at the CERN SPS”. In: *Eur. Phys. J. C* 76 (2016), p. 84. DOI: 10.1140/epjc/s10052-016-3898-y. arXiv: 1510.02703 [hep-ex].
- [206] A. Aduszkiewicz et al. “Measurements of hadron production in $\pi^+ + \text{C}$ and $\pi^+ + \text{Be}$ interactions at 60 GeV/c”. In: *Phys. Rev. D* 100.11 (2019), p. 112004. DOI: 10.1103/PhysRevD.100.112004. arXiv: 1909.06294 [hep-ex].
- [207] A. Aduszkiewicz et al. “Measurement of meson resonance production in $\pi^- + \text{C}$ interactions at SPS energies”. In: *Eur. Phys. J. C* 77.9 (2017), p. 626. DOI: 10.1140/epjc/s10052-017-5184-z. arXiv: 1705.08206 [nucl-ex].
- [208] N. Abgrall et al. “Measurement of negatively charged pion spectra in inelastic p+p interactions at $p_{lab} = 20, 31, 40, 80$ and 158 GeV/c”. In: *Eur. Phys. J. C* 74 (2014), p. 2794. DOI: 10.1140/epjc/s10052-014-2794-6. arXiv: 1310.2417 [hep-ex].

- [209] A. Aduszkiewicz et al. “Measurements of π^\pm , K^\pm , p and \bar{p} spectra in proton-proton interactions at 20, 31, 40, 80 and 158 GeV/c with the NA61/SHINE spectrometer at the CERN SPS”. In: *Eur. Phys. J. C* 77 (2017), p. 671. DOI: 10.1140/epjc/s10052-017-5260-4. arXiv: 1705.02467 [nucl-ex].
- [210] Michael Unger. “New Results from the Cosmic-Ray Program of the NA61/SHINE facility at the CERN SPS”. In: *PoS ICRC2019* (2020), p. 446. DOI: 10.22323/1.358.0446. arXiv: 1909.07136 [astro-ph.HE].
- [211] Neeraj Amin. “Pilot Study on the Measurement of the Production of Boron Isotopes in C+p Reactions at 13.5A GeV/c with NA61/SHINE”. In: *PoS ICRC2023* (2023), p. 075. DOI: 10.22323/1.444.0075.
- [212] Yoann Genolini et al. “Current status and desired precision of the isotopic production cross sections relevant to astrophysics of cosmic rays: Li, Be, B, C, and N”. In: *Phys. Rev. C* 98.3 (2018), p. 034611. DOI: 10.1103/PhysRevC.98.034611. arXiv: 1803.04686 [astro-ph.HE].
- [213] Yoann Génolini et al. “Current status and desired precision of the isotopic production cross sections relevant to astrophysics of cosmic rays. II. Fluorine to silicon and updated results for Li, Be, and B”. In: *Phys. Rev. C* 109.6 (2024), p. 064914. DOI: 10.1103/PhysRevC.109.064914. arXiv: 2307.06798 [astro-ph.HE].
- [214] J. Abraham et al. “The Fluorescence Detector of the Pierre Auger Observatory”. In: *Nucl. Instrum. Meth. A* 620 (2010), pp. 227–251. DOI: 10.1016/j.nima.2010.04.023. arXiv: 0907.4282 [astro-ph.IM].
- [215] Jan Ebr et al. “Impact of modified characteristics of hadronic interactions on cosmic-ray observables for proton and nuclear primaries”. In: *PoS ICRC2023* (2023), p. 245. DOI: 10.22323/1.444.0245.
- [216] Jiri Blazek et al. “Modified Characteristics of Hadronic Interactions”. In: *PoS ICRC2021* (2021), p. 441. DOI: 10.22323/1.395.0441.
- [217] Jiri Blazek et al. “A Study of Modified Characteristics of Hadronic Interactions”. In: *EPJ Web Conf.* 283 (2023), p. 05005. DOI: 10.1051/epjconf/202328305005. arXiv: 2303.15911 [astro-ph.HE].
- [218] The Pierre Auger Collaboration. *The Pierre Auger Observatory Upgrade - Preliminary Design Report*. 2016. arXiv: 1604.03637 [astro-ph.IM].
- [219] A. Aab et al. “Direct measurement of the muonic content of extensive air showers between 2×10^{17} and 2×10^{18} eV at the Pierre Auger Observatory”. In: *Eur. Phys. J. C* 80.8 (2020), p. 751. DOI: 10.1140/epjc/s10052-020-8055-y.
- [220] Tim Huege. “The Radio Detector of the Pierre Auger Observatory – status and expected performance”. In: *EPJ Web Conf.* 283 (2023), p. 06002. DOI: 10.1051/epjconf/202328306002. arXiv: 2305.10104 [astro-ph.IM].
- [221] Alexander Aab et al. “Measurement of the Radiation Energy in the Radio Signal of Extensive Air Showers as a Universal Estimator of Cosmic-Ray Energy”. In: *Phys. Rev. Lett.* 116.24 (2016), p. 241101. DOI: 10.1103/PhysRevLett.116.241101. arXiv: 1605.02564 [astro-ph.HE].
- [222] R. Abbasi et al. “IceTop: The surface component of IceCube. The IceCube Collaboration”. In: *Nuclear Instruments and Methods in Physics Research A* 700 (2013), pp. 188–220. DOI: 10.1016/j.nima.2012.10.067. arXiv: 1207.6326 [astro-ph.IM].

- [223] Andreas Haungs. “A Scintillator and Radio Enhancement of the IceCube Surface Detector Array”. In: *EPJ Web Conf.* 210 (2019). Ed. by I. Lhenry-Yvon et al., p. 06009. DOI: 10.1051/epjconf/201921006009. arXiv: 1903.04117 [astro-ph.IM].
- [224] M. G. Aartsen et al. “IceCube-Gen2: A Vision for the Future of Neutrino Astronomy in Antarctica”. In: (Dec. 2014). arXiv: 1412.5106 [astro-ph.HE].
- [225] R. Abbasi et al. “Density of GeV muons in air showers measured with IceTop”. In: *Phys. Rev. D* 106.3 (2022), p. 032010. DOI: 10.1103/PhysRevD.106.032010. arXiv: 2201.12635 [hep-ex].
- [226] Stef Verpoest. “Multiplicity of TeV muons in extensive air showers detected with IceTop and IceCube”. In: *PoS ICRC2023* (2023), p. 207. DOI: 10.22323/1.444.0207. arXiv: 2307.14689 [astro-ph.HE].
- [227] A. Leszczynska et al. “A multi-detector EAS reconstruction framework for IceCube”. In: *PoS ICRC2023* (2023), p. 366. DOI: 10.22323/1.444.0366.
- [228] M. Weyrauch and D. Soldin. “A Two-Component Lateral Distribution Function for the Reconstruction of Air-Shower Events in IceTop”. In: *PoS ICRC2023* (2023), p. 357. DOI: 10.22323/1.444.0357.
- [229] Rasha Abbasi et al. “Measurement of the astrophysical diffuse neutrino flux in a combined fit of IceCube’s high energy neutrino data”. In: *PoS ICRC2023* (2023), p. 1064. DOI: 10.22323/1.444.1064.
- [230] M. G. Aartsen et al. “Characteristics of the diffuse astrophysical electron and tau neutrino flux with six years of IceCube high energy cascade data”. In: *Phys. Rev. Lett.* 125.12 (2020), p. 121104. DOI: 10.1103/PhysRevLett.125.121104. arXiv: 2001.09520 [astro-ph.HE].
- [231] Rasha Abbasi et al. “Angular dependence of the atmospheric neutrino flux with IceCube data”. In: *PoS ICRC2023* (2023), p. 1009. DOI: 10.22323/1.444.1009. arXiv: 2307.14728 [astro-ph.HE].
- [232] R. Abbasi et al. “Improved Characterization of the Astrophysical Muon–neutrino Flux with 9.5 Years of IceCube Data”. In: *Astrophys. J.* 928.1 (2022), p. 50. DOI: 10.3847/1538-4357/ac4d29. arXiv: 2111.10299 [astro-ph.HE].
- [233] M. G. Aartsen et al. “Characterization of the Atmospheric Muon Flux in IceCube”. In: *Astropart. Phys.* 78 (2016), pp. 1–27. DOI: 10.1016/j.astropartphys.2016.01.006.
- [234] T. Fuchs. “Development of a Machine Learning Based Analysis Chain for the Measurement of Atmospheric Muon Spectra with IceCube”. In: *25th European Cosmic Ray Symposium* (2017). DOI: 10.48550/arXiv.1701.04067.
- [235] D. Soldin. “Atmospheric Muons Measured with IceCube”. In: *EPJ Web Conf.* 208 (2019). Ed. by B. Pattison et al., p. 08007. DOI: 10.1051/epjconf/201920808007. arXiv: 1811.03651 [astro-ph.HE].
- [236] S. Tilav et al. “Seasonal variation of atmospheric muons in IceCube”. In: *PoS ICRC2019* (2020), p. 894. DOI: 10.22323/1.358.0894.
- [237] Karolin Hymon et al. “Seasonal Variations of the Unfolded Atmospheric Neutrino Spectrum with IceCube”. In: *PoS ICRC2021* (2021), p. 1159. DOI: 10.22323/1.395.1159. arXiv: 2107.09349 [astro-ph.HE].
- [238] R. Abbasi et al. “Observation of seasonal variations of the flux of high-energy atmospheric neutrinos with IceCube”. In: *Eur. Phys. J. C* 83.9 (2023), p. 777. DOI: 10.1140/epjc/s10052-023-11679-5. arXiv: 2303.04682 [astro-ph.HE].

- [239] Paolo Desiati and Thomas K. Gaisser. “Seasonal variation of atmospheric leptons as a probe of charm”. In: *Phys. Rev. Lett.* 105 (2010), p. 121102. DOI: 10.1103/PhysRevLett.105.121102. arXiv: 1008.2211 [astro-ph.HE].
- [240] Stef Verpoest, Dennis Soldin, and Paolo Desiati. “Atmospheric muons and their variations with temperature”. In: *Astropart. Phys.* 161 (2024), p. 102985. DOI: 10.1016/j.astropartphys.2024.102985. arXiv: 2405.08926 [astro-ph.HE].
- [241] W. D. Apel et al. “The KASCADE-Grande experiment”. In: *Nucl. Instrum. Meth. A* 620 (2010), pp. 202–216. DOI: 10.1016/j.nima.2010.03.147.
- [242] T. Antoni et al. “Test of hadronic interaction models in the forward region with KASCADE event rates”. In: *J. Phys. G* 27 (2001), pp. 1785–1798. DOI: 10.1088/0954-3899/27/8/308. arXiv: astro-ph/0106494.
- [243] T. Antoni et al. “KASCADE measurements of energy spectra for elemental groups of cosmic rays: Results and open problems”. In: *Astropart. Phys.* 24 (2005), pp. 1–25. DOI: 10.1016/j.astropartphys.2005.04.001. arXiv: astro-ph/0505413.
- [244] W. D. Apel et al. “Kneelike structure in the spectrum of the heavy component of cosmic rays observed with KASCADE-Grande”. In: *Phys. Rev. Lett.* 107 (2011), p. 171104. DOI: 10.1103/PhysRevLett.107.171104. arXiv: 1107.5885 [astro-ph.HE].
- [245] W. D. Apel et al. “Ankle-like Feature in the Energy Spectrum of Light Elements of Cosmic Rays Observed with KASCADE-Grande”. In: *Phys. Rev. D* 87 (2013), p. 081101. DOI: 10.1103/PhysRevD.87.081101. arXiv: 1304.7114 [astro-ph.HE].
- [246] Donghwa Kang et al. “Results from recent analysis of KASCADE-Grande data”. In: *SciPost Phys. Proc.* 13 (2023), p. 036. DOI: 10.21468/SciPostPhysProc.13.036. arXiv: 2208.10229 [astro-ph.HE].
- [247] Sven Schoo et al. “A new analysis of the combined data from both KASCADE and KASCADE-Grande”. In: *PoS ICRC2017* (2018), p. 339. DOI: 10.22323/1.301.0339.
- [248] Juan Carlos Arteaga Velazquez et al. “Estimations of the muon content of cosmic ray air showers between 10 PeV and 1 EeV from KASCADE-Grande data”. In: *PoS ICRC2021* (2021), p. 376. DOI: 10.22323/1.395.0376.
- [249] W. D. Apel et al. “Probing the evolution of the EAS muon content in the atmosphere with KASCADE-Grande”. In: *Astropart. Phys.* 95 (2017), pp. 25–43. DOI: 10.1016/j.astropartphys.2017.07.001. arXiv: 1801.05513 [astro-ph.HE].
- [250] A. V. Glushkov et al. “Muon Puzzle in Ultra-High Energy EASs According to Yakutsk Array and Auger Experiment Data”. In: *JETP Lett.* 117.9 (2023), pp. 645–651. DOI: 10.1134/S0021364023600726. arXiv: 2304.13095 [astro-ph.HE].
- [251] Yu. A. Fomin et al. “No muon excess in extensive air showers at 100–500 PeV primary energy: EAS–MSU results”. In: *Astropart. Phys.* 92 (2017), pp. 1–6. DOI: 10.1016/j.astropartphys.2017.04.001. arXiv: 1609.05764 [astro-ph.HE].
- [252] A. G. Bogdanov et al. “Investigation of the properties of the flux and interaction of ultrahigh-energy cosmic rays by the method of local-muon-density spectra”. In: *Phys. Atom. Nucl.* 73 (2010), pp. 1852–1869. DOI: 10.1134/S1063778810110074.
- [253] A. G. Bogdanov et al. “Investigation of very high energy cosmic rays by means of inclined muon bundles”. In: *Astropart. Phys.* 98 (2018), pp. 13–20. DOI: 10.1016/j.astropartphys.2018.01.003.

- [254] J. A. Bellido et al. “Muon content of extensive air showers: comparison of the energy spectra obtained by the Sydney University Giant Air-shower Recorder and by the Pierre Auger Observatory”. In: *Phys. Rev. D* 98.2 (2018), p. 023014. DOI: 10.1103/PhysRevD.98.023014. arXiv: 1803.08662 [astro-ph.HE].
- [255] N. N. Kalmykov et al. “Muon lateral distribution function of extensive air showers: Results of the Sydney University Giant Air-shower Recorder versus modern Monte Carlo simulations”. In: *Phys. Rev. D* 105.10 (2022), p. 103004. DOI: 10.1103/PhysRevD.105.103004. arXiv: 2202.01200 [astro-ph.HE].
- [256] T. Abu-Zayyad et al. “Evidence for Changing of Cosmic Ray Composition between 10^{17} -eV and 10^{18} -eV from Multicomponent Measurements”. In: *Phys. Rev. Lett.* 84 (2000), pp. 4276–4279. DOI: 10.1103/PhysRevLett.84.4276. arXiv: astro-ph/9911144.
- [257] R. U. Abbasi et al. “Study of muons from ultrahigh energy cosmic ray air showers measured with the Telescope Array experiment”. In: *Phys. Rev. D* 98.2 (2018), p. 022002. DOI: 10.1103/PhysRevD.98.022002. arXiv: 1804.03877 [astro-ph.HE].
- [258] Flavia Gesualdi et al. “On the muon scale of air showers and its application to the AGASA data”. In: *PoS ICRC2021* (2021), p. 473. DOI: 10.22323/1.395.0473. arXiv: 2108.04824 [astro-ph.HE].
- [259] L. Cazon et al. “The muon measurements of Haverah Park and their connection to the muon puzzle”. In: *PoS ICRC2023* (2023), p. 431. DOI: 10.22323/1.444.0431.
- [260] Juan Carlos Arteaga Velazquez and D. R. Rangel. “Energy dependence of the number of muons for hadronic air showers with KASCADE-Grande”. In: *PoS ICRC2023* (2023), p. 376. DOI: 10.22323/1.444.0376.
- [261] G. Piparo et al. “Measurement of the forward η meson production rate in p-p collisions at $\sqrt{s} = 13$ TeV with the LHCf-Arm2 detector”. In: *JHEP* 10 (2023), p. 169. DOI: 10.1007/JHEP10(2023)169. arXiv: 2305.06633 [hep-ex].
- [262] R. Aaij et al. “Study of J/ψ production and cold nuclear matter effects in pPb collisions at $\sqrt{s_{NN}} = 5$ TeV”. In: *JHEP* 02 (2014), p. 072. DOI: 10.1007/JHEP02(2014)072. arXiv: 1308.6729 [nucl-ex].
- [263] Roel Aaij et al. “Measurement of the b -quark production cross-section in 7 and 13 TeV pp collisions”. In: *Phys. Rev. Lett.* 118.5 (2017). [Erratum: *Phys.Rev.Lett.* 119, 169901 (2017)], p. 052002. DOI: 10.1103/PhysRevLett.118.052002. arXiv: 1612.05140 [hep-ex].
- [264] Roel Aaij et al. “Measurement of B^+ , B^0 and Λ_b^0 production in pPb collisions at $\sqrt{s_{NN}} = 8.16$ TeV”. In: *Phys. Rev. D* 99.5 (2019), p. 052011. DOI: 10.1103/PhysRevD.99.052011. arXiv: 1902.05599 [hep-ex].
- [265] R. Aaij et al. “Measurement of the Prompt D0 Nuclear Modification Factor in p-Pb Collisions at $\sqrt{s_{NN}}=8.16$ TeV”. In: *Phys. Rev. Lett.* 131.10 (2023), p. 102301. DOI: 10.1103/PhysRevLett.131.102301. arXiv: 2205.03936 [nucl-ex].
- [266] A. S. Carroll et al. “Total Cross-Sections of π^\pm , K^\pm , p , and \bar{p} on Protons and Deuterons Between 23-GeV/c and 280-GeV/c”. In: *Phys. Lett. B* 61 (1976), pp. 303–308. DOI: 10.1016/0370-2693(76)90155-6.
- [267] A. S. Carroll et al. “Total Cross-Sections of π^\pm , K^\pm , p and \bar{p} on Protons and Deuterons Between 200 GeV/c and 370 GeV/c”. In: *Phys. Lett. B* 80 (1979), pp. 423–427. DOI: 10.1016/0370-2693(79)91205-X.

- [268] A. S. Carroll et al. “Absorption Cross-Sections of π^\pm , K^\pm , p and \bar{p} on Nuclei Between 60 GeV/c and 280 GeV/c”. In: *Phys. Lett. B* 80 (1979), pp. 319–322. DOI: 10.1016/0370-2693(79)90226-0.
- [269] J. P. Burq et al. “Soft π^-p and pp Elastic Scattering in the Energy Range 30-GeV to 345-GeV”. In: *Nucl. Phys. B* 217 (1983), pp. 285–335. DOI: 10.1016/0550-3213(83)90149-9.
- [270] M. Adamus et al. “Cross-Sections and Charged Multiplicity Distributions for π^+p , K^+p and pp Interactions at 250-GeV/c”. In: *Z. Phys. C* 32 (1986). Ed. by S. C. Loken, p. 475. DOI: 10.1007/BF01550769.
- [271] M. Adamus et al. “Study of Elastic π^+p , K^+p and pp Scattering at 250-GeV/c”. In: *Phys. Lett. B* 186 (1987), pp. 223–226. DOI: 10.1016/0370-2693(87)90284-X.
- [272] M. Adamus et al. “Charged Particle Production in K^+p , π^+p and pp Interactions at 250-GeV/c”. In: *Z. Phys. C* 39 (1988), pp. 311–329.
- [273] N. M. Agababyan et al. “Inclusive production of vector mesons in π^+p interactions at 250-GeV/c”. In: *Z. Phys. C* 46 (1990), pp. 387–395. DOI: 10.1007/BF01621026.
- [274] M. R. Atayan et al. “ π^0 and eta meson production in π^+p and K^+p collisions at 250-GeV/c”. In: *Z. Phys. C* 54 (1992), pp. 247–254. DOI: 10.1007/BF01566653.
- [275] C. Alt et al. “Inclusive production of charged pions in p+p collisions at 158-GeV/c beam momentum”. In: *Eur. Phys. J. C* 45 (2006), pp. 343–381. DOI: 10.1140/epjc/s2005-02391-9. arXiv: hep-ex/0510009.
- [276] A. Aduszkiewicz et al. “Measurements of π^\pm , K^\pm , p and \bar{p} spectra in proton-proton interactions at 20, 31, 40, 80 and 158 GeV/c with the NA61/SHINE spectrometer at the CERN SPS”. In: *Eur. Phys. J. C* 77.10 (2017), p. 671. DOI: 10.1140/epjc/s10052-017-5260-4. arXiv: 1705.02467 [nucl-ex].
- [277] A. Aduszkiewicz et al. “Measurements of production and inelastic cross sections for p+C, p+Be, and p+Al at 60 GeV/c and p+C and p+Be at 120 GeV/c”. In: *Phys. Rev. D* 100.11 (2019), p. 112001. DOI: 10.1103/PhysRevD.100.112001. arXiv: 1909.03351 [hep-ex].
- [278] A. Acharya et al. “ K_S^0 meson production in inelastic p+p interactions at 158 GeV/c beam momentum measured by NA61/SHINE at the CERN SPS”. In: *Eur. Phys. J. C* 82.1 (2022), p. 96. DOI: 10.1140/epjc/s10052-021-09976-y. arXiv: 2106.07535 [hep-ex].
- [279] ATLAS Collaboration. *Further ATLAS tunes of Pythia 8 and Pythia 6*. <https://cds.cern.ch/record/1966419>. ATL-PHYS-PUB-2014-021. Oct. 2014.
- [280] Vardan Khachatryan and others (CMS Collaboration). “Event generator tunes obtained from underlying event and multiparton scattering measurements”. In: *Eur. Phys. J. C* 76.3 (2016), p. 155. DOI: 10.1140/epjc/s10052-016-3988-x. arXiv: 1512.00815 [hep-ex].
- [281] Andy Buckley et al. “Systematic event generator tuning for the LHC”. In: *Eur. Phys. J. C* 65 (2010), pp. 331–357. DOI: 10.1140/epjc/s10052-009-1196-7. arXiv: 0907.2973 [hep-ph].
- [282] Diederik P. Kingma and Jimmy Ba. “Adam: A Method for Stochastic Optimization”. In: Dec. 2014. arXiv: 1412.6980 [cs.LG].